Uncertainty Analysis of the ICRP Human Respiratory Tract Model applied to Interpretation of Bioassay Data for Depleted Uranium

M R Bailey and M Puncher

ABSTRACT

Measurements of uranium excreted in urine have been widely used to monitor possible exposure to depleted uranium (DU) by personnel who have served in areas where DU munitions were used in conflicts. A study has been carried out to provide guidance on the most appropriate parameter values to be used in assessing intakes and doses from urine samples taken at long times (100 to 10,000 days) after possible intakes, and to assess the overall uncertainty in the results. As part of this study, information relating to the application of the ICRP Human Respiratory Tract Model has been reviewed, and from it, central values, ranges and distributions were assigned to parameter values defining respiratory tract deposition of appropriate DU aerosols, and clearance of DU from the respiratory tract. An analysis was carried out of the sensitivity to variation in each parameter value, of committed lung dose and effective dose calculated from a measurement of DU in urine. Generally, the most important parameters were those defining dissolution of the DU in the respiratory tract: the fraction that dissolves rapidly and the slow (long-term) dissolution rate. The overall uncertainty in dose (ratio of maximum to minimum) was estimated to be about 50 at 10 days after intake and about a factor of 7–10 at 1000–10,000 days. Nevertheless, the maximum estimated dose from a measurement of 1 nanogram DU in urine was less than 1 millisievert up to 5000 days after intake. This report complements reports that consider uncertainties in the ICRP model that describes the behaviour of uranium after entry to the blood, and the possible effects on urinary excretion of alteration in kidney function resulting from uranium toxicity.

This study was partly funded by the Defence Science and Technology Laboratory under Contract No RD034-9781

Centre for Radiation, Chemical and Environmental Hazards
Radiation Protection Division
Chilton, Didcot, Oxfordshire OX11 0RQ

Approval: March 2007
Publication: June 2007
£20.00
ISBN 978-0-85951-591-7

EXECUTIVE SUMMARY

Measurements of uranium excreted in urine have been widely used to monitor possible exposures to depleted uranium (DU) by personnel who have served in areas where DU munitions were used in conflicts. In the UK, the Depleted Uranium Oversight Board (DUOB) oversaw a testing programme for UK military veterans and eligible non-military personnel who wished to know whether they had been significantly exposed to DU in the 1991 Gulf War, or during operations in the Balkans from 1994. The test method adopted is based on measurement of uranium isotopic ratios and total uranium excretion in urine.

A study has been carried out to provide guidance on the most appropriate parameter values to be used in assessing intakes and doses from urine samples taken at long times (100 to 10,000 days) after possible intakes, to provide estimates of the overall uncertainties on the results, and recommendations on the most appropriate research to provide information to reduce such uncertainties. As part of the study, information relating to the application of the ICRP Human Respiratory Tract Model (HRTM) to such assessments has been reviewed. From that review, central values, ranges and distributions (probability density functions, PDFs) were assigned to parameter values defining respiratory tract deposition of appropriate DU aerosols, and clearance of DU from the respiratory tract. This report complements two others, which consider uncertainties in the ICRP model that describes the behaviour of uranium after entry to the blood, and the possible effects on urinary excretion of alteration in kidney function resulting from uranium toxicity.

The reviews carried out in support of the assessments made by The Royal Society Working Group on the Health Hazards of Depleted Uranium Munitions (RSWG) formed the starting point for the literature review. Consideration was given to Level I and Level II exposure scenarios as defined by the RSWG (and others), because these are considered to have potential to give rise to the highest exposures. Level I represents people in a vehicle when it is struck by a DU penetrator or first responders who enter immediately afterwards. Level II represents people who work on or in contaminated vehicles. However, an important difference in approach was that the RSWG assessment was prospective. Assessments were made of intakes, committed doses and maximum concentrations of uranium in the kidneys ($^{max}[U]_k$) based on estimated exposures (time-integrated air concentrations) in selected scenarios. The present work is concerned with retrospective assessments based on urine samples from individuals. Information that has become available since publication of the RSWG assessments in 2001 was also reviewed, in particular the extensive information on the characteristics of aerosols formed by the impact of DU penetrators on armoured vehicles provided by the Capstone Aerosol Study.

For exposures to aerosols formed within a struck vehicle, more than 80 sets of measurements of size distribution made within 5 minutes after impact on non-DU armour are available from the Capstone Study. From these, representative central values and ranges were taken to be: activity median aerodynamic diameter (AMAD) 2.5 μm (range 0.4 – 13 μm) and geometric standard deviation (GSD) 6 (range 2 – 15). The relatively few measurements made outside struck vehicles and through resuspension by

disturbance during recovery work activities inside struck vehicles (about 10 each) were consistent with these values, and so they were chosen to represent all Level I and II exposures.

Deposition in each part of the respiratory tract is determined by the size distribution of the inhaled aerosol, and on the breathing characteristics of the person. For the latter, information was drawn largely from a review carried out in support of a project to assess uncertainties in the results of reactor accident consequence assessment computer codes. HRTM parameter values for heavy exercise and light exercise were taken to be central values for Level I and II respectively. It was considered that ventilation rates (m^3 h^{-1}) might range from 0.5 to 2 times the central value, with similar contributions to that range coming from variation in breathing frequency and from variation in tidal volume.

Clearance of material deposited in the respiratory tract results from movement of particles (particle transport) by mechanisms such as mucus flow, mainly to the throat where they are swallowed, but also to regional lymph nodes, and by dissolution and uptake of dissociated material into the blood (absorption). In the HRTM the two are assumed to act independently: particle transport rates depend on the respiratory tract region, but not on the material, while rates of absorption to blood depend on the material but not on the region. For particle transport, HRTM default values were taken to be central values. Based on detailed discussion in ICRP Publication 66, which describes the HRTM and its basis, for each particle transport rate, a range of a factor of three either side of the central value was taken here to account for uncertainty in the central value and inter- and intra-subject variability around it. For simplicity, it was assumed that all particle transport rates are correlated, *i.e.* all rates are increased or decreased by the same factor. Important model uncertainties were identified relating to the slow phase of particle transport in the bronchial tree. To address these, an alternative model of slow bronchial clearance, based on recent experimental data, was also applied.

In the HRTM, absorption of uranium from the respiratory tract to blood is described by three parameters: the fraction that dissolves rapidly, f_r; the dissolution rate of the rapid fraction, s_r (d^{-1}); and the dissolution rate of the slow fraction, s_s (d^{-1}). Following the approach taken by the RSWG, consideration was given both to *in vitro* results on materials that are directly relevant, and to *in vivo* results on similar uranium oxides. However, with the availability of the comprehensive Capstone data somewhat more weight was given here to the *in vitro* data than by the RSWG. Values selected for f_r were simply rounded from the corresponding *in vitro* data. Values selected for s_r and s_s took account of both. Central values and ranges were first selected for impact and combustion aerosols separately. Values were then selected for DU dust that might be of either origin, but more weight was given to results for impact aerosols as this mechanism seems likely to generate larger amounts of respirable dust. From these, representative central values and ranges were taken to be: f_r = 0.15 (range 0.01 – 0.5); s_r = 3 d^{-1} (range 0.3 – 20 d^{-1}) and s_s = 0.002 d^{-1} (range 0.0001 – 0.005 d^{-1}). Appropriate values were also derived for the fractional absorption from the gastrointestinal (GI) tract to blood of material cleared from the respiratory tract to the GI tract.

An analysis was carried out of the sensitivity to uncertainty and variability in each parameter value, of committed effective dose, $E(50)$, $H_{Lung}(50)$ and $^{max}[U]_k$ for unit intake

of DU, and that calculated from a measurement of DU in urine. Most results were calculated with the internal dosimetry code IMBA Professional. For expediency and accuracy, a program was written that automated the process by setting the relevant parameter values within IMBA and calling its dose and bioassay prediction subroutines iteratively. Low, central and high values were taken for each parameter in turn and the result compared with that obtained using central values of all parameters. For absorption to blood, Type M and S default values were included for comparison. Results for $E(50)$ and $H_{Lung}(50)$ were very similar and so are considered together. This reflects the fact that for inhalation of uranium in moderately soluble or insoluble forms, lung dose makes the dominant contribution to effective dose.

For doses per unit intake (DPUI), some parameters were identified in all four categories (aerosol size; breathing; absorption to blood and particle transport) for which the range in values led to changes from the result using the central value of more than 20%.

For doses assessed from a measurement of DU in a 24-hour urine sample at times in the range 100–10,000 days after intake, generally the same sub-set of parameter values leading to large changes was identified as for DPUI. However, for AMAD the effect was the opposite of that observed for DPUI: an increase in AMAD led to a lower DPUI, but a higher dose assessed from a urine sample. This demonstrates the importance of selecting realistic parameter values. It is possible that a parameter value chosen to be 'conservative' for prospective dose assessments, *i.e.* to overestimate the DPUI, will lead to underestimation of dose in a retrospective assessment. The largest changes arose through variation in parameters defining dissolution of the DU in the respiratory tract, in particular, the slow (long-term) dissolution rate. Uncertainties in the particle transport rates relating to slow clearance in the bronchial tree were next in order of importance, but variations in most other particle transport rates had little effect.

Generally a similar sub-set of parameter values leading to changes greater than 20% was identified for ${}^{max}[U]_k$, as for doses. However, in some cases the effects were in the opposite direction from those for doses. Changes to the dissolution parameter values had most effect, especially changes to the fraction that dissolves rapidly, f_r.

An assessment of 'indicative' uncertainties in doses and ${}^{max}[U]_k$ assessed from a urine sample, based on simple combinations of uncertainties related to individual parameters, was carried out in advance of the full uncertainty analysis. Combinations of high and low parameter values were used to give an 'indication' of the overall uncertainty in doses and ${}^{max}[U]_k$ assessed from measurement of DU in a 24-hour urine sample at times in the range 10–10,000 days after intake. 'Central' values of dose and ${}^{max}[U]_k$ were calculated using the central values chosen for all parameters. 'Minimum' and 'maximum' values were obtained using all combinations of high and low parameter values as described above.

For the full uncertainty analysis, Monte Carlo simulations were performed using a new software tool: the IMBA Uncertainty Analyser. This code has been developed for calculating full probabilistic uncertainties on prospective and retrospective dosimetry calculations, and implements Bayesian inference procedures. The code samples parameters from the HRTM and GI tract model, using random or Latin Hypercube sampling methods. The software sets the sampled parameters within IMBA and then

calls its dose and bioassay prediction subroutines iteratively. A Latin Hypercube sample of 10^4 variates was constructed for each parameter from its assigned PDF. For each of 10^4 iterations of the Monte Carlo, a sample set of HRTM parameter values was configured in IMBA by the IMBA Uncertainty Analyser program. IMBA calculated the results needed to derive $E(50)$ and $H_{Lung}(50)$ assessed from 1 ng DU measured in a 24-hour urine sample, at 10 logarithmically-spaced times between 10 and 10,000 days after an intake by inhalation. From the distributions of 10^4 values of $E(50)$ or $H_{Lung}(50)$, calculated for each time point, the median, lower 2.5-percentile ($L_{2.5\%}$) and upper 97.5-percentile ($U_{97.5\%}$) were calculated.

For the median, $E(50)$ assessed from 1 ng DU d^{-1} increases from about 0.1 μSv at 10 days after intake to about 1 mSv at 10,000 days. At 10 days after intake, $L_{2.5\%}$ is about a factor of 10 below the median and $U_{97.5\%}$ is about a factor of 6 above it, giving an overall range ($U_{97.5\%}/L_{2.5\%}$) of about 50. As the time between intake and sampling increases, the range decreases, so that between 1000 and 10,000 days, $U_{97.5\%}$ is between 7 and 10 times $L_{2.5\%}$. Despite the large uncertainty, even $U_{97.5\%}$ values of $E(50)$ assessed from 1 ng DU d^{-1} are below 1 mSv up to 5000 d. A similar pattern was found for $H_{Lung}(50)$.

For the purpose of this study it is assumed that intakes occur entirely by inhalation, although there could be a contribution from ingestion such as that resulting from inadvertent hand-to-mouth transfer. It was shown that for the conditions considered here, doses assessed from a urine sample are generally much lower following ingestion than following inhalation.

The median from the uncertainty analysis lies close to the central value from the indicative analysis, as expected. The range of values obtained in the full uncertainty analysis is narrower than that obtained from the indicative analysis, even though two additional sources of uncertainty were included: intersubject variation in deposition in the extrathoracic airways, and model uncertainties in slow bronchial clearance, demonstrating that the indicative analysis overestimates the range. However, the minimum values from the indicative analysis are close to the $L_{2.5\%}$ values at all times, whereas the maximum values from the indicative analysis are consistently higher than $U_{97.5\%}$ especially at times up to 1000 days after intake.

For the 'indicative' uncertainty analysis of ${}^{max}[U]_k$ assessed from 1 ng DU d^{-1}, the central value increases from about 10^{-5} μg per gram at 10 days after intake, to about 0.1 μg per gram at 10,000 days. At 10 days after intake the minimum is about a factor of four below the central value and the maximum is about a factor of two above it. At later times, the range increases, so that between 200 and 10,000 days, the maximum is between 300 and 900 times the minimum. Nevertheless, despite the large uncertainty (which is probably overestimated, as it was for the indicative uncertainty analysis of doses), even maximum assessed values of ${}^{max}[U]_k$ from 1 ng DU d^{-1} are below 1 μg per gram at all times considered.

For the first part of the sensitivity analyses, consideration is given to doses (and ${}^{max}[U]_k$) resulting from 1 mg DU. For the second part of the sensitivity analyses, and for the uncertainty analyses, consideration is given to doses (and ${}^{max}[U]_k$) assessed from a

measurement of 1 ng DU in urine. It is considered that the results can be scaled linearly to other intakes and measurements over wide ranges.

Recommendations were made for research on HRTM parameter values to reduce uncertainties in doses (and $^{max}[U]_k$) assessed from measurements of DU in urine. The sensitivity analysis identified parameters related to absorption to blood as those having the largest effect on assessed doses (and $^{max}[U]_k$). There is scope for research to define better the probability distribution of rates of absorption of DU from the lungs. It is therefore recommended that consideration be given to conducting limited *in vivo* measurements of long-term dissolution of suitable particles containing DU, a major objective of which would be to validate extrapolation of the results of *in vitro* tests to man.

The variability in some parameter values associated with the exposure scenario limits the potential for research in advance to reduce uncertainties. Since parameter values such as AMAD can vary so greatly according to the exposure conditions, however well their distributions are known, there will be considerable uncertainty about the values relevant to exposure of any individual in a particular incident. Consideration should therefore be given to a study to design a monitoring programme that might be carried out on exposed personnel, to reduce uncertainties in their assessed doses, by providing information on the behaviour of the material to which they were actually exposed.

CONTENTS

1 Introduction 1
1.1 Background 1
1.2 Objectives and scope 3

2 Human respiratory tract model parameter values 3
2.1 The ICRP Human Respiratory Tract Model 3
2.1.1 Morphometry 4
2.1.2 Physiology 5
2.1.3 Respiratory tract deposition of particles 5
2.1.4 Clearance 9
2.1.5 Dose calculation 12
2.2 Selection of HRTM parameter values and ranges 14
2.2.1 The Capstone Aerosols Study 16
2.3 Respiratory tract deposition 17
2.3.1 Aerosol size distributions 18
2.3.2 Exercise level and ventilation rates 21
2.3.3 Breathing mode 24
2.3.4 Intersubject variation in nasal deposition efficiency 24
2.4 Particle transport from the respiratory tract 25
2.4.1 Variability 25
2.4.2 Uncertainty 26
2.4.3 Modifying factors 26
2.4.4 Model uncertainties 26
2.4.5 Particle transport parameter values and ranges 28
2.4.6 Particle transport parameter distributions 29
2.5 Absorption to blood from the respiratory tract 29
2.5.1 Direct measurements of dissolution of DU formed from penetrator impacts 30
2.5.2 Direct measurements of dissolution of DU formed in fires 33
2.5.3 Uranium speciation 34
2.5.4 Dissolution of uranium oxides 35
2.5.5 Absorption parameter values for assessments of DU exposures 37
2.6 Summary 41

3 Methods used in the sensitivity and uncertainty analyses 42
3.1 Computer Codes 43
3.2 Composition of Depleted Uranium 43
3.3 Individual parameter sensitivity analysis of HRTM parameter values 44
3.3.1 Deposition 44
3.3.2 Absorption to blood 44
3.3.3 Particle transport 45
3.3.4 Bioassay and dose calculations 45
3.3.5 Data Analysis 45
3.4 Probabilistic uncertainty analysis 46
3.4.1 The Monte Carlo simulation 46
3.4.2 Data processing and statistical analyses 47

4 Results and discussion 47
4.1 Sensitivity of radiation doses to inhalation parameter values 47

4.1.1 Results of sensitivity analysis 50
4.2 Uncertainty analysis 54

5 Conclusions 57

6 Recommendations for research to reduce uncertainties 60

7 Acknowledgements 61

8 References 61

APPENDIX A 66
Indicative uncertainty analysis of the HRTM applied to interpretation of bioassay data for depleted uranium 66
A1 Introduction 66
A2 Variation in respiratory tract deposition 67
A3 Sensitivity analysis of maximum kidney concentrations to inhalation parameter values 70
A4 Indicative uncertainty analysis of HRTM parameter values 75

1 INTRODUCTION

1.1 Background

Measurements of uranium excreted in urine have long been used to monitor the exposure of workers to materials containing uranium, notably in the production and processing of nuclear reactor fuel. During the last few years urine analysis has been used by authorities in several countries to monitor possible exposure to depleted uranium (DU) by personnel who have served in areas in which DU munitions were used in conflicts: the 1991 and 2003 Gulf Wars, and operations in the Balkans (*e.g.* Portuguese Nuclear and Technological Institute, 2001; Roth et al, 2001; Meddings and Haldiman 2002; Ough et al, 2002; McDiarmid et al, 2004).

In the UK, the Depleted Uranium Oversight Board (DUOB) was established in 2001 to oversee the development of a testing programme for UK military veterans and eligible non-military personnel who wished to know whether they had been significantly exposed to DU in the 1991 Gulf War, or during operations in the Balkans from 1994. The test method adopted was based on measurement of uranium isotopic ratios and total uranium excretion in urine (Parrish et al., 2006). DU has a higher ^{238}U:^{235}U isotopic ratio than natural uranium. Hence, if DU is being excreted following exposure, there will be elevation of the ^{238}U:^{235}U ratio in urine above the value of 137.9 that is normally found from excretion of natural uranium from the diet. Altogether 464 veterans underwent testing in the main programme, including two who were tested twice. Most had served in the armed forces during the Gulf War (219), the Balkans campaign (80) or both (123). None of the veterans tested had detectable exposure to DU (DUOB, 2007).

Using existing available knowledge about the behaviour of materials containing uranium after their entry to the body, it is in principle possible to calculate, from the amount of DU excreted in urine per day, the original intake (amount that entered the body), and from it quantities related to risks of health effects. Based on current understanding, the most important quantities are the radiation dose to the lungs, the effective dose, and the maximum concentration of uranium in the kidneys ($^{max}[U]_k$).

There is currently considerable interest in ultrafine particles (mainly from fossil fuel combustion) in the ambient air, and their possible role in adverse health effects (e.g. Kreyling et al 2004). (In this context ultrafine particles are usually defined as particles with physical diameters less than 0.1 μm.) There is a growing body of evidence that some adverse health effects of air pollution may be related to the number or surface area concentrations of inhaled ultrafine particles rather than the mass concentration, which is expected to determine radiation effects and kidney damage. However, at present it is not possible to quantify the effects of ultrafine particles, nor is it known whether ultrafine DU particles would cause such effects. Consideration of effects related specifically to ultrafine particles was therefore beyond the scope of this project.

The relationships between exposure to DU by inhalation or ingestion and radiation doses and ($^{max}[U]_k$) are complex, but reasonably well understood. Inhaled material that is deposited in the respiratory tract is absorbed into the blood at a rate depending on its solubility in body fluids, but is also removed, mainly towards the throat, where it is

swallowed, at rates that vary from time-scales of minutes in the nose, to years in the deep lungs. Most of the uranium absorbed into blood is excreted rapidly, but some is deposited in tissues throughout the body, notably the skeleton, where it can be retained for many years, before being returned to the blood, and either redeposited or excreted.

Because of the large-scale use of uranium in nuclear fuel production, its behaviour in the body has been studied extensively since the 1940s, enabling sophisticated models to be developed to describe its behaviour. Nevertheless, significant generic uncertainties remain, which affect the uncertainty, or "confidence interval" that might be associated with assessments of radiation doses (or $^{max}[U]_k$) from urine samples. In addition, some parameter values associated with the DU material to which an individual is exposed (particle size distribution, dissolution characteristics) will depend on the specific circumstances of formation (penetrator impact or fire) and of the exposure. Similarly, some parameters associated with the individual will be subject to biological variability and/or depend on the circumstances of exposure (e.g., breathing rate).

This is the first of three reports produced by HPA to address a requirement within the MOD DU Research Programme for a review of work on biokinetic modelling related to uranium and an assessment of its relevance to DU issues. In addition to providing an overall introduction to the project, it addresses factors relating to the ICRP Human Respiratory Tract Model (HRTM, ICRP, 1994a) and its application to munitions DU. Uncertainties (ranges and distributions) related to parameter values used in the HRTM are estimated. An analysis is carried out of the sensitivity, to variation in each parameter value, of doses calculated from a measurement of DU in urine. An assessment is made of uncertainties in doses assessed from a urine sample, but considering only uncertainty and variability in HRTM parameter value. It concludes with consideration of research relating to HRTM parameter values that might be undertaken to improve the assessment of intakes and doses.

An Appendix describes an assessment of 'indicative' uncertainties in doses assessed from a urine sample, based on simple combinations of uncertainties related to individual parameters, which was carried out in advance of the full uncertainty analysis. Again only uncertainty and variability in HRTM parameter values are considered in this report. However, it also includes sensitivity and indicative uncertainty analyses of $^{max}[U]_k$ assessed from a urine sample, although these were beyond the scope of the contract.

The second report (Harrison et al, 2007) addresses issues relating to the ICRP model for the behaviour of uranium that has entered the blood (systemic model, ICRP, 1995b) and estimates uncertainties related to parameter values used in that model. It includes assessments of indicative and overall uncertainties in doses assessed from a urine sample, considering only uncertainty and variability in systemic model parameter values, and consideration of work relating to systemic model parameter values that might be undertaken to improve the assessment of intakes and doses. It concludes with an overall assessment of uncertainties in doses assessed from a urine sample, considering uncertainty and variability in both HRTM and systemic model parameter values.

The third report (Hodgson et al, 2007) addresses the issue of whether alteration of kidney function at high uranium kidney concentrations might affect urinary excretion of uranium and hence assessments based on urine sampling.

1.2 Objectives and scope

The objectives of this report are to:

- Review information relevant to the selection of HRTM parameter values.
- Recommend the most appropriate HRTM parameter values for use in biokinetic modelling relating to intakes of DU munitions debris.
- Estimate appropriate ranges and frequency distributions for values of each relevant HRTM parameter.
- Carry out a sensitivity analysis to examine the effects of uncertainty and variability in these parameter values, the relative importance of each parameter and the likely uncertainty in interpreting urine analysis data following intakes of DU munitions debris
- Carry out an analysis of the uncertainty in doses assessed from a urine sample, considering only uncertainty and variability in HRTM parameter values.

Note that for the purpose of this study it is assumed that intakes occur entirely by inhalation, although there could be a contribution from ingestion such as that resulting from inadvertent hand-to-mouth transfer. As shown in Section 4.2, doses assessed from a urine sample are generally much lower following ingestion than following inhalation.

2 HUMAN RESPIRATORY TRACT MODEL PARAMETER VALUES

Two exposure scenarios are considered here, since they are recognised as having potential for significant intakes in e.g. the assessments carried out by the Royal Society Working Group on the Health Hazards of Depleted Uranium Munitions (RSWG, Royal Society, 2001, 2002):

- 'Level I' exposures, which apply to personnel present in a vehicle struck by a DU round, and first responders who enter soon after: predominantly inhalation of the cloud of dust formed directly from the impact of a DU penetrator on armour plate.
- 'Level II' exposures, which apply to personnel working in or on vehicles contaminated with DU dust: predominantly inhalation of resuspended DU originating from either impacts or combustion within struck vehicles.

2.1 The ICRP Human Respiratory Tract Model

The HRTM is described in detail in ICRP Publication 66 (ICRP, 1994a). Summaries are given in the ICRP Publications (68, 71, 72, 78, 88, 95) in which it is applied (ICRP, 1994b; 1995a; 1996; 1997; 2001; 2002; 2004), and elsewhere (Bailey; 1994; Bailey et al, 1998; 2003). An outline is given here.

The main functions of the HRTM are to provide:

- A qualitative and quantitative description of the respiratory tract as a route for radionuclides to enter the body.
- A method to calculate radiation doses to the respiratory tract for any exposure.
- A method to calculate the transfer of radionuclides to other tissues.

The HRTM is comprehensive. It applies to:

- Assessing doses from exposures, and assessing intakes from bioassay measurements.
- Radionuclides associated with particles (aerosols) of all sizes of practical interest (0.0006–100 μm) and to gases and vapours.
- All members of the population, giving reference values for children aged 3 months, 1, 5, 10 and 15 years, and adults. Guidance is provided for taking into account the effects of factors such as smoking, diseases and pollutants, and specific information relating to the inhaled material and/or the exposed subjects.

2.1.1 Morphometry

In the HRTM the respiratory tract is represented by five regions, based on differences in radio-sensitivity, deposition and clearance (Figure 1). The extrathoracic (head and neck) airways (ET) are divided into ET_1, the anterior nasal passage (front of the nose), and ET_2, which consists of the posterior nasal and oral passages, the pharynx and larynx. The thoracic regions (the lungs) are Bronchial (BB: trachea, generation 0, airway generations 1-8), Bronchiolar (bb: airway generations 9–15), and Alveolar-Interstitial (AI, the gas exchange region). Lymph nodes are associated with the extrathoracic and thoracic airways (LN_{ET} and LN_{TH} respectively). Target cells are identified in each region: e.g. the basal cells of the epithelium in both ET regions; basal and secretory cells in the bronchial epithelium. Reference values of dimensions that define the mass of tissue containing target cells in each region for dose calculations, are given. They are assumed to be independent of age and sex.

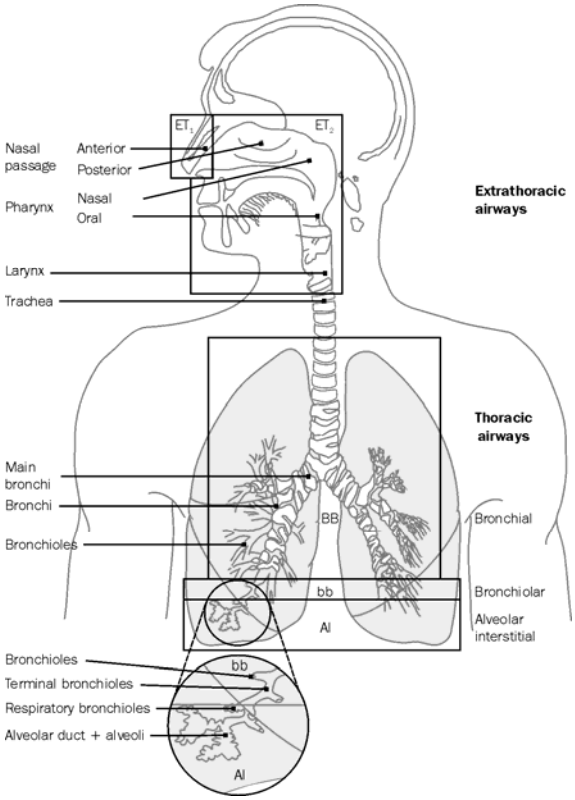

Figure 1 Respiratory tract regions defined in the HRTM

2.1.2 Physiology

Breathing characteristics (frequency and volume) are the main HRTM parameters that depend on age and physical activity. The key relevant ventilation parameters are: (1) breathing mode, the distribution of inhaled air between nose and mouth; (2) breathing frequency, f_R, the number of breaths per minute; and (3) tidal volume, V_T, the volume of air inhaled per breath. The ventilation rate, the volume of air inhaled per unit time, is calculated from f_R, and V_T. Reference values of these parameters are recommended for the population groups noted above, for four levels of exercise: sleep, sitting, light and heavy exercise, and taking account of both nose- and mouth-breathing. These were combined with habit survey data to give the reference volumes inhaled per working shift or per day. Thus light work is a combination of light exercise and sitting. These parameters determine intakes per unit exposure (time-integrated air concentration) but are also used with the deposition model to determine regional deposition.

2.1.3 Respiratory tract deposition of particles

Deposition refers to the initial processes that determine how much of the material in the inhaled air remains behind after exhalation.

The behaviour of an airborne particle depends on its size, shape and density. If the particle is spherical, its size can be uniquely defined by its geometric diameter. If it is not spherical its size is usually described in terms of an 'equivalent diameter' – the diameter of a sphere (or circle) which gives the same result as the particle when

measured in the same way. For example, the volume equivalent diameter, d_e, is the diameter of a sphere with the same volume as the particle.

There are three main mechanisms that affect the behaviour of airborne particles in the respiratory tract (Figure 2): gravitational sedimentation, inertial impaction and Brownian motion (diffusion). These mechanisms also determine their behaviour in the ambient air and in many air sampling instruments.

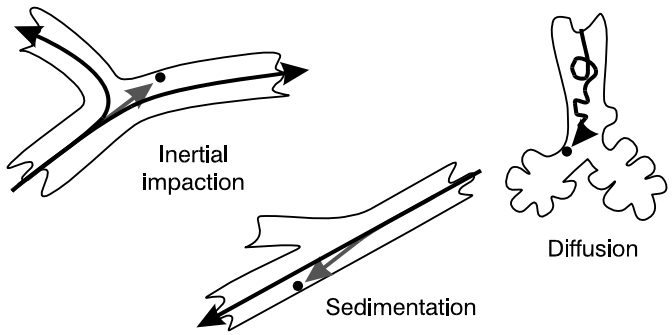

Figure 2 Main mechanisms of particle deposition in the respiratory tract (after Yeh *et al*., 1976)

Sedimentation and impaction are "aerodynamic" effects that are important above about 0.1 μm and increase with increasing size. The particle's behaviour can be represented by the aerodynamic equivalent diameter, d_{ae}, the diameter of a unit density sphere that has the same terminal settling velocity in air as the particle of interest. In many practical situations d_{ae} approximates to $d_e\ (\rho)^{½}$, where ρ is the particle density.

Diffusion is a "thermodynamic" effect that is important below about 1 μm and increases with decreasing size. (In the transition size-range, about 0.1 μm–1.0 μm, particle motion is influenced by both aerodynamic and thermodynamic effects). The behaviour can be represented by the thermodynamic equivalent diameter, d_{th}, the diameter of a spherical particle with the same diffusion coefficient in air as the particle of interest. Because diffusion does not depend on particle density, d_{th} approximates to the 'physical' or 'geometric' diameter of the particle, and is assumed in the HRTM to be equal to d_e.

The particles produced by any source generally have a wide range of sizes. A collection of airborne particles (solid or liquid) is known as an aerosol. In order to describe the size of the whole aerosol, and its behaviour, it is useful to represent it by a mathematical function. The one most frequently used for aerosols is the 'log-normal' distribution. The log-normal function is often suitable for describing the distribution of a parameter that shows a wide range of values. It is described by the median diameter, which is the 50th percentile particle size, and the geometric standard deviation (GSD, or σ_g), which is approximately the ratio of the 50th percentile size to the 16th percentile size.

For a radioactive aerosol, the amount of activity per unit size, rather than the number of particles, is usually considered. When sedimentation and impaction dominate, the aerosol should be characterised by the activity median aerodynamic diameter, AMAD: 50% of the activity is associated with particles of d_{ae} larger than the AMAD. When diffusion dominates, the aerosol should be characterised by the activity median thermodynamic diameter, AMTD: 50% of the activity is associated with particles larger

than the AMTD. In the HRTM it is assumed, by default, that σ_g is a function of AMTD, increasing from a value of 1.0 at 6 nm to a value of 2.5 above about 1 μm.

The HRTM deposition model evaluates the fraction of activity in the inhaled air that is deposited in each region. Deposition in the ET regions was determined mainly from experimental data. For the lungs, a theoretical model was used to calculate particle deposition in each region, and to quantify the effects of the subject's lung size and breathing rate. The regions are treated as a series of filters during both inhalation and exhalation. The efficiency of each was evaluated by considering aerodynamic and thermodynamic processes acting competitively.

Figure 3(a) gives the fraction of inhaled activity deposited in each region as a function of aerosol size for a reference worker. (The HRTM default value of 3 g cm^{-3} was used for the particle density). As indicated above, for particle diameters below about 0.1 μm diffusion dominates, so AMTD is the appropriate parameter to characterise the aerosol. Above 1 μm the aerodynamic processes of gravitational sedimentation and inertial impaction dominate, so AMAD is the appropriate parameter. Between 0.1 and 1 μm both contribute. In Figure 3 results are therefore shown as functions of AMTD up to 1 μm and of AMAD above 0.1 μm. In the transition size-range (0.1–1 μm) values are given for both AMAD and AMTD. The pattern in Figure 3(a) illustrates the deposition mechanisms outlined above and also the effectiveness of the nose as a filter. The smallest particles (~1 nm) are mainly deposited in the extrathoracic (ET) airways by diffusion. As particle size increases, deposition by diffusion decreases and more particles penetrate to, and deposit in, the bronchial (BB), bronchiolar (bb) and alveolar-interstitial (AI) regions in turn. A maximum in AI deposition occurs at about 20 nm (0.02 μm). With further increase in size, fewer particles deposit even in the AI region, and a large fraction of the inhaled particles are exhaled again. Sedimentation and impaction then become increasingly effective, and deposition in the ET airways increases. The decrease in ET deposition at AMAD > 10 μm results from reduced 'inhalability': because of their inertia, some particles in the inhaled air do not enter the nose and mouth.

In Figure 3(b) regions have been grouped together in combinations which are likely to influence dose. For example, for a very soluble (Type F) material, all the activity that deposits in the respiratory tract (except that in ET_1) reaches blood quickly, so dose may well be proportional to total deposition in the lungs combined with that in region ET_2 (lungs+ET_2). Expressed another way, the dose depends on total deposition excluding that in region ET_1, since it is assumed that there is no absorption to blood or clearance to the GI tract from ET_1.

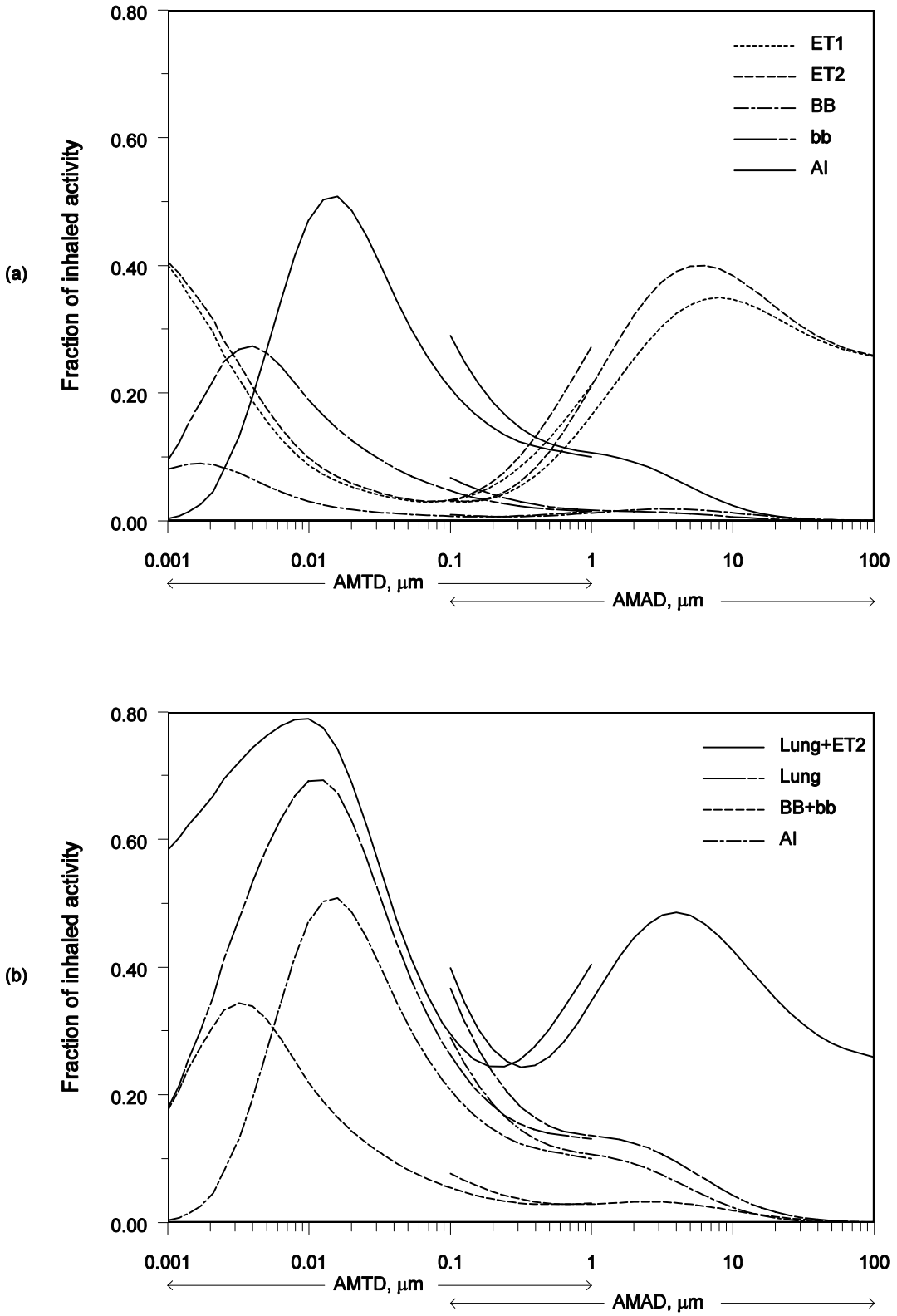

Figure 3 Deposition in (a) each respiratory tract region and (b) combinations of regions as predicted by the HRTM for a reference worker, as a function of aerosol median size. In the transition size-range (0.1–1 µm) values are given for both AMAD and AMTD (ICRP 2002, Figure 4.3).

2.1.4 Clearance

The HRTM describes several routes of clearance from the respiratory tract (Figure 4), which involve three general processes. Material deposited in ET_1 is assumed to be removed by nose blowing and wiping. In other regions clearance results from a combination of movement of particles towards the GI tract and lymph nodes (particle transport), and movement of radionuclides from the respiratory tract into the blood and hence body fluids (absorption).

It is assumed that:

- All clearance rates are independent of age and sex.
- Particle transport rates are the same for all materials.
- Absorption into blood, which is material specific, occurs at the same rate in all regions except ET_1, where none occurs.

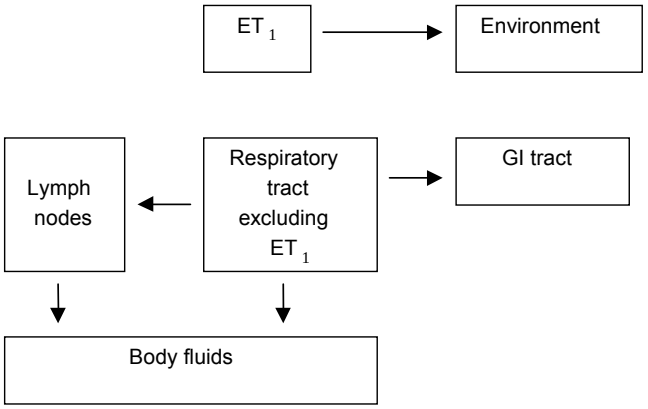

Figure 4 Routes of clearance from the respiratory tract

Fractional clearance rates vary with time, but to simplify calculations are represented by combinations of compartments that clear at constant rates. Since particle transport rates are the same for all materials, a single compartment model applies to all (Figure 5 and Table 1). It was based, so far as possible, on human experimental data.

The model as shown in Figure 5 would describe the retention and clearance of a completely insoluble material. However, there is in general simultaneous absorption to body fluids of material from all the compartments except ET_1.

Table 1 Reference values of parameters for the compartment model to represent time-dependent particle transport from human respiratory tract (*ICRP Publication 66, Table 17*)

A. Clearance rates

Pathway	From	To	Rate, d^{-1}	Half-time*
$m_{1,4}$	AI_1	bb_1	0.02	35 d
$m_{2,4}$	AI_2	bb_1	0.001	700 d
$m_{3,4}$	AI_3	bb_1	0.0001	7000 d
$m_{3,10}$	AI_3	LN_{TH}	0.00002	-
$m_{4,7}$	bb_1	BB_1	2	8 h
$m_{5,7}$	bb_2	BB_1	0.03	23 d
$m_{6,10}$	bb_{seq}	LN_{TH}	0.01	70 d
$m_{7,11}$	BB_1	ET_2'	10	100 min
$m_{8,11}$	BB_2	ET_2'	0.03	23 d
$m_{9,10}$	BB_{seq}	LN_{TH}	0.01	70 d
$m_{11,15}$	ET_2'	GI tract	100	10 min
$m_{12,13}$	ET_{seq}	LN_{ET}	0.001	700 d
$m_{14,16}$	ET_1	Environment	1	17 h

B. Partition of deposit in each region between compartments†

Region or deposition site	Compartment	Fraction of deposit in region assigned to compartment‡
ET_2	ET_2'	0.9995
	ET_{seq}	0.0005
BB	BB_1	0.993 - f_s
	BB_2	f_s
	BB_{seq}	0.007
bb	bb_1	0.993 - f_s
	bb_2	f_s
	bb_{seq}	0.007
AI	AI_1	0.3
	AI_2	0.6
	AI_3	0.1

*The half-times are approximate since the reference values are specified for the particle transport rates and are rounded in units of d^{-1}. A half-time is not given for the transport rate from AI_3 to LN_{TH}, since this rate was chosen to direct the required amount of material to the lymph nodes. The clearance half-time of compartment AI_3 is determined by the sum of the clearance rates from it.

†See *ICRP Publication 66 Paragraph 181, Chapter 5* for default values used for relating f_s to d_{ae}.

‡It is assumed that the slow-cleared fraction f_s is size-dependent. For modelling purposes f_s is taken to be:

$f_s = 0.5$ for $d_{ae} \leq 2.5 \sqrt{(\rho/\chi)}$ µm

$f_s = 0.5\, e^{-0.63\,(d_{ae}\,\sqrt{\chi/\rho}-2.5)}$ for $d_{ae} > 2.5\sqrt{\rho/\chi}$ µm

Absorption to blood is a two-stage process: dissociation of the particles into material that can be absorbed into blood (*dissolution*); and absorption into blood of soluble material and of material dissociated from particles (*uptake*). Both stages can be time-dependent. The simplest representation of time-dependent *dissolution* is to assume that a fraction (f_r) dissolves relatively rapidly, at a rate s_r, and the remaining fraction (1 – f_r) dissolves more slowly, at a rate s_s (Figure 6). Provision is made in the HRTM for only two

fractions, to avoid undue complexity, because it was considered that there would not often be information available to justify the use of more. *Uptake* to body fluids of dissolved material can usually be treated as instantaneous. In some situations, however, a significant fraction of the dissolved material is absorbed slowly. To enable this to be taken into account, the HRTM includes compartments in which activity is retained in each region in a 'bound' state. However, in the HRTM it is assumed by default that uptake is instantaneous, and the 'bound' state is not used.

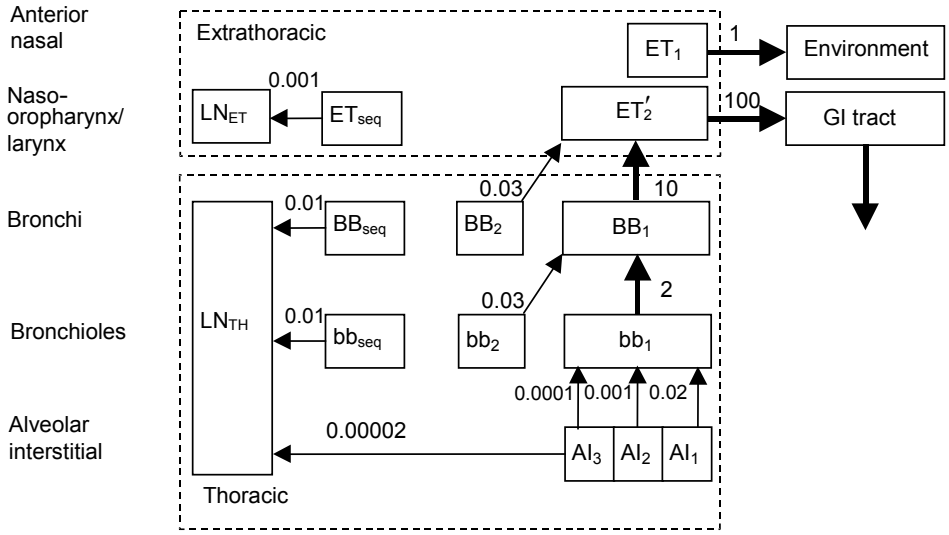

Figure 5 Compartment model representing time-dependent particle transport from each respiratory tract region in the HRTM. Rates shown alongside arrows are reference values in units of d^{-1} (Table 1).

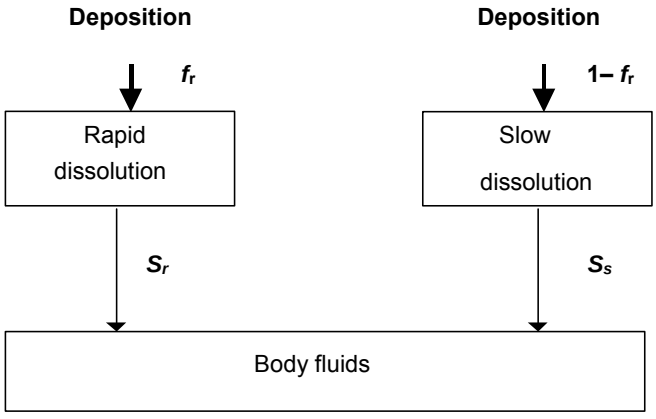

Figure 6 Compartment model representing time-dependent dissolution, followed by instantaneous uptake to body fluids. A fraction f_r of the deposit is initially assigned to the compartment labelled "Rapid dissolution", and the rest ($1–f_r$) of the deposit is initially assigned to the compartment labelled "Slow dissolution".

It is recommended (ICRP, 1994a; 1994b; 2002) that material-specific rates of absorption should be used for compounds for which reliable experimental data exist. For other compounds, default values of parameters are recommended, according to whether the absorption is considered to be fast (Type F), moderate (M) or slow (S), corresponding broadly to inhalation Classes D, W and Y in the ICRP Publication 30 (ICRP, 1979) model (Table 2).

Table 2 Default absorption parameter values for Type F, M, and S materials (ICRP, 1994a)*

Type		F(fast)	M (moderate)	S (slow)
Fraction dissolved rapidly	f_r	1	0.1	0.001
Dissolution rates:				
Rapid (d^{-1})	s_r	100	100	100
Slow (d^{-1})	s_s	-	0.005	0.0001

*The values of f_r, s_r and s_s in this table are close approximations to the reference values.

These absorption rates, expressed as approximate half-times, and the corresponding amounts of material deposited in each region that reach blood can be summarised as follows:

Type F: 100% absorbed with a half-time of 10 minutes. There is rapid absorption of almost all material deposited in the lungs (BB, bb, and AI), and 50% of material deposited in ET_2. The other 50% of material deposited in ET_2 is cleared to the GI tract by particle transport.

Type M: 10% absorbed with a half-time of 10 minutes and 90% with a half-time of 140 d. There is rapid absorption of about 10% of the deposit in BB and bb; and 5% of material deposited in ET_2. About 70% of the deposit in AI eventually reaches the blood.

Type S: 0.1% absorbed with a half-time of 10 minutes and 99.9% with a half-time of 7000 d. There is little absorption from ET, BB, or bb, and about 10% of the deposit in AI eventually reaches the blood.

For absorption Types F, M, and S, all the material deposited in ET_1 is removed by extrinsic means. Most of the material deposited in other regions that is not absorbed is cleared to the GI tract by particle transport. The small amounts transferred to lymph nodes continue to be absorbed into body fluids at the same rate as in the respiratory tract.

2.1.5 Dose calculation

The deposition and clearance models enable the amounts of activity throughout the respiratory tract at any time after intake to be calculated. The dosimetric model enables the resulting doses to each part of the lungs to be calculated.

For dosimetric purposes, the respiratory tract is treated as two tissues: the thoracic airways (TH) and the extrathoracic airways (ET). It is considered that some regions in both TH and ET are more sensitive to radiation than others. To take account of these differences in sensitivity between tissues, the equivalent dose H_i to each region i is multiplied by a factor, A_i, representing the region's estimated radiosensitivity relative to

that of the whole organ. The weighted sum is the equivalent dose to the thoracic airways (given as 'lungs' in the tables of dose coefficients) or ET airways respectively:

$$H_{TH} = H_{BB}\, A_{BB} + H_{bb}\, A_{bb} + H_{AI}\, A_{AI} + H_{LN_{TH}}\, A_{LN_{TH}} \quad (1)$$

$$H_{ET} = H_{ET_1}\, A_{ET_1} + H_{ET_2}\, A_{ET_2} + H_{LN_{ET}}\, A_{LN_{ET}} \quad (2)$$

The tissue weighting factor, w_T, of 0.12 specified for lungs in ICRP Publication 60 (ICRP, 1991) is applied to the equivalent dose to the thoracic airways, H_{TH}, to calculate its contribution to effective dose. The extrathoracic airways were included in the list of remainder tissues and organs in ICRP Publication 68 (ICRP, 1994b). Hence when the equivalent dose to the extrathoracic airways, H_{ET}, is higher than any other organ dose (as it often is), a w_T of 0.025 is applied to H_{ET} to calculate its contribution to effective dose.

The recommended values of A_i (the fraction of w_T assigned to each region) are given in ICRP Publication 66, Table 31 (Table 3), and are assumed to be independent of age and sex.

The dose to each respiratory tract region is taken to be the dose to the cells at risk (target cells) in that region, and is calculated as the average dose to the target tissue in that region. In the alveolar region (AI) and lymph nodes (LN_{TH} and LN_{ET}) the cells at risk are taken to be distributed throughout the region, and the average dose to the whole region is calculated. For the regions making up the conducting airways (ET_1, ET_2, BB and bb) the target cells are considered to lie in a layer of tissue at a certain range of depths from the airway surface.

In each respiratory tract region there are also several possible sources of radiation. In bb, for example, particles in the fast phase of clearance (bb_1, Figure 5) are taken to be in a layer of mucus above the cilia; particles in the slow phase of clearance (bb_2) are taken to be in the fluid between the cilia; particles retained in the airway wall (bb_{seq}) are taken to be in macrophages which lie in a layer which is further from the surface than the target cells; activity "bound" to the epithelium is uniformly distributed in it. Account is also taken of irradiation from activity present in the alveolar region.

For each source/target combination, only a fraction of the energy emitted in the source is absorbed in the target: the 'Absorbed Fraction'. ICRP Publication 66, Annexe G provides photon Absorbed Fractions as a function of energy for the thoracic (TH) and extrathoracic (ET) airways as sources (and all other organs as targets) and for TH and ET as targets (and all other organs as sources). For each respiratory tract region, and each source/target combination (see above), ICRP Publication 66, Annexe H provides Absorbed Fractions for non-penetrating radiations: (alpha particles, beta particles and electrons) in each case as a function of energy. To obtain these absorbed fractions, a single cylindrical geometry was used to represent each region of the conducting airways. The representative bronchus for BB is 5 mm in diameter and the representative bronchiole for bb is 1 mm diameter (ICRP 66, Paragraphs 48 and 54).

Table 3 Target tissues of the respiratory tract (based on ICRP 1994a, Table 31)

Organ	Region	Target cells	Assigned fractions* A_i, of w_T
Extrathoracic airways	ET_1 (anterior nose)	Basal	0.001
	ET_2 (posterior nose, mouth, pharynx, larynx)	Basal	0.998
	LN_{ET} (lymphatics)	‡	0.001
Thoracic airways (lungs)	BB (bronchial)	Secretory (BB_{sec}) Basal (BB_{bas})	0.333†
	bb (bronchiolar)	Secretory	0.333
	AI (alveolar-interstitial)	‡	0.333
	LN_{TH} (lymphatics)	‡	0.001

*Reference values *ie*., the recommended default values for use in the model. Independent of age and sex. †The dose to BB, H_{BB}, is calculated as the arithmetic mean of the doses to BB_{sec} and BB_{bas}.

‡Average dose to region calculated.

2.2 Selection of HRTM parameter values and ranges

As noted above, based on reviews of information then available the RSWG selected parameter values for central and worst-case estimates of doses and maximum kidney concentrations ($^{max}[U]_k$) for a set of scenarios intended to represent the range of battlefield exposures. RSWG parameter values for Level I and Level II inhalation exposures are given in Tables 4 and 5. These form a natural starting point for the selection made here. However, there is an important difference in context between this analysis and that of the RSWG. Here we consider the "retrospective" assessment of doses (and $^{max}[U]_k$) for an individual, based on a urine sample. The RSWG assessment was "prospective", considering the doses and $^{max}[U]_k$ arising from postulated exposure scenarios. For that situation it was recognised that the dominant uncertainty was in the exposure (time-integrated air concentration), and in the light of that it was reasonable to ignore some other components of uncertainty. In a retrospective assessment however, the intake is assessed from the urine concentration through the HRTM, and factors affecting e.g. the initial deposition pattern are relatively more important than they are in a prospective assessment.

Table 4 Parameter values for Level I inhalation of impact aerosol. Except where indicated, parameter values are only given where they differ from those used in ICRP Publication 68 (default) to calculate dose coefficients for workers for UO_2 and U_3O_8 (Royal Society 2001, Table 14: References are made to other tables in Royal Society 2001).

Parameter	Central estimate	Worst case (radiation)	Worst case (chemical toxicity)
Subject exercise level, type	Heavy exercise	Heavy exercise, habitual mouth breather	Heavy exercise, habitual mouth breather
AMAD, μm	2 (table G2)	0.8 (lowest reported in table G2)	0.8 (lowest reported in table G2)
GSD	13 (table G2, in particular Chambers et al. 1982)	18 (highest reported in table G2)	18 (highest reported in table G2)
Density ρ, g cm^{-3}	9 (UO_2 and U_3O_8 are ~11.0 and ~8.4 respectively. Mainly U_3O_8)	11 (UO_2)	11 (UO_2)
Shape factor, χ	1.5 (default)	1.5 (default)	1.5 (default)
Rapid dissolution fraction, f_r	0.3 (Typical of table F3)	0.1 (Lowest from table G3)	0.5 (Highest from table G3)
Rapid dissolution rate, s_r, d^{-1}	1 (Typical of U compounds table A5)	0.4 (Low value for U compounds, table A5)	14 (High value for U compounds, table A5)
Slow dissolution rate, s_s, d^{-1}	0.001 (Typical of U_3O_8 *in vivo*, table A5)	0.0001 (as Type S, see table A3)	0.0015 (Highest for U_3O_8 or UO_2 *in vivo*, table A5)
Gut uptake factor, f_1	0.002 (default for Type S)	0.02 (default for Types M and F)	0.02 (default for Types M and F)

Table 5 Parameter values for Level II or III inhalation of resuspension aerosol (impact or combustion) within vehicle. Except where indicated, parameter values are only given where they differ from those used in ICRP Publication 68 to calculate dose coefficients for workers for UO_2 and U_3O_8. Justification given only where also different from Table 4 (Royal Society 2001, Table 15: References are made to other tables in Royal Society 2001)

Parameter	Central estimate	Worst case (radiation)	Worst case (chemical toxicity)
Subject exercise level, type of breathing	Heavy work (7 h light exercise + 1 h heavy exercise, ICRP Publication 66, table 6)	Heavy exercise, habitual mouth breather	Heavy exercise, habitual mouth breather
AMAD, μm	5 (default workplace)	1 (resuspension aerosols normally 'coarse', >1 μm)	1 (resuspension aerosols normally 'coarse', >1 μm)
GSD	2.5 (default)	4 (Upper bound for aerosol from single source)	4 (Upper bound for aerosol from single source)
Density ρ, g cm^{-3}	9	11	11
Rapid dissolution fraction, f_r	0.2 (Mid-way between typical values, table 14 for impacts and table 18 for combustion)	0.005 (Lowest for combustion in table 18)	0.5 (Highest for impact in table 14)
Rapid dissolution rate, s_r, d^{-1}	1	0.4	14
Slow dissolution rate, s_s, d^{-1}	0.001	0.0001	0.0015
Gut uptake factor, f_1	0.002	0.02	0.02

Consideration is also given to information that has become available since the RSWG reports were issued in 2001 and 2002. The most important source is the Capstone Aerosols Study (Parkhurst et al, 2004a; 2004b) and its associated Human Health Risk Assessment (HHRA, Guilmette et al, 2004).

2.2.1 The Capstone Aerosols Study

The Capstone Aerosols Study involved the generation and characterisation of DU aerosols created by the perforation of an Abrams tank and a Bradley Fighting Vehicle (BFV) with large calibre depleted uranium (LC-DU) penetrators. A series of tests was carried out in which LC-DU penetrators impacted target vehicles inside an enclosure. Phases I-III used a "Ballistic Hull and Turret" (BHT), a vehicle shell stripped of flammable material, instrumentation etc. In particular, the BHT had no ventilation system. Phase IV used an operational Abrams tank.

Phase I (Abrams tank BHT with conventional armour) consisted of seven shots. Four shots crossed the turret (two of them 13 minutes apart in a single test, i.e., a double shot), two were fired into the gun breech (to maximise aerosol formation), and one was fired into the hull.

Phase II (BFV BHT) consisted of three shots: two of them 14 minutes apart in a single test through the scout compartment, and one through the turret to maximise aerosol formation.

Phase III (Abrams tank BHT with DU armour) consisted of two shots, both through the DU armour fitted to the turret.

Phase IV (operational Abrams tank with DU armour) consisted of four shots. Three were firings of non-DU munitions. One was more relevant, involving a DU penetrator fired through DU armour. It therefore enabled a comparison to be made of a BHT (Phase III) with an operational vehicle.

Three shots were retrospective, simulating Operation Desert Storm (ODS) incidents, while the others were prospective, providing information for possible future incidents.

Extensive sampling and aerosol characterisation were carried out. In Phases I-III, there were four main sampling positions within the vehicle, corresponding to the four tank crew: commander, driver, gunner, and loader. At each position nine pairs of air samplers were run in a pre-set time sequence starting 5 seconds after impact (to avoid damage from blast and fragments). Each pair consisted of a filter that collected total aerosol (all the airborne particles in the volume of air drawn through it), and a cascade impactor* (CI), which separated the particles collected into nine fractions according to their aerodynamic diameter. Thus DU air concentrations and aerodynamic size distributions were obtained as functions of time.

In addition, two other types of air sampler were operated inside the vehicle. One was a moving filter sampler (MVF), which collected particles on a tape of filter that was wound past the sampler inlet, and which started immediately after impact. The other was a

* The cascade impactor has long been the most widely used instrument for measuring aerodynamic size distributions. Suction is used to draw air through one or more orifices in a plate, producing a high velocity jet (or jets). A collection plate perpendicular to the jet creates a rapid change in direction. The inertia of larger particles causes them to impact on the collection plate, while the air and smaller particles flow around it. In a cascade impactor there are several such stages in series, each consisting of an orifice plate and a collection plate designed to collect successively smaller particles, followed by a 'back-up' filter to collect particles that pass the final stage.

cascade cyclone*, which provided much larger amounts of sized material than the CI, but collected a single set of samples over the entire period from 5 seconds to 2 hours after impact.

For Shot PI-1 the back-up filter of the cascade cyclone was replaced by a parallel-flow diffusion battery (PFDB) to fractionate the sub-micron particles. However, it did not function properly, a problem attributed to leakage, which could not be corrected (the PFDB is a complicated apparatus designed for laboratory use), and for the remaining tests the standard back-up filter was used.

The Phase IV tests were not designed specifically to evaluate DU aerosols, and space for samplers was restricted. Some sampling was carried out in three tests. Typically five CI were attached to mannequins at the driver and loader positions, with the MVF and cyclone in the driver's compartment.

To provide information on particle shape, structure and composition, some samples were analysed by x-ray diffraction (XRD), others by scanning electron microscopy (SEM) and energy dispersive spectroscopy (EDS). To provide material-specific information to characterise absorption of uranium into circulating body fluids from particles deposited in the lungs, *in vitro* dissolution tests were carried out on 27 samples, mainly from the cascade cyclone stages.

Aerosol measurements were also carried out during recovery operations several hours after impact. Some personnel wore personal CI, and for two shots (in Phase I) the loader's sampling array was used. Some personnel also wore cotton gloves, which were measured to provide information for assessing inadvertent ingestion through hand-to-mouth transfer.

Some air sampling was conducted outside the vehicle, using high volume air samplers and CI, but only a few samples were taken in each test. The priority of the study was to obtain information on aerosols within the vehicle, and this determined its location within an enclosure. However, the presence of the enclosure limited the value of aerosol data collected outside the vehicle.

2.3 Respiratory tract deposition

There are four main factors that determine respiratory tract deposition and its variability:

- Aerosol size distribution
- Exercise level and hence ventilation rate
- Breathing mode (nose versus mouth breathing)

* A cyclone, like an impactor, uses inertia to separate the aerosol into aerodynamic size fractions. The air is drawn tangentially into a tapered cylinder, and as the air flows round the circumference, the larger particles impact on the inner surface, from where they fall into a collecting chamber. The air and smaller particles are drawn from the axis of the cylinder to the next stage. Its main advantage over the cascade impactor is its higher capacity: much larger masses can be collected for further study without overloading. Its main disadvantage is that the stage cut-offs are less sharp – there is much more overlap in the particle sizes collected in each stage. It is also bulkier.

- Inter- and intra-subject variability in deposition for a given aerosol size distribution, ventilation rate and breathing mode.

The first three of these are relatively straightforward. The fourth is much more complex, because each respiratory tract region acts as a particle filter in series during inhalation and exhalation. Thus deposition in each affects the amount of aerosol reaching the next region (ICRP, 1994a; Bailey et al, 1997; Guilmette et al, 1998). For this study, it was judged that the most important filters to consider were those of the extrathoracic (ET) airways, because these are the first in the series, deposition is so high in them, and deposition in ET determines the fraction of inhaled aerosol that penetrates to the more radiosensitive lungs.

Appropriate parameter values and ranges are considered in turn below. However, because the analysis here concerns estimates of dose and kidney concentration from a urine sample, rather than an exposure (time integrated air concentration), the total deposition is not of importance, only the relative distribution between regions.

2.3.1 Aerosol size distributions

Measurements of DU aerosol size distributions made following the impact of DU penetrators on armour plate are summarised in Table 6. In all cases cascade impactors (CI) were used, and results were expressed as mass (or activity) median aerodynamic diameter, MMAD or AMAD and geometric standard deviation, GSD. Table 6 is based on a review carried out in support of the RSWG assessment (Bailey, 2002a), which includes a summary of relevant aspects of each report. Table 6 has, however, been updated (as have Tables 14 and 16–18, which relate to dissolution rates and chemical forms). The RSWG assessment concluded that for initial exposure near a target it is reasonable to take MMAD ~2 μm, with a large GSD, ~10 (Table 4), but, at later times or further away to take lower values, ie MMAD 1 μm, with GSD ~2.5, the HRTM defaults for environmental exposure. The AMADs measured by Chazel et al (2003) are consistent with that, although the GSDs are smaller close to the impact.

Table 6 Parameters of log-normal aerosol size distributions from DU penetrator impacts (partly based on Royal Society 2001, Table G2)

Report		MMAD, μm	GSD	"Respirable fraction" (%)*
Reports obtained				
Hanson et al., 1974	Entrance chamber : Exit chamber :	2.1 – 3.3 2.4 – 4.2	1.8 – 3.3 1.8 – 3.1	42 – 64
Glissmeyer and Mishima, 1979		0.8 – 3.1	1.6 – 18	51 – 70
Patrick and Cornette, 1978	†		†	
Chambers et al., 1982		1.6 (1.4 – 2.0)	13 (12 – 17)	~70
Brown, 2000	inside outside	3.7 (1.1 – 7.5) 1.8 (1.3 – 2.7)	3.5 (2.8 – 4.2) 4.1 (3.9 – 4.5)	
Chazel et al, 2003	Glacis shot, outside	1.05	3.7	
	Turret shot, outside	2	2.5	
Capstone: Parkhurst et al 2004b‡	BFV First 10 sec: BFV After 10 sec: Abrams First 10 sec: Abrams After 10 sec: Abrams DU armour First 10 sec: After 10 sec:	0.6 – 4 0.4 – 4 0.2 – 8 0.3 – 7 0.8 – 8 0.1 – 5		
*Reports (restricted distribution) not obtained (OSAGWI 2000, Tab L)***				
Gilchrist et al., 1979	High volume, preferred Low volume	2.1 5.8		

* Here the term "respirable fraction" is used to mean the fraction of the airborne material that is small enough to be readily resuspended and inhaled, i.e., less than about 10 μm d_{ae}, and not, as usually defined for occupational health purposes, to mean the fraction of the aerosol that if inhaled could reach the alveolar region, i.e., the deep lungs. However, different definitions are used in different reports.

† Size distribution was not measured, but a qualitative statement is made that a very wide range size was observed: from fragments >50 μm to submicron.

‡ No concise summary was found in the Capstone Report. These ranges are based on Attachment 1, Table 6.40, which gives results individually for each type of shot and time. BFV refers to Bradley Fighting Vehicle.

**A number of reports relating to DU hazards are cited in documents published by US Government related sources, but are restricted in distribution, and so were not available to the authors. Summaries of several important restricted documents are given in OSAGWI, 2000 Tab L, and provided the information given here.

2.3.1.1 Capstone Study: Level 1 inside vehicle

Far more comprehensive results are available from the Capstone Study (Parkhurst et al., 2004a; 2004b). Table 6.25 of Attachment 1 to Parkhurst et al (2004b), lists AMADs (based on fitted unimodal log-normal distributions) inside vehicles for each shot, sampling position and time after impact. Table 5.25 gives corresponding values of aerosol GSDs. However, it is noted that generally more acceptable fits were obtained using bi-modal rather than single distributions, and in many cases even a bimodal distribution did not fit well. The HHRA made use of the original CI data rather than fitted functions. Nevertheless, fitted log-normal distributions do provide simple measures of the size distributions, which were assumed to be adequate for the present exercise. To obtain relevant representative values, results were selected as follows:

- Phases I and II: i.e. shots fired against conventional (non-DU) armour, since, so far as we know, DU armour is fitted only to US vehicles.
- Measurements made during the first 5 minutes after impact. For vehicles without mechanical ventilation operating, the DU air concentration is much higher during the

first few minutes than subsequently (see e.g. Table S1 of Attachment 1 to Parkhurst et al, 2004b). The RSWG assessment and the HHRA considered exposure durations of 1 and 5 minutes as most likely for personnel in a struck vehicle.

This still gave 84 measurements, which are summarised in Table 7. They are broadly consistent with the RSWG assessment. During the first minute, the AMAD is typically a few microns, and the distributions are wide, with typical GSD about 6. As expected, measurements made during the next few minutes show somewhat smaller AMADs and GSDs, but not dramatically different, and therefore averages are also shown for the full data set (0 – 5 minutes). From this, representative central values and ranges are taken to be AMAD 2.5 μm (range 0.4 – 13 μm) and GSD 6 (range 2 – 15).

Table 7 Measurements of AMAD of DU aerosol after impact of LC-DU penetrator on non-DU armour

	AMAD			GSD		
	Time after impact (minutes)			Time after impact (minutes)		
	0 – 1	1 – 5	0 – 5	0 – 1	1 – 5	0 – 5
No of measurements	35	49	84	35	49	84
Range	0.18-22 (μm)	0.55-41 (μm)	0.18-41 (μm)	2.1-14	1.3-13	1.3-14
Arithmetic mean	4.1 (μm)	3.3 (μm)	3.6 (μm)	7.0	4.8	5.7
Geometric mean	2.7 (μm)	2.0 (μm)	2.3 (μm)	6.5	4.4	5.7
GSD	2.6	2.3	2.4	1.54	1.55	1.6
Upper bound*	18 (μm)	10 (μm)	13 (μm)	15.3	10.5	14.6
Lower bound**	0.41 (μm)	0.38 (μm)	0.38 (μm)	2.7	1.8	2.2

*Based on geometric mean/$(GSD)^2$ **Based on geometric mean x $(GSD)^2$

2.3.1.2 Capstone Study: Level 1 outside vehicle

Relatively few measurements were made with CI outside the vehicle, the priority of the Capstone Study being on exposures inside. Results are given in Table 5.28 of Attachment 1 to Parkhurst et al (2004b). Because they were so difficult to fit with either unimodal or bimodal log-normal distributions using regression analysis, unimodal distributions were also fit using "professional judgement". For the shots in Phases I and II (conventional armour), there are nine sets of results. Parameter values obtained using professional judgement give for AMAD a geometric mean value of 3.0 μm (range 1 – 9 μm) and for GSD a geometric mean value of 5 (range 1.5 – 16). These are similar to those obtained inside the vehicle (Section 2.4.1.1.).

2.3.1.3 Capstone Study: Level 2 inside vehicle

Measurements were made using one of the sampling arrays during recovery operations following shots PI-6 and PI-7. Results are given in Table 5.27 of Attachment 1 to Parkhurst et al (2004b). (In addition, two recovery personnel wore CI, but the results were not analysed for size distribution.) There are 13 sets of results, which for AMAD give a geometric mean value of 2.7 μm (range 1 – 17 μm) and for GSD a geometric mean value of 6 (range 2 – 11). These are again similar to those obtained inside the vehicle directly after impact (Section 2.4.1.1.).

2.3.1.4 Aerosol size parameter values and ranges

Based on all the discussion above, it seems reasonable to use the most comprehensive data set, i.e. the measurements made inside vehicles in the Capstone study (Section

2.4.1.1). The other, more limited sources are consistent with it. Thus, representative central values and ranges are taken to be AMAD 2.5 μm (range 0.4 – 13 μm) and GSD 6 (range 2 – 15) for both Level I and Level II scenarios.

2.3.1.5 Aerosol size parameter distributions

For the AMAD, based on the information above, a log-normal probability density function (PDF) with a median of 2.3 μm and GSD of 2.4 was adopted, which gives a symmetric 95% probability range over the interval 0.4 to 13 μm.

Similarly, for the aerosol GSD, a log-normal probability density function (PDF) with a median of 5.7 and GSD of 1.6 was adopted, which gives a symmetric 95% probability range over the interval 2.2 to 14.6, which is consistent with that above (2 – 15).

2.3.2 Exercise level and ventilation rates

The Commission of the European Communities (CEC) and the United States Nuclear Regulatory Commission (USNRC) conducted a joint project to assess uncertainties in the results of Accident Consequence Assessment (ACA) codes. One phase of this project established uncertainty distributions over the major relevant parameters in health effects models, using panels of experts. Panel members provided estimates of the median, 5-percentile and 95-percentile values of selected parameters, using expert judgement, and documentation to support their judgements. NRPB-M763 (Bailey et al, 1997) gives documentation in support of the judgements made by one member of the Expert Panel on Internal Dosimetry (M R Bailey). The following is largely based on Bailey et al (1997), which gives further details. Note, however, that Bailey et al (1997) were estimating the uncertainty in the central value of each parameter, ie, the uncertainty in the population mean value, rather than intersubject variation about that mean. Furthermore, emphasis was placed on the ventilation rate, because for a prospective study, the ventilation rate has a much greater effect on intake (which is directly proportional to it), than on the deposition pattern (ICRP, 2002).

2.3.2.1 HRTM approach

The ventilation rate (i.e., the volume of air inhaled per unit time) is the more important of the two main factors that relate exposure (time-integrated air concentration, Bq s m^{-3}), to intake in Bq. The other factor is inhalability (also known as aspiration efficiency), which is the ratio of the particle concentration in the air entering the respiratory tract to that in the ambient air. The inertia of particles larger than a few microns increases the concentration in the air entering the nose or mouth when facing into a wind, and reduces it otherwise, the average net effect being to reduce it to about half that in the ambient air. Inhalability is here considered with deposition, as it is in the HRTM.

The approach taken in the HRTM is described in detail in Annexe B (Respiratory Physiology) of ICRP Publication 66 (1994a). It follows that taken previously by ICRP in its report on Reference Man (ICRP, 1975). Reference levels of physical exercise are defined, in this case four: sleep, sitting, light exercise (LE), and heavy exercise (HE). Exercise levels for adult males were chosen as follows:

- Light exercise: one-third of highest work load completed (W_{max} measured by Godfrey et al, 1971). This corresponds to working in laboratories and workshops; active house cleaning; painting, woodworking, etc.
- Heavy exercise: two-thirds of W_{max}. Firemen, construction workers, farmers, athletes, etc might spend up to 2 hours per day at this level.
- For each reference subject, reference values were determined from review of the literature, for the primary quantities: breathing frequency (f_R) (breaths per minute) and ventilation rate (B) (m^3 h^{-1}) for the four reference levels of exercise. (The breathing frequency is required as an input to the deposition model, as is the ventilation rate). Values for adults are shown in Table 8 (V_T is tidal volume).

Table 8 Ventilation parameters for adults (based on ICRP 1994a, Table B.15)

	Sleep			Sitting		
Maximum workload, %:	8			12		
Breathing Parameters	f_R (min^{-1})	V_T (L)	B (m^3 h^{-1})	f_R (min^{-1})	V_T (L)	B (m^3 h^{-1})
Male	12	0.625	0.45	12	0.75	0.54
Female	12	0.444	0.32	14	0.464	0.39
	Light exercise			Heavy exercise		
Maximum workload, %:	32			64		
Breathing Parameters	f_R (min^{-1})	V_T (L)	B (m^3 h^{-1})	f_R (min^{-1})	V_T (L)	B (m^3 h^{-1})
Male	20	1.25	1.5	26	1.923	3.0
Female	21	0.992	1.25	33	1.364	2.7

Central values and confidence intervals on mean ventilation rates estimated by Bailey et al (1997) are shown in Table 9 (converted from L per minute to m^3 h^{-1}). The ICRP values (Table 8) were taken for the central values.

Table 9 Uncertainty in mean ventilation rates (m^3 h^{-1})

	Male			Female		
	x_5	x_{50}	x_{95}	x_5	x_{50}	x_{95}
Sleep	0.36	0.45	0.78	0.27	0.32	0.54
Sitting	0.48	0.54	0.90	0.33	0.39	0.66
LE	1.32	1.50	2.70	0.84	1.25	1.80
HE	1.80	3.00	4.80	1.80	2.7	3.00

Hofmann et al (2001) measured f_R and V_T in a group of 11 young non-smoking subjects breathing spontaneously at rest. Mean values: f_R = 14.6 per minute; V_T = 0.66 L, were similar to the ICRP values for males (Table 8), although the group included males and females. There was much greater variation in f_R (range 8-27 per minute), than in V_T (range 0.46 – 0.90 L). Minute volumes gave a mean of 9.8 L, and range of 4.3 – 16.2 L, corresponding to ventilation rates of 0.59 (0.26 – 0.97 m^3 h^{-1}).

Heyder et al (1982) studied intersubject variation in total deposition of inhaled particles during (i) controlled breathing (ii) spontaneous breathing at rest (iii) spontaneous

breathing after exercise (running up and down three flights of stairs). Although individual values of f_R and ventilation rate were not reported, some inferences can be drawn. For spontaneous breathing at rest the mean period of a breathing cycle was 4.3 s, with an individual range of 2.8 – 5.6 s. This gives a mean value of f_R of 14 per minute (similar to Table 8 for sitting) and a range of 10.7 – 21 per minute. After exercise, the mean period of a breathing cycle was 3.6 s, with an individual range of 2.4 – 4.8 s, giving a mean value of f_R of 17 per minute and a range of 12.5 – 25. These are only about 20% greater than at rest. Conversely, the mean flow rate after exercise was nearly three times higher than at rest. Thus the main effect of exercise observed was to increase the tidal volume. This differs from the ICRP values (Table 8), which show similar increases in the two parameter values.

2.3.2.2 Breathing parameter values and ranges

Based on the above, for this exercise, we take the ICRP values of ventilation rate and frequency for light and heavy exercise to be central values for Level II and Level I exposures, respectively. We assume that the breathing rate could be a factor of two higher or lower, that variability in the frequency and tidal volume are correlated (high frequency corresponds to high tidal volume) and contribute equally, i.e., variation in each is a factor of 1.4, giving the ranges shown in Table 10.

Table 10 Estimated ranges in breathing parameter values

	Light Exercise (Level II)			Heavy Exercise (Level I)		
	Minimum	Mean	Maximum	Minimum	Mean	Maximum
B (m^3 h^{-1})	0.75	1.5	3	1.5	3	6
f_R (per minute)	14	20	28	19	26	36
V_T (L)	0.9	1.25	1.8	1.3	1.9	2.8

2.3.2.3 Breathing parameter distributions

For the ventilation rate, B, it was assumed that the subjects were equally likely to be undertaking either light or heavy exercise during exposure. To derive the PDF for ventilation rate, 10^4 variates were generated using a Latin Hypercube sampling method (McKay et al 1979), from each of two log-normal distributions with medians of 1.5 and 3 m^3 h^{-1} and GSDs of 1.4. The $2x10^4$ variates were then combined to give a new distribution. Although not log-normal itself, it was found that this distribution could be approximated by a log-normal distribution with a median of 2 m^3 h^{-1} and GSD of 1.6.

For the breathing frequency it was assumed that f_R was 100% linearly correlated with B, according to the following relationship:

$$f_R = 4B + 13$$

This relationship was determined by linear regression of f_R on B using the combined minimum, central and maximum values for B and f_R for light and heavy exercise in Table 10. Tidal volume was calculated from B and f_R.

2.3.3 Breathing mode

Since the filtration efficiencies of the nose and mouth are different, a subject's breathing mode (fraction of inhaled air passing through the nose, F_n) affects the amount of inhaled material that deposits in ET and in the lungs. Niinimaa *et al*, (1980, 1981) found that, in studies of 30 healthy young adults, 20 subjects ("normal augmenters") switched to oro-nasal breathing, typically at a ventilation rate of about 2.1 m^3 h^{-1} (i.e., between light exercise and heavy exercise). Five subjects ("nose breathers") continued to breathe through the nose even when exercising vigorously. Four subjects, who were habitual "mouth breathers", breathed oro-nasally (through the nose and mouth together) at all levels of exercise. The remaining subject showed no consistent pattern. Malarbet *et al*, (1994) conducted studies similar to those of Niinimaa *et al*, and found broadly similar results in adults. For this exercise the normal augmenters are taken for the central estimate, and habitual nose- and mouth-breathers are taken to give ranges.

In accordance with a review by Miller *et al*, (1988), the HRTM uses the distribution of air between nose and mouth measured by Niinimaa *et al*, for "normal augmenters", and "mouth-breathers", as given in Table 11.

Table 11 Percentage of total ventilatory airflow passing through the nose in normal nasal augmenters (nose breathers) and in mouth breathers (ICRP Publication 66, Table 11)

	F_n, %		
Level of exercise	Normal nasal augmenter	Mouth breather	Nose breather
Sleep	100	70	100
Rest (sitting)	100	70	100
Light exercise	100	40	100
Heavy exercise	50	30	100

2.3.3.1 Breathing mode distribution

To derive a PDF for F_n, the distribution of breathing mode types, based on the volunteers studied by Niinimaa *et al* (1980, 1981) was assumed to consist of 20 normal augmenters, 4 mouth breathers and 5 nose breathers. Taking the F_n values for light and heavy exercise from Table 11, and assuming that subjects exposed to DU were equally likely to have been in light or heavy exercise during exposure, the following F_n values are obtained (fraction of time spent in breathing mode in parentheses): F_n =0.3 (0.07), F_n =0.4 (0.07), F_n =0.5 (0.34), F_n =1 (0.54). A right-angled triangular distribution with minimum at 0.2 and vertex at 1 was considered a reasonable representation of the data.

2.3.4 Intersubject variation in nasal deposition efficiency

In the HRTM (ICRP 1994a), aerosol deposition in the compartments ET_1 and ET_2 is modelled by two mathematical filters (for aerodynamic and thermodynamic deposition mechanisms) which determine the amounts of aerosol deposited in these regions during inhalation and exhalation. ICRP Publication 66 (ICRP 1994a) states that intersubject variation in the deposition efficiency of each filter can be modelled by multiplying the constant *a*, given in the equations for the deposition filters in Table 12 of ICRP Publication 66 (ICRP 1994a), with variable *c*. The variation in the deposition efficiency of the ET regions can be achieved by assigning to *c* values of 3.3 or 3.3^{-1}, for the

aerodynamic filter, and 1.4 or 1.4^{-1} for the thermodynamic filter. This process was modelled in the present investigation by assigning to *c* a log-normal distribution with a median of 1 and GSD of $3.3^{1/2}$ (aerodynamic) or $1.4^{1/2}$ (thermodynamic). The ET_1 and ET_2 filters were scaled independently, and thus four values of *c* were randomly generated during each Monte Carlo calculation.

PDF of parameter *c*:

Aerodynamic filter: Log-normal (median=1, GSD=1.82).

Thermodynamic filter: Log-normal (median=1, GSD=1.18).

2.4 Particle transport from the respiratory tract

The HRTM particle transport clearance model is described in Section 2.2.4 (Figure 5 and Table 1). The derivation of each of the corresponding parameter values is described in detail in ICRP Publication 66 Annexe E (Bailey and Roy, 1994). Consideration is given to uncertainty in each central value, intersubject variation, and modifying factors (e.g. lung disease). Bailey et al (1997) give a similar discussion, with some updating. The overall approach, described in Section E 1.1 of ICRP Publication 66 Annexe E is outlined below here (Sections 2.4.1 to 2.4.3).

As far as possible these parameter values were based on observations on humans, since particle transport rates are known to vary markedly between species. Ideally each value would be based on carefully conducted studies designed to measure that parameter. The uncertainty in the reference value would then be given by the 95% confidence interval on the mean and the variability by the 95% limits on intersubject variation. However, few human lung clearance parameters have been measured directly in this way.

2.4.1 Variability

Three clearance rates for which the distributions have been obtained in humans are identified: mucociliary transport in the posterior nasal passage; mucociliary transport in the trachea; and alveolar clearance at 200 d after inhalation. In each case most measurements conformed well to a log-normal distribution, with similar geometric standard deviations (GSD): 1.6, 1.8, and 1.7, respectively. (Note, however, that, for nasal and alveolar clearance, about 20% of cases showed clearance slower than predicted by such a distribution.) It is not surprising that a similar degree of variation should be seen in mucociliary clearance rates in the nasal passage and trachea, since similar mechanisms are involved. It is interesting, however, that a similar distribution occurs for alveolar clearance, which is determined by the behaviour of alveolar macrophages. This result gives support to the proposition, made below, that a similar distribution be assumed for those clearance rates that have not been measured directly.

For a log-normal distribution with median x_{50}, approximately 95% of values lie between x_{50}/GSD^2 and $x_{50}.GSD^2$. The observed distributions of human particle transport rates suggest a typical value for GSD of 1.7, and hence a value for GSD^2 of about 3. It is therefore proposed in ICRP Publication 66 that, in the absence of specific information,

intersubject variation in any clearance rate be represented by a log-normal distribution with x_{50} equal to the reference value, and GSD = 1.7. This gives 95% confidence limits at $x_{50}/3$ and $3x_{50}$.

2.4.2 Uncertainty

It is recognised that in general, the reference values for particle transport rates are based on indirect information and their choice involved a considerable element of judgement. The combination of a high degree of intersubject variation and possible systematic errors means that the uncertainties in the reference values are large and difficult to quantify. It was therefore assumed that the uncertainty in the reference value is log-normally distributed, and thus that there is a 95% probability that the true mean value lies within a factor Φ_u of the chosen reference value. The values selected for Φ_u depended on the quality of information available, and are in general derived in the relevant sections of ICRP Publication 66 Annexe E. For the majority of rates, Φ_u was taken to be 3, but for a few rates lower values were estimated, e.g. rapid clearance from BB and bb (Φ_u = 1.5, Φ_u = 2 respectively) (Bailey and Roy, 1994).

2.4.3 Modifying factors

As discussed in ICRP Publication 66 Annexe E, the effects of many factors on respiratory tract clearance rates have been investigated, notably age, diseases, pharmacological agents, and air pollutants. The most frequently studied factors are smoking (both acute and chronic effects) and respiratory disease; the most common endpoints have been mucociliary clearance from the nasal passage or tracheobronchial tree. However, while effects have often been observed, the results are usually qualitative, i.e., an increase or (more often) a decrease in clearance. Only in a few cases, do sufficient data exist to enable the effect on a clearance parameter to be quantified. In such cases, a modifying factor Φ_m is given in ICRP Publication 66, Table 19. Such factors were proposed for:

- the "fast" phase of particle transport from the BB and bb regions (compartments BB_1 and bb_1), decreases due to several lung diseases, cigarette smoking, and sleep
- the AI region, a decrease due to cigarette smoking only.

Proposed values of Φ_m were generally between 0.3 and 0.7.

2.4.4 Model uncertainties

For two aspects of the model there are recognised uncertainties that go beyond uncertainty in a parameter value, and relate to the model structure.

2.4.4.1 Clearance from the nasal passage

The HRTM assumes that of material deposited in the extrathoracic (ET) airways, about 50% is deposited in ET_1 (the front of the nose), which is cleared by nose blowing at a rate of 1 d^{-1}, and the rest is deposited in ET_2 (back of nose, pharynx, etc.), which clears to the GI tract at a rate of 100 d^{-1}. However, there was little information available in

1994 to characterise clearance from ET_1. Recent experiments (Smith, 2003) have shown that for 1–6 μm particles, of the material deposited in ET:

- only about 15% deposits in ET_1 and is cleared by nose blowing (in about a day)
- about 60% deposits in ET_1 and is cleared to the GI tract (via ET_2) on a time-scale of hours to days
- the remaining 25% deposits in ET_2 and is cleared to the GI tract in about 10 minutes.

These results are consistent with earlier observations, but provide the additional information needed to quantify the behaviour more realistically. However, the sensitivity analysis (Section 4.1 below) showed that variations in particle transport rates from the nose had little effect on either doses per unit intake or assessments of doses from urine sample measurements. The considerable effort that would be required to implement this model change in the software was therefore not justified for this project.

2.4.4.2 Clearance from bronchial and bronchiolar airways

The HRTM assumes that a size-dependent fraction (50% below 2.5 μm geometric diameter, and decreasing with size above 2.5 μm) of particles deposited in the bronchial (BB) and bronchiolar (bb) regions clears with a half-time of about 20 d, much slower than traditionally assumed for particle clearance from the bronchial tree (Figure 5 and Table 1). This was mainly based on a series of experiments in which subjects inhaled radiolabelled particles as a small ('shallow') bolus at the end of each breath. Its inclusion in the HRTM has a significant effect on inhalation doses for some important radionuclides, including moderately soluble uranium, but it remains controversial (Bailey et al, 1995).

In a recent series of human studies carried out in collaboration between the Karolinska Institute, Sweden and the Swedish Radiation Protection Institute (SSI), large (6-μm aerodynamic diameter, d_{ae}) particles were inhaled extremely slowly (Anderson et al, 1995; Falk et al, 1997, 1999; Philipson et al, 2000; Svartengren et al, 1995; 2001). Theoretically most particles should be deposited in the bronchioles under these conditions. It was found that the fraction of particles retained at 24 hours after deposition (R_1) was much greater than the fraction of particles predicted to deposit in the alveolar region, supporting the view that there is a significant slow clearance phase from the conducting airways. However, the results suggest that the slow-cleared fraction is a function of the particles' aerodynamic properties and hence their site of deposition, rather than their geometric size (Philipson et al, 2000). Furthermore, when clearance was followed for 6 months after administration, lung retention (as a fraction of R_1) could be well represented by a two-component exponential function with half-times of about 4 days (35%) and 200 days (Falk et al, 1999). When 6-μm d_{ae} particles were inhaled at a normal rate, a much smaller fraction was associated with the 4-day component. The KI and SSI groups interpret the findings as indicating that the slow phase of clearance from TB (the 4-day component) represents clearance from the smaller bronchioles (Svartengren et al, 2001).

More recently, experiments have been carried out at HPA-RPD to address this issue directly (Smith et al 2007a, 2007b). Participants inhaled a shallow bolus containing

polystyrene particles labelled with indium-111, and gold particles labelled with gold-198. The particles have the same d_{ae} (5 μm in the first set of experiments and 8 μm in the second set), and so their deposition patterns in the respiratory tract should be the same. However, because of the large difference in densities (1.05 g cm^{-3} for polystyrene, and 19 g cm^{-3} for gold) their geometric diameters are 5 and 1 μm respectively, and the slow cleared fractions assumed by the HRTM are 0.1 and 0.5 respectively. For each subject, clearance of the two particles was very similar, supporting the Swedish interpretation, rather than the HRTM.

Further studies are in progress to develop a revised model of slow clearance from the bronchial tree, based on these new observations, as well as the original bolus studies. For the purpose of this exercise a simple alternative model has been applied, based on the Swedish interpretation. For simplicity, this model is referred to here as the KI Model, and it is assumed that:

- in the bronchiolar (bb) region all particles are cleared slowly to the BB region at a rate of 0.2 d^{-1} ($t_{½}$ ~3.5 d) (except for the small, 0.7%, sequestered fraction, as in the HRTM, Figure 5).
- in the bronchial (BB) region there is no slow clearance, and all particles are cleared to GI tract by mucociliary action at a rate of 10 d^{-1} (except for the small, 0.7%, sequestered fraction, as in the HRTM, Figure 5)

Table 12 shows the particle transport clearance rates for the bronchial tree in the HTRM (taken from Table 1) and the corresponding rates to implement the simple alternative KI model.

Table 12 Median values of parameters for particle transport clearance from the bronchial (BB) and bronchiolar (bb) regions (see Figure 5 and Table 1)

Clearance rates				
			Rate, d^{-1}	
Pathway	From	To	HRTM	KI Model
$m_{4,7}$	bb_1	BB_1	2	**0.2**
$m_{5,7}$	bb_2	BB_1	0.03	**0.2**
$m_{6,10}$	bb_{seq}	LN_{TH}	0.01	0.01
$m_{7,11}$	BB_1	ET_2'	10	10
$m_{8,11}$	BB_2	ET_2'	0.03	**10**
$m_{9,10}$	BB_{seq}	LN_{TH}	0.01	0.01

2.4.5 Particle transport parameter values and ranges

Observed intersubject variability suggests that a reasonable range is to take a factor of three either side of the central value. Similar, or somewhat lower, factors apply to uncertainties in the central value and most quantifiable modifying factors. For simplicity, a range of a factor of three either side of the central value is taken here.

2.4.6 Particle transport parameter distributions

Based on the information above, it was assumed that variation in any clearance rate could be represented by a log-normal distribution with median equal to the reference value, and GSD = 1.7. For simplicity, it is assumed that all particle transport rates are correlated, i.e. all rates are increased or decreased by a factor of three. This is likely to result in some overestimation of the range, but to some degree offsets the underestimation resulting from not combining distributions in all three factors (uncertainty, variability and modifying factors). It seems reasonable to expect some correlation, since similar mechanisms (mucociliary action, macrophage mobility) are involved in more than one pathway. Andersen et al (1974) made direct comparisons of nasal and bronchial clearance rates in the same subjects. They found a correlation, but only a weak one. Furthermore, the sensitivity analysis (Section 4.1 below) showed that variations in most particle transport rates (except those relating to slow bronchial clearance) had little effect on either doses per unit intake or assessments of doses from urine sample measurements.

For the uncertainty analysis all particle transport rates were multiplied by a random variable *c* taken from a log-normal distribution (median=1, GSD=1.7). To take account of the alternative ('KI') model of slow clearance in the bronchial tree, it was considered equally probable that the median rates were either the values adopted in the HRTM (ICRP 1994a) and given in Table 1, or the KI rates proposed in Section 2.4.4.2 (Table 12). To achieve this in the Monte Carlo simulations, the HRTM rates or the KI Model rates were randomly selected as the median values prior to multiplying them by the factor *c*. This was engineered so that exactly half of all calculations were performed with either the HRTM rates or the KI Model set of rates.

PDF of scaling factor *c*: Log-normal (median=1, GSD=1.7)

2.5 Absorption to blood from the respiratory tract

The representation of absorption to blood in the HRTM is described in Section 2.2.4 (Figure 6 and Table 2). There are two routes by which information can be used to assess absorption parameter values for relevant forms of DU:

- direct measurements on DU formed from penetrator impacts or in fires
- determination of the chemical forms of uranium produced, combined with information relating to those forms.

For use with the HRTM, it is necessary to estimate values of three parameters (Figure 6):

- the fraction that dissolves rapidly, f_r
- the dissolution rate of the rapid fraction, s_r, d^{-1}
- the dissolution rate of the slow fraction, s_s, d^{-1}

These are easily obtained from *in vitro* tests where the undissolved fraction is expressed as a two-component exponential function. However, determination from the results of *in vivo* studies requires application of an appropriate model to assess values from the results, which will typically be of excretion rates and organ contents at a limited number of times after administration.

2.5.1 Direct measurements of dissolution of DU formed from penetrator impacts

In several studies measurements have been made of the rate of dissolution of particles formed from the impact of a DU penetrator on armour plate, in a medium designed to be a simulant of the fluid present in the lungs, with which the particle might be in contact after inhalation. Such "*in vitro* dissolution" tests have a number of advantages over *in vivo* studies, in which particles are deposited in the lungs of laboratory animals, including cost and ease of interpretation, and so are more frequently used. However, dissolution rates, like chemical reaction rates in general, are potentially very sensitive to conditions, and therefore great care is needed to be reasonably sure that the results are representative of dissolution in the human lungs. The advantages and disadvantages of *in vitro* and *in vivo* methods to determine dissolution *in vivo* are discussed in ICRP (2002).

Results are summarised in Table 13. In a recent study by Mitchell and Sunder (2004) material was administered to rats. However, only rough estimates of f_r and s_s can be made from the results. Although it has the merit of being an *in vivo* study, it is of little value for this analysis, because of factors including lack of information about the material, its large particle size, and the short duration of measurements. All other measurements of DU penetrator impact aerosols were made *in vitro*, and used broadly similar procedures. Again, by far the most comprehensive results come from the Capstone Study (Parkhurst et al., 2004b: summarised in its Attachment 1, page 5.70, with full details in Appendix E), which are therefore considered here in some detail. Dissolution in simulated lung fluid was measured for 46 days on 27 samples. Most of these were obtained using a cascade cyclone, or 'cyclone train': a series of cyclones, which collected progressively smaller aerodynamically sized fractions. Time-dependent retention of undissolved DU was fitted by two- and/or three-component exponential functions. Table 14 summarises the parameters of the fitted functions.

Table 13 Dissolution characteristics of material formed from DU penetrator impacts (Partly based on Table G3 of Royal Society, 2001)

Report	Fraction dissolved rapidly (%)	Dissolution rate of the rapid fraction, d^{-1}	Dissolution rate of the slow fraction, d^{-1}	Duration of measurements, d
Reports obtained				
Glissmeyer and Mishima, 1979	43 (34 – 49) respirable 15 (11 – 18) total	–	<0.01 <0.01	28
Scripsick et al., 1985a,b	25 (air filter) respirable 4 (core sample) respirable	4.7 1.7	0.004 0.0014	~30
Chazel et al, 2003	47 (glacis) 57 (turret)	0.06 0.07	0.00018 0.00034	30
Mitchell and Sunder, 2004	~5	~1	–	7
Capstone: Parkhurst et al 2004b	1 – 28	0.1 – 30	0.0004 – 0.0095	46
*Reports (restricted distribution) not obtained (OSAGWI 2000, Tab L)**				
Jette et al., 1990	24 – 43 "Class D"	–	–	?
Parkhurst et al., 1990	17 "soluble"	–	–	?

* A number of reports relating to DU hazards are cited in documents published by US Government related sources, but are restricted in distribution, and so were not available to the authors. Summaries of several important restricted documents are given in OSAGWI, 2000 Tab L, and provided the information given here.

Table 14 Results of *in vitro* dissolution tests carried out in the Capstone Aerosol study

				Two-component			Three-component exponential retention function						
Phase	Shot	Sample Description	Fig	A_1(%)	B_1 (d^{-1})	B_2 (d^{-1})	A_1(%)	B_1 (d^{-1})	A_2(%)	B_2 (d^{-1})	B_3 (d^{-1})	R(30) %	R(180) %
I	2	driver IOM filter, sampling period 1	E.2	7.8	2.1	0.0014	4.7	5.7	4.7	0.18	0.00091	88.2	76.9
I	2	driver IOM filter, sampling period 3	E.3	13.8	2.4	0.0033	8	8.2	8.8	0.2	0.0022	77.9	56.0
I	2	driver IOM filter, sampling period 4	E.4	18.5	4.1	0.0034	14.9	6	7.5	0.14	0.0018	73.6	56.1
I	2	driver IOM filter, sampling period 6	E.5	13.6	1.9	0.0028	8.3	5	8.7	0.15	0.0016	79.2	62.2
I	2	driver IOM filter, sampling period 7	E.6	9.2	3.9	0.0039	7.2	6.2	4.2	0.13	0.0032	80.6	49.8
I	2	cyclone stage 2	E.7	13.9	13.7	0.0014	12.8	17.1	3	0.14	0.00073	82.4	73.8
I	3/4	cyclone stage 3	E.8	27.5	11	0.0069	22.3	21.7	13.5	0.15	0.0032	58.5	36.1
I	3/4	cyclone stage 4	E.9	21.6	26.1	0.0080	20	31.5	21	0.043	0.0021	61.2	40.4
I	3/4	cyclone stage 5	E.10	27.2	31.7	0.0095	21.1	63	8.2	1.9	0.0084	55.0	15.6
I	3/4	cyclone back-up filter	E.11	1	25.7	0.0009						96.5	**84.8**
I	7	cyclone stage 1	E.12	28.2	4.1	0.0033	24.9	5.1	10.2	0.084	0.00067	64.4	57.5
I	7	cyclone stage 2	E.13	11.8	14.2	0.0018	10.2	21.8	5	0.11	0.00062	83.4	75.8
I	7	cyclone stage 3	E.14	25.9	4.5	0.0006	18.1	11.4	12.9	0.21	0.0025	64.0	44.0
I	7	cyclone stage 4	E.15	25.7	8.1	0.0050	20.1	16.2	10.9	0.19	0.0026	63.9	43.2
I	7	cyclone stage 5	E.16	21.9	21.8	0.0059	19.5	29.2	12	0.083	0.0024	64.7	44.5
I	7	cyclone back-up filter	E.17	10.5	4.2	0.0019	6.8	14.5	6.4	0.19	0.001	84.3	72.5
II	1/2	cyclone stage 2	E.18	18.9	6.7	0.0033	17.4	7.8	4.7	0.091	0.0022	73.2	52.4
II	1/2	cyclone stage 3	E.19	19.8	6.6	0.0039	13.2	15.8	7.6	1.1	0.0035	71.3	42.2
II	1/2	cyclone stage 4	E.20	27.1	6.4	0.0068	25.6	7.1	16.8	0.039	0.0024	58.8	37.4
II	1/2	cyclone stage 5	E.21	27.6	10.5	0.0066	26	12.2	11.2	0.055	0.0034	58.9	34.1
II	1/2	cyclone back-up filter	E.22	15	6.7	0.0029	14	7.7	8.8	0.039	0.001	77.6	64.5
III	2	cyclone stage 4	E.23	4	1.8	0.0013	2.7	3.8	7.5	0.044	0	91.8	**89.8**
III	2	cyclone stage 5	E.24	4.6	2.8	0.0024	4.6	2.8	80	0.0029	4E-17	88.7	62.9
III	2	cyclone back-up filter	E.25	11	3.9	0.0014	9.8	4.8	4.5	0.061	0.00041	85.4	79.6
I	1	PFDB screen assembly 7	E.26	20.5	0.084	0.0014	3.1	2.9	24.6	0.049	0.0000031	77.9	72.3
I	5	DU cone bulk powder	E.27	1.4	6.2	0.0004						97.4	**91.6**
I	5	DU cone size separated	E.28	6.3	16.2	0.0015	5.7	20.7	1.3	0.23	0.0013	89.4	73.6
												TypeF<13	TypeS>84
		Geometric mean		12.5	5.7	0.0026	11.3	10.1	8.6	0.1			

IOM = Institute of Medicine personal air sampler.

Based on the two-component fits, values of the rapid fraction, f_r, ranged from 1% to 28%, broadly similar, but somewhat lower in range than in the previous studies (4%–57%, Table 13). Values of the slow dissolution rate, s_s, ranged from 0.0004 to 0.0095 d^{-1}, broadly similar, but somewhat higher in range than the previous studies (0.0002 to 0.004 d^{-1}, Table 13). Thus there was considerable variation between samples, especially in the fraction that dissolved rapidly. There appeared to be some correlation between the initial and final dissolution rates: the higher the dissolution in the first day, the faster the long term dissolution rate.

In the Capstone Report the dissolution characteristics were compared with both the ICRP Publication 30 lung model defaults (Classes D, W and Y) and HRTM defaults (Types F, M, S). For the former, each sample tested was assigned proportions to each Class (Parkhurst et al., 2004b, Table 5.37). For the latter, the Capstone Report notes qualitatively that most samples resemble Type M, but some (e.g. PI-3/4 cyclone back-up filter, and the "DU cone") Type S. It points out (Appendix E, page E.11) that such variation is not surprising given the heterogeneity of both physical and chemical forms of the uranium-containing aerosols. ICRP Publication 71 (ICRP, 1995a) gives quantitative criteria for assigning materials to Types F, M and S. Based on these criteria, for *in vitro* dissolution tests, a material would be assigned to Type F if the amount remaining undissolved at 30 days was less than 13%, and to Type S if the amount remaining undissolved at 180 days was more than 84%. Otherwise it is assigned to Type M. These amounts are given in Table 14 (calculated here from the fitted functions: the amounts at 180 days are predicted values, since the tests stopped at 46 days). On those criteria, no samples would be assigned to Type F, but in addition to the two identified in the Capstone Report, PIII-2 cyclone stage 4 would be assigned to Type S. The rest would be assigned to Type M. Note, however, that comparisons with the ICRP default values are only to put the results in perspective: the specific parameter values are used here.

The Capstone report noted that the absence of Type F behaviour suggested that the conditions were not conducive to the formation of highly oxidised forms of uranium such as UO_3 or UO_4. However, it also notes the possibility that further oxidation could occur as a result of weathering, and therefore the results apply "directly to exposures that occur relatively soon after a DU impact event (minutes to weeks)" (Parkhurst et al., 2004b Attachment 1, Page 5.70).

Discussion in Appendix E (Parkhurst et al., 2004c) considers the effect of particle size, and is summarised below here. The simplest assumption is that dissolution at the particle surface is the rate-determining step. In that case, the dissolution rate depends on specific surface area (SSA), ie, the fractional dissolution rate should increase with decreasing particle size (Mercer, 1967).

Sets of cyclone stage data were measured from 4 shots (Table 14, and shown in detail in Parkhurst et al., 2004c Figs E.29-E.32):

- PI-3/4 Stages 2, 3, 4, 5, back-up.
- PI-7 Stages 1, 2, 3, 4, 5, back-up.
- PII-1/2 Stages 2, 3, 4, 5, back-up.
- PIII-2 Stages 4, 5, back-up.

If the dissolution rate increases with SSA, the rate should increase with increasing stage number, and be highest for the back-up filter, which collects the smallest particles. However, this is not apparent from the cyclone samples.

- PI-3/4 dissolution rate: back-up <2 <3,4 <5. The back-up filter is slowest, but in theory should be fastest.
- PI-7 dissolution rate: back-up, 2 <1,3,4,5. Similar to PI-3/4. The main difference between samples is in the rapid fraction. The long-term rates were all similar.
- PII-1/2 dissolution rate: back-up, <2,3 <4,5. As above. Back-up low, but others as expected. Main difference in rapid fraction.
- PIII-2 dissolution rate: Stage 4 <5 <back-up, as expected.

The five Institute of Medicine personal air sampler (IOM PI-2 driver position) samples were collected in sequence (1) 5-35 sec; (3) 1.30-3.30 min; (4) 3.30-7.30 min; (6) 15.30-31.30 min; (7) 32.30-60.30 min; and would therefore be expected to have sequentially smaller particles, as the larger ones were removed by sedimentation. Hence the dissolution rates were expected to be in the order 1<3<4<6,7, but the observed rates (Fig E.33, Table E.4) were 1<3,6,7<4: the order appears almost random.

Two tests were carried out on the “Cone sample”, the “DU cone”, which was formed when a metal fragment ignited and burned on the floor of the Abrams BHT following Shot PI-5, and was almost entirely DU oxide. It is therefore more relevant to combustion than penetrator aerosols. “Unseparated” was bulk powder, and “Separated” was size-segregated by sedimentation in alcohol. “Separated” had both a larger rapid fraction and higher slow rate, consistent with sedimentation removing larger particles, and size-dependent dissolution.

Thus there was no clear trend of dissolution with particle size. The Capstone Report noted that two confounding factors were:

1) cyclone cut-offs are not sharp, so there was considerable overlap in size distribution between stages.
2) heterogeneity of particle composition, shape etc. A review of SEM results showed several distinctly different forms of uranium-bearing particle.

The effect of the target was also considered, by comparing the same cyclone stage from different shots (Parkhurst et al., 2004c, Figs E.35-E.39). However it was concluded that there were conflicting findings, and overall, it was “difficult to discern consistent trends”.

Although comprehensive, the results of the Capstone Study have some limitations. The dissolution tests ran for 46 days, at which time most of the material remained undissolved, and so the results have to be extrapolated in time. The main limitation however, is that the dissolution tests were all carried out *in vitro*, and there is no discussion in the Capstone reports of potential problems of extrapolation of the results to the human lungs.

2.5.2 Direct measurements of dissolution of DU formed in fires

There have been a number of studies relating to the effects of fire on DU munitions and penetrators, to address concerns about fires during storage or transport. In several,

measurements were made of dissolution *in vitro*, which as noted above, should be treated with caution. Results are summarised in Table 15. The rapid fraction is typically a few percent, and the slow rate of the order of 0.001 d^{-1}, both broadly similar to the results for penetrator impact aerosols.

Table 15 Dissolution characteristics of material formed from combustion of uranium (Partly based on Table H4 of Royal Society, 2001)

Report	Fraction dissolved rapidly (%)	Dissolution rate of the rapid fraction, d^{-1}	Dissolution rate of the slow fraction, d^{-1}	Duration of measurements, d
Reports obtained				
Mishima et al 1985	0.5 (<10 μm d_{ae})	–	0.0005	60
Scripsick et al 1985a	6 – 10 (Respirable)	0.4 – 10	0.0017 – 0.0034	~30
Parkhurst et al 2004b	1.4 (Cone bulk powder)	6.2	0.0004	46
	6.3 (Cone size separated)	16	0.0015	46
*Reports (restricted distribution) not obtained (OSAGWI 2000, Tab L)**				
Haggard et al 1986	4 (“within 10 days”)	–	–	?
Parkhurst et al 1990	6.8 (“slightly soluble”)	–	–	?

* see footnote to Table 13

2.5.3 Uranium speciation

X-ray analysis was used in several studies to identify the oxides present and to attempt to quantify the proportions. Results are summarised in Tables 16 and 17 respectively, for DU produced from penetrator impacts, and from combustion. Studies of penetrator impacts generally indicate that most of the crystalline uranium oxide is present as UO_2 or U_3O_8 or intermediates (U_3O_7 and U_4O_9). However, there is variation in the oxides chosen (Table 16), perhaps reflecting the difficulty in distinguishing between some, as noted in the Capstone Report. Chazel *et al*, like the Capstone Study, report U_4O_9 to be an important constituent. Glissmeyer and Mishima (1979) noted that the proportion of U_3O_8 may increase with decreasing size. This is consistent with the Capstone report observation that the proportion of U_3O_8/UO_3 (which could not be distinguished) increased with decreasing size. Following combustion, most of the uranium is reported to be present as U_3O_8, with a small amount of UO_2 (Table 17).

A further complication is that the aerosol formed following penetration of armour by a DU round will contain material derived from the armour. Thus analysis of the cyclone samples in the Capstone Study showed that a high percentage of the mass of material collected was uranium: approximately 40-70% for the Abrams BHT and about 25% for the BFV BHT. Aluminium and iron were the other main metal constituents. Aluminium varied the most by phase, being highest in Phase II and lowest in Phase III. Other major constituents included titanium, zinc, and copper. There is insufficient information available to enable the dissolution characteristics of a particular uranium-metal mixture to be predicted, but the varied elemental composition probably contributes to the variability in dissolution characteristics observed.

Table 16 Chemical composition of material formed from DU penetrator impacts (Partly based on Table G4 of Royal Society, 2001)

Report	Amorphous (%)	UO_2 (%)	U_3O_8 (%)
Glissmeyer and Mishima, 1979		25	75
Patrick and Cornette, 1978	*	*	*
Scripsick *et al*., 1985(a,b)	–	60 (air filter, total)	40
	20	18 (air filter, respirable)	62
	–	97 (core sample, total)	3
	–	54 (core sample, respirable)	46
Chazel et al, 2003			30-40†
Mitchell and Sunder, 2004		9	44‡

* Qualitative: Air samples mainly U, Fe. Soil also Si, Al and W. † also 25-40% U_4O_9 and 20% UO_3

‡ also 47% U_3O_7

Table 17 Chemical composition of material formed from combustion of uranium (Based on Table H5 of Royal Society, 2001)

Report	UO_2 (%)	U_3O_8 (%)
Reports obtained		
Elder and Tinkle 1980	0.2 – 4	96 – 99.8
Scripsick et al 1985a	<0.02 – 1.3 (respirable)	98.7 – >99.98
*Reports not obtained (OSAGWI 2000, Tab L)**		
Haggard et al 1986	"Predominantly"	
Parkhurst et al 1999	~100%	

* see footnote to Table 13

2.5.4 Dissolution of uranium oxides

As described in the previous section, following the impact of a DU penetrator, or combustion of DU objects in a fire, any DU inhaled is likely to be in oxide form, predominantly UO_2, U_3O_8 or intermediates (U_3O_7 and U_4O_9). The processing of uranium into reactor fuel elements may involve one or more oxide forms, and as a result there have been many *in vivo* studies of the biokinetics of uranium following the deposition of the various oxides in the lungs (usually of rats), and *in vitro* studies of the dissolution of uranium oxides under conditions intended to simulate lung deposition.

As noted above, ICRP Publication 71 (ICRP, 1995a) included a brief review of information relating to inhalation of different chemical forms, updating the reviews in ICRP Publication 30, but with emphasis on environmental exposure. ICRP Publication 71 also introduced criteria for assigning compounds to the three HRTM default absorption Types (F, M or S) on the basis of experimental data. In discussing the behaviour of each compound, consideration was given to the assignment to the appropriate absorption Type. With respect to uranium oxides it made the following observations:

"Uranium trioxide, ammonium diuranate (ADU) and uranium octoxide are found in various hydration states alone or more often mixed in various proportions in industrial processes. The human data from accidental intakes (West et al., 1979; Eidson, 1990), and from monitoring data in workers from processing facilities (Barber and Forrest, 1995), the many animal studies in rats, dogs and monkeys (Morrow et al., 1972; Eidson

and Damon, 1985a,b; Stradling et al., 1985b; Métivier et al., 1992), and extensive in vitro studies (Mansur, 1988; Hengé-Napoli et al., 1989) show that the behaviour depends on particular processes but, in most cases, is consistent with assignment to Type M, although pure UO_3 would be assigned to Type F. Considerable variation in the behaviour of U_3O_8 was observed, with some studies indicating Type M behaviour and others Type S.

Human studies have shown that UO_2 can be very insoluble (Pomroy and Noel, 1981; Price, 1989). Experiments in rats, dogs, monkeys and baboons (Leach et al., 1973; Stradling et al., 1989; Métivier, et al., 1992) also support the assignment of UO_2 to Type S."

In more recent studies, efforts have been made to derive specific values of HRTM absorption parameters. In doing so consideration has to be given to the extent of binding of dissolved uranium to lung tissues (Section 2.4), but experimental evidence suggests that this is unimportant. Cooper *et al*. (1982) and Ellender (1987) followed the behaviour of ^{233}U after instillation of uranyl nitrate and bicarbonate into the pulmonary (AI) region of the lungs of rats. Cooper *et al*. (1982) found that less than 2% of the initial lung deposit (ILD) remained at 7 days. Ellender (1987) found that about 3% remained at 30 d. Detailed analysis, however, indicated that clearance over this period was mainly by particle transport, and that the results did not provide evidence for binding of uranium (Hodgson, *et al*., 2000).

Hodgson, *et al*. (2000) derived HRTM absorption parameter values for a number of uranium compounds produced during the manufacture of nuclear fuel, using the results of previously published experiments. Values for uranium oxides are given in Table 18. Ansoborlo *et al.* (2002) compiled HRTM parameter values for uranium compounds handled during nuclear fuel fabrication in France. *In vivo* results for pure oxides are also given in Table 18. For each compound there is considerable variation, reflecting differences in methodology, and in the physico-chemical properties of the materials. However, there is a marked distinction between the relatively soluble UO_4 and UO_3, for which f_r, the rapidly-dissolving fraction is more than 50%, and the relatively insoluble U_3O_8 and UO_2, for which f_r is <10% and for UO_2 about 1%.

Table 18 Summary of absorption parameter values for uranium oxides (Partly based on Royal Society, 2001 Table A5)

Compound	Absorption parameters			Reference
	f_r	s_r, d^{-1}	s_s, d^{-1}	
UO_4 (n=4)	0.87	0.93	0.024	Ansoborlo et al., 2002
UO_3	0.75	14	0.02	Bailey et al., 1998
UO_3	0.92	1.4	0.0036	Hodgson et al., 2000
UO_3	0.71	0.28	0.0011	Ansoborlo et al., 2002
U_3O_8	0.044	0.49	0.00035	Hodgson et al., 2000
U_3O_8	0.046	2.3	0.0012	Ansoborlo et al., 2002
U_3O_8	0.03	2.1	0.00038	Ansoborlo et al., 2002
UO_2 – Non-ceramic	0.011	0.95	0.00061	Hodgson et al., 2000
UO_2 – Ceramic	0.008	1.3	0.00026	Hodgson et al., 2000
UO_2	0.03	1.3	0.0015	Ansoborlo et al., 2002
UO_2	0.01	nd	0.00049	Ansoborlo et al., 2002
UO_2	0.01	nd	0.00058	Ansoborlo et al., 2002
Defaults (ICRP 68)				
Type F	1	100	—	
Type M	0.1	100	5.0×10^{-3}	
Type S	0.001	100	1.0×10^{-4}	

nd = Not determined

2.5.5 Absorption parameter values for assessments of DU exposures

Different approaches were taken in the two major recent assessments to estimating appropriate HRTM parameter values for assessing the behaviour of DU deposited in the respiratory tract and hence organ doses and maximum kidney uranium concentrations.

2.5.5.1 Royal Society (2001)

The Royal Society (2001) assessment considered a wide range of battlefield exposures to DU aerosols originating from the impact of DU penetrators on armour, and from DU involved in fires. It aimed at obtaining "central estimates" of doses and kidney concentrations, which would be typical for those exposed under a given set of conditions, and "worst cases", which it was unlikely that any individual would exceed. In each case, the values of f_r were based on the information then available from *in vitro* studies (Tables 14 and 16). These gave a central value of 0.3 (range 0.1–0.5) for aerosols formed from impacts and a central value of 0.05 (range 0.05–0.1) for aerosols formed by combustion. The former was applied to assessment of Level I exposures (Table 4). For Level II and III exposures within vehicles, it was considered that the DU dust resuspended might have been formed by either impact or combustion, and therefore the parameter values chosen, a central value of 0.2 (range 0.005–0.5) encompass both (Table 5).

Results of *in vivo* experiments on U_3O_8 and UO_2 (Table 18) were used to assess the central values of the rapid dissolution rate s_r (1 d^{-1}) and the slow dissolution rate s_s (0.001 d^{-1}) for both types of aerosol. The range of values taken for s_r (0.4–14 d^{-1}) was based on the range observed for uranium oxides (Table 18). The range of values taken for s_s was from 0.0001 d^{-1} (as for default Type S) to 0.0015 d^{-1} (the highest value for

U_3O_8 or UO_2 in Table 18). However, a number of limitations of the data in Table 18 were recognised:

- It is difficult to determine dissolution rates less than about 0.001 d^{-1} in such experiments, and so there will be considerable errors on the values of s_s.
- The studies were conducted on rats: it is assumed that the same rates apply to man.
- As noted above, s_s depends on the physical and chemical form of the material, its mode of formation and 'history' before inhalation. There are some obvious differences between the DU aerosols formed in penetrator impacts and/or fires and the industrial uranium oxides studied *in vivo*:
  - The DU is not pure uranium but typically contains 0.75% titanium
  - In impacts in particular, the oxide may be a mixture of uranium with other metals from the target, notably iron and/or aluminium.

2.5.5.2 Capstone: Guilmette et al., 2004

The Capstone Human Health Risk Assessment (HHRA, Guilmette et al., 2004) considered only aerosols formed within a vehicle struck by a large calibre DU penetrator, and only used information derived from the Capstone Aerosol Study (Parkhurst et al., 2004a, 2004b). As noted above (Section 2.6.1) dissolution in simulated lung fluid was measured for 46 days on 27 samples, many of which were fractionated by size. Time-dependent retention of undissolved DU was fit by two- and/or three-component exponential functions. The HHRA incorporated the results (taking the more detailed three-component fits) into a probabilistic assessment that derived distributions of doses for each exposure scenario, using the results of the cascade impactor measurements to give distributions of DU air concentrations as functions of particle size and time after impact. Appropriate sets of absorption parameter values (according to the scenario and size) were assigned to each size fraction.

2.5.5.3 Respiratory tract absorption parameter values and ranges

Since the objectives and scope of this analysis are similar to those of the Royal Society Working Group (RSWG) assessment, a similar approach is taken, but the values are updated taking account of the more recent data now available. The absorption parameter values chosen for the RSWG assessment (Tables 4 and 5) are shown in Table 19. Those for Level I were based on impact aerosols, those for Level II either impact or combustion. The only differences are in the central and low values of f_r, which were lower for combustion aerosols and hence for Level II. As noted above, values of f_r were based on the available relevant *in vitro* studies and values of s_r and s_s were based on *in vivo* studies on uranium oxides. No recent relevant *in vivo* experiments were identified, other than that of Mitchell and Sunder (2004), which was considered not to be useful here (Section 2.5.1).

For comparison, Table 19 also summarises the *in vitro* results now available. For each set the geometric mean was taken as the "central value", with the highest and lowest values giving the range. All but two of the Capstone *in vitro* studies (Table 14) relate to

impact aerosols, and their summary statistics are given. Results for all impact aerosols, including the others from Table 13 are similar, because most of the results are from the Capstone study.

Table 19 Parameter values for absorption from the respiratory tract to blood

	f_r			s_r (d^{-1})			s_s (d^{-1})		
	Central	Range		Central	Range		Central	Range	
		Low	High		Low	High		Low	High
Royal Society Level I (Table 4)	0.3	0.1	0.5	1	0.4	14	0.001	0.0001	0.0015
Royal Society Level II (Table 5)	0.2	0.005	0.5	1	0.4	14	0.001	0.0001	0.0015
Capstone (impact aerosols)	0.14	0.01	0.28	5	0.1	30	0.0028	0.0006	0.0095
All in vitro impact aerosols	0.17	0.01	0.57	4	0.1	30	0.0024	0.0002	0.0095
All in vitro combustion aerosols	0.05	0.005	0.1	3	0.4	16	0.0014	0.0004	0.0034
Proposed values and ranges									
Impact aerosols	0.2	0.01	0.5	3	0.3	20	0.002	0.0001	0.005
Combustion aerosols	0.05	0.01	0.1	3	0.3	20	0.001	0.0001	0.002
Impact or combustion aerosols	**0.15**	**0.01**	**0.5**	**3**	**0.3**	**20**	**0.002**	**0.0001**	**0.005**

Selecting the parameter values for use in this analysis (and potentially other analyses until other information becomes available) from the available information is a matter of judgement. Values are selected for impact and combustion aerosols separately. Values are also selected for DU dust that might be of either origin, but more weight is given to results for impact aerosols as this mechanism seems likely to generate larger amounts of respirable dust. Following the approach taken by the RSWG, consideration is given to both the *in vitro* results on material which are directly relevant, and *in vivo* results on similar uranium oxides. However, with the availability of the comprehensive Capstone data rather more weight is given here to the *in vitro* data. Values selected for the rapid fraction, f_r, are simply rounded from the corresponding *in vitro* data. Values selected for the rapid and slow dissolution rates, s_r and s_s, take account of both.

2.5.5.4 Respiratory tract absorption parameter distributions

Normal and log-normal probability density functions (PDFs) were fitted to the two-component Capstone data given in Table 14, using the statistics software MINITAB® 12 (Minitab Inc. PA, USA) for Windows®. A normal distribution (mean=0.16, standard deviation=0.09) gave an acceptable fit to the fraction that dissolved rapidly (variable A_1 in Table 14) data ($p<0.23$). However, the tail of this distribution (upper 95-percentile, $U_{95\%}$ = 0.34) did not include the higher values for the rapid fraction determined by Glissmeyer and Mishima (1979) and others given in Table 13. A log-normal distribution (median=0.15, GSD=2), gave better support over the range of values in Tables 14, 15 and 20.

Log-normal distributions gave acceptable fits to the rapid dissolution rate (variable B_1 in Table 14) (median=5.7, GSD=3.3) ($p<0.06$), and slow dissolution rate (variable B_2 in Table 14) (median=0.0026, GSD=2.2) ($p<0.51$). Log-normal PDFs were therefore chosen to represent the absorption parameters. Median and GSDs for these

distributions were chosen that gave the best support over the range of values for "Impact or combustion aerosols" given in the final row of Table 19.

PDF of f_r: Log-normal (median=0.15, GSD=2)

PDF of s_r: Log-normal (median=3 d^{-1}, GSD=3)

PDF of s_s: Log-normal (median=0.001 d^{-1}, GSD=3)

2.5.5.5 GI tract uptake fraction, f_1 parameter values and ranges

Values are also needed for the fractional absorption in the GI Tract (f_1 value) for material cleared to it from the respiratory tract by particle transport. The ICRP default f_1 values for uranium are 0.02 for Type F and Type M forms and 0.002 for Type S (ICRP 1994b, 1995a). Most of the combinations of parameter values proposed in Table 19 correspond to Type M, according to the ICRP Publication 71 criteria (Section 2.5.1). Exceptions, which are Type S, are low f_r (0.01) and low s_s (0.0001 d^{-1}) and for combustion aerosols central f_r (0.05) and low s_s (0.0001 d^{-1}). There appear to be no specific studies aimed at determining f_1 values for DU aerosols. Chazel et al (2003) did, however, measure dissolution in HCl at pH 3, to simulate acid rain, which may give some guidance to dissolution in the acidic conditions in the stomach. The fraction dissolved rapidly was somewhat higher than that in Gamble's solution, intended to simulate serum (68% versus 57% for the turret shot and 65% versus 47% for the glacis shot), but qualitatively similar. However, this would represent dissolution of the dust *into* a form that was available for absorption in the GI tract, rather than absorption itself.

Data on the absorption of different forms of uranium in the GI Tract have been reviewed in ICRP Publication 69 (1995b) and by Harrison *et al* (2001) and Leggett and Harrison (1995). For uranium in drinking water ingested by volunteers individual values ranged from less than 0.0025 up to about 0.06, with central values of about 0.01–0.02. Taken with results of animal experiments with soluble forms of uranium (e.g. nitrate) a value for f_1 of 0.02 was adopted by ICRP (1995b) for dietary forms of uranium ingested by adults. It was also noted that data from animal studies provide information on the relative uptake of uranium ingested in different chemical forms, showing that absorption is strongly dependent on the solubility of the compound. Compared to soluble forms, absorption is roughly half as great for UO_4 or UO_3, and 1–2 orders of magnitude lower for UCl_4, U_3O_8, UO_2 and UF_4. That gives values of 0.0002-0.002 for U_3O_8 and UO_2, assuming an f_1 of 0.02 for nitrate in Table 6 of Leggett and Harrison (1995). Thus the value of 0.02 is effectively an upper bound on the central value for a given form of uranium, since it applies to soluble forms. For a mixture of soluble and insoluble forms, it would be expected to apply to the fraction present in soluble forms. Given the findings of Chazel et al (2003), it was judged that there was likely to be a positive correlation between higher *in vitro* dissolution in simulated lung fluid and greater absorption in the GI tract. Thus f_r was taken to be the fraction of material in soluble form, and for the uncertainty analysis it was assumed that f_1 was equal to $0.02*f_r$. The distribution of f_r is assumed to be log-normal with a median of 0.15 and GSD of 2. Hence the distribution of f_1 is assumed to be log-normal with a median of 0.003 and GSD of 2. Taking the range to be from $0.003/GSD^2$ to $0.003*GSD^2$ gives a range of values of f_1 from lower 5-

percentile, $L_{5\%}$ = 0.0008 to $U_{95\%}$ = 0.012. This range is largely below the default value for Type M (0.02), and extends below that for Type S (0.002).

2.5.5.6 GI tract uptake fraction, f_1 distribution

As discussed above in deriving a range of values the distribution of f_1 is assumed to be log-normal with a median of 0.003 and GSD of 2.

2.6 Summary

As noted in Section 2.1, there are three main sets of HRTM parameter values relevant to this analysis: those that determine the initial pattern of deposition in the respiratory tract, those that determine particle transport rates from each part of the respiratory tract, and those that determine the rate of absorption to blood. These are discussed in detail in Sections 2.3, 2.4, and 2.5, respectively.

Consideration has been given to Level I exposures for which heavy exercise and impact aerosols are here considered most likely, and to Level II exposures, for which light exercise, and a mixture of impact and combustion aerosols seem most likely. However, the central values and ranges of deposition parameter values for light and heavy exercise (Table A2) are not greatly different, and neither are the absorption parameter values for impact aerosols or mixed impact and combustion aerosols (Table 19). (Particle transport rates are the same for both scenarios.) For this analysis, to reduce the number of variables, it is preferable to have a single set of parameter values. The deposition values for heavy exercise from Tables 10 and 11 (which show a somewhat greater range than those for light exercise), and the absorption values for “impact or combustion aerosols” from the last row of Table 19 were therefore used.

The central values of inhalation parameter values proposed for retrospective assessments (from urine sampling) of exposures to DU from penetrator impacts or fires are listed in Table 20. Ranges of values of each parameter for use in the sensitivity analysis also given (Low and High).

Table 20 Central values of inhalation parameter values proposed for retrospective assessments (from urine sampling) of exposures to DU from penetrator impacts or fires (particle density 9 g cm^{-3}, shape factor 1.5). Ranges for the sensitivity analysis are also given (Low and High).

Parameter		Unit	Value			Source table (and figure)
			Low	Central	High	
Aerosol						A2
AMAD		µm	0.4	2.5	13	
Aerosol GSD			2	6	15	
Breathing						A2
Nasal fraction (mode), F_n			0.3	0.5	1	11
Ventilation rate, B		$m^3\ h^{-1}$	0.75	3	6	10
Frequency, f_R		$minute^{-1}$	14	26	36	10
Absorption to blood						20 (Figure 6)
Rapid fraction, f_r			0.01	0.15	0.5	
Rapid dissolution rate, s_r		d^{-1}	0.3	3	20	
Slow dissolution rate, s_s		d^{-1}	0.0001	0.002	0.005	
GI tract absorption, f_1			0.0008	0.003	0.012 (0.002)*	
Particle transport rates (KI model in parentheses)						4, 12 (Figure 5)
$m_{1,4}$	AI_1 to bb_1	d^{-1}	6.67E-3	0.02	0.06	
$m_{2,4}$	AI_2 to bb_1	d^{-1}	3.33E-4	0.001	0.003	
$m_{3,4}$	AI_3 to bb_1	d^{-1}	3.33E-5	1E-4	3E-4	
$m_{3,10}$	AI_3 to LN_{TH}	d^{-1}	6.67E-6	2E-5	6E-5	
$m_{4,7}$	bb_1 to BB_1	d^{-1}	0.67 *(0.067)*	2 *(0.2)*	6 *(0.6)*	
$m_{5,7}$	bb_2 to BB_1	d^{-1}	0.01 *(0.067)*	0.03 *(0.2)*	0.09 *(0.6)*	
$m_{6,10}$	bb_{seq} to LN_{TH}	d^{-1}	3.33E-3	0.01	0.03	
$m_{7,11}$	BB_1 to ET_2'	d^{-1}	3.33	10	30	
$m_{8,11}$	BB_2 to ET_2'	d^{-1}	0.01 *(10)*	0.03 *(10)*	0.09 *(30)*	
$m_{9,10}$	BB_{seq} to LN_{TH}	d^{-1}	3.33E-3	0.01	0.03	
$m_{11,15}$	ET_2' to GI tract	d^{-1}	33.3	100	300	
$m_{12,13}$	ET_{seq} to LN_{ET}	d^{-1}	3.33E-4	0.001	0.003	
$m_{14,16}$	ET_1 to environment	d^{-1}	0.333	1	3	

Default value of 0.02 for Type M was used in the sensitivity analysis

3 METHODS USED IN THE SENSITIVITY AND UNCERTAINTY ANALYSES

For the first part of the sensitivity analyses, consideration is given to doses (and $^{max}[U]_k$) resulting from unit intake, which is taken to be 1 mg DU. The choice of 1 mg is arbitrary but consistent with usage in assessments such as that carried out by the Royal Society

(2001, 2002). For the second part of the sensitivity analyses, and for the uncertainty analyses, consideration is given to doses (and $^{max}[U]_k$) assessed from a measurement of 1 ng DU in urine. Again the choice of 1 ng is arbitrary, but considered appropriate since urinary excretion rates are typically in the range 1–30 ng l^{-1} (Ting et al 1999) and it is possible to measure DU at 0.3 ng d^{-1} against a background of 10 ng d^{-1} natural uranium (Parrish et al, 2006). It is considered that the results can be scaled linearly to other intakes and measurements over wide ranges, because all the ICRP models used are linear, first-order models, i.e., all the rate constants are independent of the amount of uranium present. It is recognised that at very high lung loadings, greater than about 1 gram dust per kilogram of lung tissue, reduced particle transport from the alveolar region would occur (ICRP 1994a, paragraphs E29 and E67). However, dissolution and absorption to blood may well be less affected. Hodgson et al (2007) considered whether alteration of kidney function at high uranium kidney concentrations might affect urinary excretion of uranium and hence assessments based on urine sampling. They found that available measurements in humans of the ratio of uranium urinary excretion to kidney concentration show no obvious change in this ratio up to kidney concentrations of at least 3 μg uranium g^{-1} of kidney.

3.1 Computer Codes

Most of the bioassay predictions and committed doses were calculated using the internal dosimetry code IMBA Professional (Birchall et al 2003, 2006), which implements the HRTM (ICRP, 1994a), the ICRP Publication 30 GI tract model (ICRP, 1979) and the ICRP Publication 69 (ICRP, 1995b) systemic model for uranium.

To carry out the sensitivity analysis expediently, and to reduce the potential for human error, a separate program was written in Microsoft Visual Basic 6.0 that automated IMBA Professional. This program set the relevant parameter values within IMBA and then called its dose and bioassay prediction subroutines iteratively.

For the uncertainty analysis, the Monte Carlo simulations were performed using a new software tool developed at HPA: The IMBA Uncertainty Analyser (Puncher and Birchall 2007). This code has been developed for the purpose of calculating full probabilistic uncertainties on prospective and retrospective dosimetry calculations, and implements Bayesian inference procedures. The code samples parameters from the HRTM (ICRP 1994a) and GI tract model (ICRP, 1979), using random or Latin Hypercube sampling methods. The software sets the sampled parameters within IMBA and then calls its dose and bioassay prediction subroutines iteratively.

Another of the HPA's internal dosimetry codes, PLEIADES (Fell et al, 2007) was used to generate Figure 7 (Section 4.1.1) which shows uptake to blood from various sites of deposition following inhalation of DU.

3.2 Composition of Depleted Uranium

For these analyses, the isotopic composition of DU was taken to be that adopted in the assessments made by the RSWG (Royal Society, 2001), as listed in Table 21. The four

uranium isotopes are all long-lived, and emit alpha particles of similar energy. They therefore have similar dose coefficients (doses per unit intake). The isotopic composition of the DU does however determine its specific activity (Bq of uranium isotopes per mg), and so the dose from intake of 1 mg. Even for natural uranium, the specific activity (25.3 Bq mg^{-1}, Royal Society 2001) is less than a factor of two higher than for the DU composition given in Table 21 (14.9 Bq mg^{-1}), and therefore uncertainties in dose resulting from uncertainties in the DU composition are likely to be small. Furthermore, in practice it should be possible to determine the relevant composition from samples collected in the field, and so uncertainty associated with the composition of DU is not included in this analysis. The calculations include any contributions from radioactive decay products of the uranium isotopes formed within the body. Possible contributions from trace contaminants (plutonium, neptunium, americium and fission products) were not included, because information currently available suggests that they are unlikely to add more than about 1% to the doses from the uranium isotopes present in the DU (Royal Society 2001, Annex D, Section D2).

Table 21 Composition of DU (AEPI 1995)

Isotope	Mass fraction, %	Activity in 1 mg DU, Bq	Activity fraction, %
^{234}U	0.001	2.31	15.53
^{235}U	0.20	0.16	1.07
^{236}U	0.0003	0.007	0.05
^{238}U	99.8	12.42	83.35

3.3 Individual parameter sensitivity analysis of HRTM parameter values

Separate sets of calculations were performed to investigate the sensitivity of committed effective doses, $E(50)$, committed equivalent lung doses, $H_{Lung}(50)$, and maximum kidney concentrations $^{max}[U]_k$, µg uranium per gram kidney (Appendix A), to the value of each parameter. 'Low', 'central' and 'high' values for each parameter (Table 20) were selected as follows.

3.3.1 Deposition

For the aerosol parameters central values and ranges are taken from Section 2.3.1.4 to be AMAD 2.5 µm (range 0.4 – 13 µm) and GSD 6 (range 2 – 15). The values for breathing represent the low and high values given in Tables 10 and 11 for light or heavy exercise. The central values are those for heavy exercise in Tables 10 and 11.

3.3.2 Absorption to blood

The absorption parameters f_r, s_r and s_s were taken from the 'low', 'central' and 'high' ranges for *"Impact or combustion aerosols"* given in the final row of Table 19. The values for default Type M and Type S absorption were also included for comparison purposes. For fractional absorption from the GI tract (f_1), the central value taken for the

sensitivity analysis was the default value for Type M (0.02), but values of 0.003 and 0.0008 were included for comparison.

3.3.3 Particle transport

The 'central' rates were taken to be the ICRP HRTM default values given in Table 1. Low and high sets of particle transport rates were obtained by dividing the HRTM particle transport rate constants (given in Table 1) by a factor of three or multiplying the constants by a factor of three respectively (Section 2.4.5, Table 20). The KI Model was included by comparing results using its central values (Table 12) with all HRTM central values (Table 1).

3.3.4 Bioassay and dose calculations

Initially, urine bioassay predictions and dose calculations were performed for the 'central' sets of HRTM parameter values. This was performed as follows:

1. The 'central' sets of deposition, absorption and particle transport parameter values were configured in IMBA by the client program.
2. The predicted 24-hour DU urine excretion (ng d^{-1}) after an inhalation of 1 mg of DU was calculated at 100, 500, 1000, 5000 and 10000 days after the intake.
3. The committed effective dose, $E(50)$ and committed equivalent lung dose, $H_{Lung}(50)$, were calculated for the 1-mg intake of DU.
4. The maximum predicted kidney concentration of DU ($^{max}[U]_k$, µg uranium per gram kidney) was calculated for the 1-mg intake of DU.
5. Using the values calculated in steps 3 and 4, and assuming that a quantity of 1 ng of DU had been detected in a 24-hour urine sample, E(50), $H_{Lung}(50)$, and $^{max}[U]_k$ were calculated from the predicted urine bioassay quantities at each time point as follows.

$$Q_T = Q_{mg} / U_T \quad (3)$$

Where:

Q_T is the required quantity of $E(50)$, $H_{Lung}(50)$, and $^{max}[U]_k$ predicted from the urine bioassay.

Q_{mg} is the $E(50)$, $H_{Lung}(50)$, and $^{max}[U]_k$ calculated for an acute inhalation of 1 mg of DU.

U_T is the urine excretion of DU in ng d^{-1} at time T after an intake of 1 mg of DU.

Steps 1 to 5 were repeated. However, each time the high or low value for a single parameter was substituted for its central value. In one run, for example, the central values for all parameters were configured in IMBA except that the AMAD was assigned the low value of 0.4 instead of the central value of 2.5.

3.3.5 Data Analysis

To determine the effect on calculated dose, or kidney concentration, of varying any single parameter between its low or high value a 'sensitivity factor' was calculated as

follows: the doses and $^{max}[U]_k$ for the central values including the perturbed parameter, determined from the predicted bioassay at each time point, were divided by the corresponding value calculated using the central values for all of the parameters (the first set of calculations in the analysis). For example, to determine the effect on E(50) from substituting the low value of 14 for the central value of 26 for respiratory frequency f_R (per minute), the following ratio was calculated:

$$R = E(50)_{frl}/E(50)_c \quad (4)$$

Where:

R is the 'sensitivity' factor. This will be >1 if the lower limit of the respiratory frequency increases the dose with respect to the central value, or <1 if it decreases the dose.

$E(50)_{frl}$ is the effective dose when the respiratory frequency has its low value, but all other parameters are assigned their central values.

$E(50)_c$ The effective dose calculated when all HRTM parameters are assigned their central values.

3.4 Probabilistic uncertainty analysis

The PDFs derived for the inhalation parameters and gut uptake fraction, f_1, have been given earlier and are summarised in Table 22. A Latin Hypercube sampling procedure (McKay *et al* 1979) was employed in the present study. This method was developed to permit efficient sampling over the full support of a PDF. It is particularly useful when only small sample sizes are permitted because, for instance, calculation times are long, or the sampled PDFs are asymptotic with long "tails" (e.g. a log-normal distribution with a large GSD).

3.4.1 The Monte Carlo simulation

A Latin Hypercube sample of 10^4 variates was constructed for each parameter from its assigned PDF. For f_r and aerosol GSD, this meant that a small fraction of values were outside of the permitted range for these parameters (>1 for f_r, <1 for aerosol GSD). When this occurred, the parameters were set to unity. This occurred for 0.3% of values of f_r and 0.01% of values of aerosol GSD.

Two separate Monte Carlo simulations were performed in order to monitor convergence of the calculated sample distributions.

For each iteration of the Monte Carlo, the following steps were performed:

1. The sample vector of HRTM parameter values was configured in IMBA by the IMBA Uncertainty Analyser program.
2. The predicted 24-hour DU urine excretion (ng d^{-1}) after an inhalation of 1 mg of DU was calculated at times T=10, 20, 50, 100, 200, 500, 1000, 2000, 5000 and 10,000 days after the intake.
3. The committed effective dose, $E(50)$ and committed equivalent lung dose, $H_{Lung}(50)$, were calculated in IMBA for an acute inhalation of 1 mg of DU.

Steps 1-2 were repeated 10^4 times.

3.4.2 Data processing and statistical analyses

The data for the 10^4 runs were imported into Microsoft® Excel 97®. Using the values calculated in steps 2 and 3 of the Monte Carlo, and assuming that a quantity of 1 ng of DU had been detected in a 24-hour urine sample, $E(50)$ and $H_{Lung}(50)$ were calculated from the predicted urine bioassay quantities at each time using Equation (3).

For the 10^4 values of dose, $E(50)$ or $H_{Lung}(50)$, calculated for each T, the following sample statistics were calculated: the mean, median, 2.5-percentile and 97.5-percentile. The percentage differences between the sample statistics for the two simulations were also calculated.

Table 22 Parameters and distributions used in the probabilistic uncertainty analysis.

Parameter	Distribution	Median	GSD
Aerosol parameters			
AMAD	Log-normal	2.3	2.4
GSD	Log-normal	5.7	1.6
Breathing parameters			
B	Log-normal	2	1.6
f_R	f_R =4B+13	21	1.2
Breathing mode			
F_n	Triangular	0.2[a]	1[b]
ET_1, ET_2 aerodynamic filter efficiency	Log-normal	1	1.82
ET_1, ET_2 thermodynamic filter efficiency	Log-normal	1	1.18
Particle transport rates			
All rates scaled by factor c [c]	Log-normal	1	1.7
Absorption parameters			
f_r	Log-normal	0.15	2
s_r	Log-normal	3	3
s_s	Log-normal	0.001	3
f_1	f_1=0.02 f_r	0.003	2

[a]minimum of right angled triangle, [b]vertex of right angled triangle. [c]The median particle transport rates adopted in the HRTM or KI Model.

4 RESULTS AND DISCUSSION

4.1 Sensitivity of radiation doses to inhalation parameter values

Table 20 lists the parameter values chosen as 'central' (typical) values, and ranges. Table 23 summarises the analysis of the sensitivity to inhalation parameter values of doses (effective and lung) for unit intake of DU. Results for maximum kidney concentration $^{max}[U]_k$, are given in Appendix A. Thus, doses (and $^{max}[U]_k$) were

calculated for an intake of 1 mg DU, using the central parameter values. The value of each parameter in turn was changed to its 'low' and 'high' value, the result recalculated and presented as the ratio to that obtained using all central values, i.e. the 'sensitivity factor'. Thus if a 'low' value gives a ratio greater than 1.0 it means that the dose is higher if calculated with that value than if calculated with the central value. To identify parameters that can have an 'important' impact (worthy of further discussion), ratios ≤ 0.8, and ≥ 1.2 are shown in bold font. (A criterion of 20% difference was chosen because it identified a reasonable number of parameters in each case.) It should be noted that in many cases the sensitivity of the output (dose or $^{max}[U]_k$) to changes in a particular parameter value will be dependent on the set of central values themselves. For example, the central value of the slow dissolution rate, s_s, is 0.002 d^{-1}, and so changes to the slowest particle transport rate from the AI region 0.0001 d^{-1} will have little effect, because overall retention is dominated by dissolution. Changes to this particle transport rate would have had more effect if a lower value of s_s had been chosen.

For comparison, results for HRTM default Type M and Type S absorption parameter values are also given. For these, all four absorption parameter values are set to their default values simultaneously, but other parameter values (aerosol, breathing, particle transport) remain at the DU central values given in Table 20:

- For Type M: f_r = 0.1; s_r = 100 d^{-1}; s_s = 0.005 d^{-1}; f_1 = 0.02
- For Type S: f_r = 0.001; s_r = 100 d^{-1}; s_s = 0.0001 d^{-1}; f_1 = 0.002

Note that for Type M the value of f_r is close to the central value (0.15), and that of s_s is the same as the 'high' value. For Type S the value of f_r is only 10% of the 'low' value (0.01), and that of s_s is the same as the 'low' value.

For fractional absorption from the GI tract (f_1), the central value taken for the sensitivity analysis was the default value for Type M (0.02), but median and low values of 0.003 and 0.0008 derived for the uncertainty analysis were included for comparison.

Table 23 Sensitivity to inhalation parameter values of doses (effective and lung) for unit intake of DU

				Ratio to central values	
Parameter	Low/ High	Value	Unit	E(50)	$H_{Lung}(50)$
Aerosol					
AMAD	Low	0.4	μm	**1.53**	**1.52**
AMAD	High	13	μm	**0.60**	**0.60**
Aerosol GSD	Low	2		**1.39**	**1.40**
Aerosol GSD	High	15		1.07	1.07
Breathing					
Nasal fraction (mode), F_n	Low	0.3		**1.21**	**1.21**
Nasal fraction (mode), F_n	High	1		**0.45**	**0.45**
Ventilation rate, B	Low	0.75	$m^3\ h^{-1}$	0.92	0.92
Ventilation rate, B	High	6	$m^3\ h^{-1}$	1.05	1.05
Frequency, f_R	Low	14	$minute^{-1}$	1.09	1.09

Parameter		Low/ High	Value	Unit	Ratio to central values E(50)	Ratio to central values $H_{Lung}(50)$
Frequency, f_R		High	36	$minute^{-1}$	0.95	0.95
Absorption to blood						
Rapid fraction, f_r		Low	0.01		1.15	1.16
Rapid fraction, f_r		High	0.5		**0.62**	**0.60**
Rapid dissolution rate, s_r		Low	0.3	d^{-1}	1.01	1.01
Rapid dissolution rate, s_r		High	20	d^{-1}	1.00	1.00
Slow dissolution rate, s_s		Low	1E-4	d^{-1}	**1.59**	**1.62**
Slow dissolution rate, s_s		High	0.005	d^{-1}	0.84	0.83
Type M					0.83	0.82
Type S					**1.80**	**1.83**
GI tract absorption, f_1		Low	0.0008		1.00	1.00
GI tract absorption, f_1		Central	0.003		1.00	1.00
Particle transport rates		(Fig. 5; Table 1)				
$m_{1,4}$	AI_1 to bb_1	Low	6.67E-3	d^{-1}	1.01	1.01
$m_{1,4}$	AI_1 to bb_1	High	0.06	d^{-1}	0.99	0.99
$m_{2,4}$	AI_2 to bb_1	Low	3.33E-4	d^{-1}	1.04	1.04
$m_{2,4}$	AI_2 to bb_1	High	0.003	d^{-1}	0.95	0.95
$m_{3,4}$	AI_3 to bb_1	Low	3.33E-5	d^{-1}	1.00	1.00
$m_{3,4}$	AI_3 to bb_1	High	3E-4	d^{-1}	1.00	1.00
$m_{3,10}$	AI_3 to LN_{TH}	Low	6.67E-6	d^{-1}	1.00	1.00
$m_{3,10}$	AI_3 to LN_{TH}	High	6E-5	d^{-1}	1.00	1.00
$m_{4,7}$	bb_1 to BB_1	Low	0.67	d^{-1}	1.05	1.05
$m_{4,7}$	bb_1 to BB_1	High	6	d^{-1}	0.98	0.98
$m_{5,7}$	bb_2 to BB_1	Low	0.01	d^{-1}	**1.54**	**1.55**
$m_{5,7}$	bb_2 to BB_1	High	0.09	d^{-1}	**0.79**	**0.78**
$m_{6,10}$	bb_{seq} to LN_{TH}	Low	3.33E-3	d^{-1}	1.01	1.01
$m_{6,10}$	bb_{seq} to LN_{TH}	High	0.03	d^{-1}	1.00	1.00
$m_{7,11}$	BB_1 to ET_2'	Low	3.33	d^{-1}	1.01	1.00
$m_{7,11}$	BB_1 to ET_2'	High	30	d^{-1}	1.00	1.00
$m_{8,11}$	BB_2 to ET_2'	Low	0.01	d^{-1}	**1.67**	**1.69**
$m_{8,11}$	BB_2 to ET_2'	High	0.09	d^{-1}	**0.74**	**0.73**
$m_{9,10}$	BB_{seq} to LN_{TH}	Low	3.33E-3	d^{-1}	1.03	1.03
$m_{9,10}$	BB_{seq} to LN_{TH}	High	0.03	d^{-1}	0.98	0.98
$m_{11,15}$	ET_2' to GI tract	Low	33.3	d^{-1}	1.00	1.00
$m_{11,15}$	ET_2' to GI tract	High	300	d^{-1}	1.00	1.00
$m_{12,13}$	ET_{seq} to LN_{ET}	Low	3.33E-4	d^{-1}	1.00	1.00
$m_{12,13}$	ET_{seq} to LN_{ET}	High	0.003	d^{-1}	1.00	1.00
$m_{14,16}$	ET_1 to environment	Low	0.333	d^{-1}	1.00	1.00
$m_{14,16}$	ET_1 to environment	High	3	d^{-1}	1.00	1.00
KI Model (Table 12)					**0.56**	**0.54**

4.1.1 Results of sensitivity analysis

4.1.1.1 Dose per unit intake

Results for effective dose and lung dose (Table 23) are very similar and so are discussed together. This reflects the fact that for inhalation of uranium in moderately soluble or insoluble forms, lung dose makes the dominant contribution to effective dose. This in turn is a reflection of the systemic biokinetics: most uranium that enters the bloodstream is excreted rapidly, and only a small fraction is deposited in organs such as liver and skeleton. Important parameters are identified in all four categories: aerosol size; breathing; absorption to blood and particle transport.

For aerosol size, increased doses result from a smaller AMAD or GSD, which both result in higher lung deposition (Table A1, Heavy exercise). However, the lower AMAD mainly increases deposition in the bronchiolar (bb) and alveolar (AI) regions, whereas the lower GSD mainly increases deposition in the bronchial (BB) region. A higher AMAD correspondingly reduces lung deposition and dose, but the larger GSD has little effect.

For breathing parameters, the fraction breathed through the nose, F_n, is important: as expected reducing F_n, and correspondingly increasing the fraction breathed through the mouth, increases lung deposition and doses. However, the volume inhaled per unit time and the breathing frequency have little effect.

Of the absorption parameters, an increase in the fraction dissolved rapidly, f_r, reduces doses, while a decrease in the slow dissolution rate, s_s, increases them. Both follow from their effects on lung retention. As expected, doses for Type M are very similar to those for the 'high' value of s_s, while doses for Type S are similar to those for the 'low' value of s_s.

Changes to most of the particle transport rates have little effect on doses per unit intake. (Hence the assumption made in the indicative uncertainty analysis, that all particle transport rates are positively correlated, is unlikely to have a major effect on the results). The exceptions are the rates relating to 'slow bronchial clearance' in the BB and bb regions (compartments BB_2 and bb_2 in Figure 5). As noted in Section 2.4.4.2 above, it has been known for some time that retention of activity in these compartments makes a major contribution to lung dose and effective doses for inhaled moderately soluble uranium (Bailey et al, 1995). This results from a combination of several factors:

- Significant deposition in these regions, especially for mouth breathing
- Close proximity of the source (airway surface) to the target cells (10–50 μm below the surface in BB and 4–12 μm below the surface in bb), resulting in a large absorbed fraction of energy for alpha-particle emissions
- Small mass of the target tissue, a few grams, compared to about 1 kg for the alveolar region
- High presumed radiation sensitivity for BB and bb regions reflected in high apportionment factors (Table 3).

Similarly, application of the alternative 'KI' Model for slow bronchial clearance results in doses about 50% of those assessed with the HRTM.

4.1.1.2 Dose per unit measurement (assessed from a urine sample)

Table 24 summarises the sensitivity to inhalation parameter values of effective doses assessed from measurement of DU in a 24-hour urine sample at a series of times in the range 100–10,000 days after intake. Only effective doses are presented in Table 24 because the pattern for lung doses is so similar. Again ratios ≤ 0.8, and ≥ 1.2 are shown in bold font. Generally the same sub-set of parameter values as for dose per unit intake is identified as 'important'. The exception is that particle transport from compartment AI_2 is also identified here. In the HRTM, the AI region is represented by three compartments (Figure 5). For a moderately soluble but long-lived radionuclide, most transformations in the AI region will take place in AI_2. Of activity deposited in AI, 60% is assigned to AI_2. Particle transport from AI_1 is faster. Although particle transport from AI_3 is slower, overall retention is determined by the slow dissolution rate, for which the central value (0.002 d^{-1}) is much greater than the particle transport rate from AI_3 (0.0001 d^{-1}).

Table 24 Summary of sensitivity to inhalation parameter values of effective doses for 1 ng of DU in a 24-hour urine sample at 100–10,000 days after intake

Parameter	Low/ High	Value	Unit	Ratio to central values				
Days after intake				100	500	1000	5000	10000
Aerosol								
AMAD	Low	0.4	µm	**0.80**	**0.77**	**0.78**	0.85	0.86
AMAD	High	13	µm	**1.38**	**1.50**	**1.47**	1.19	1.18
Aerosol GSD	Low	2		**1.30**	**1.34**	**1.33**	**1.26**	**1.26**
Aerosol GSD	High	15		0.97	0.96	0.96	0.98	0.98
Breathing								
Nasal fraction (mode), F_n	Low	0.3		1.08	1.08	1.08	1.08	1.08
Nasal fraction (mode), F_n	High	1		**0.68**	**0.67**	**0.67**	**0.68**	**0.68**
Ventilation rate, B	Low	0.75	$m^3\ h^{-1}$	1.06	1.05	1.05	1.06	1.06
Ventilation rate, B	High	6	$m^3\ h^{-1}$	1.13	1.15	1.15	1.10	1.10
Frequency, f_R	Low	14	$minute^{-1}$	0.81	**0.79**	**0.80**	0.84	0.84
Frequency, f_R	High	36	$minute^{-1}$	1.14	1.16	1.15	1.11	1.11
Absorption to blood								
Rapid fraction, f_r	Low	0.01		1.07	1.00	1.01	**1.37**	**1.39**
Rapid fraction, f_r	High	0.5		**0.77**	1.01	0.94	**0.44**	**0.43**
Rapid dissolution rate, s_r	Low	0.3	d^{-1}	1.02	1.01	1.01	1.05	1.06
Rapid dissolution rate, s_r	High	20	d^{-1}	0.98	1.00	0.99	0.92	0.92
Slow dissolution rate, s_s	Low	1E-4	d^{-1}	**8.82**	**10.28**	**4.21**	**0.59**	**0.56**
Slow dissolution rate, s_s	High	0.005	d^{-1}	**0.47**	**1.39**	**3.86**	**0.74**	**0.72**
Type M				**0.44**	**1.30**	**3.55**	**0.67**	**0.65**
Type S				**26.4**	**12.21**	**4.97**	**0.67**	**0.62**
GI tract absorption, f_1	Low	0.0008		1.04	1.01	1.01	1.08	1.09
GI tract absorption, f_1	Central	0.003		1.04	1.01	1.01	1.07	1.00
Particle transport rates	(Fig. 5; Table 1)							
$m_{1,4}$ AI_1 to bb_1	Low	6.67E-3	d^{-1}	0.89	0.99	1.01	0.97	0.97
$m_{1,4}$ AI_1 to bb_1	High	0.06	d^{-1}	1.06	1.00	1.00	1.01	1.01
$m_{2,4}$ AI_2 to bb_1	Low	3.33E-4	d^{-1}	1.00	**0.81**	**0.65**	0.90	0.92

Parameter		Low/ High	Value	Unit	Ratio to central values				
Days after intake					100	500	1000	5000	10000
$m_{2,4}$	AI_2 to bb_1	High	0.003	d^{-1}	1.05	**1.79**	**2.17**	1.17	1.15
$m_{3,4}$	AI_3 to bb_1	Low	3.33E-5	d^{-1}	1.00	0.99	0.98	1.00	1.00
$m_{3,4}$	AI_3 to bb_1	High	3E-4	d^{-1}	1.00	1.02	1.05	1.01	1.01
$m_{3,10}$	AI_3 to LN_{TH}	Low	6.67E-6	d^{-1}	1.00	1.00	1.00	1.00	1.00
$m_{3,10}$	AI_3 to LN_{TH}	High	6E-5	d^{-1}	1.00	1.00	1.00	1.00	1.00
$m_{4,7}$	bb_1 to BB_1	Low	0.67	d^{-1}	1.05	1.05	1.05	1.05	1.05
$m_{4,7}$	bb_1 to BB_1	High	6	d^{-1}	0.98	0.98	0.98	0.99	0.99
$m_{5,7}$	bb_2 to BB_1	Low	0.01	d^{-1}	**1.47**	**1.54**	**1.54**	**1.52**	**1.52**
$m_{5,7}$	bb_2 to BB_1	High	0.09	d^{-1}	**0.80**	**0.79**	**0.79**	**0.79**	**0.79**
$m_{6,10}$	bb_{seq} to LN_{TH}	Low	3.33E-3	d^{-1}	1.01	1.01	1.01	1.01	1.01
$m_{6,10}$	bb_{seq} to LN_{TH}	High	0.03	d^{-1}	1.00	1.00	1.00	1.00	1.00
$m_{7,11}$	BB_1 to $ET2'$	Low	3.33	d^{-1}	1.00	1.00	1.00	0.99	0.99
$m_{7,11}$	BB_1 to $ET2'$	High	30	d^{-1}	1.00	1.00	1.00	1.01	1.01
$m_{8,11}$	BB_2 to $ET2'$	Low	0.01	d^{-1}	**1.52**	**1.67**	**1.67**	**1.63**	**1.63**
$m_{8,11}$	BB_2 to $ET2'$	High	0.09	d^{-1}	**0.76**	**0.74**	**0.74**	**0.74**	**0.74**
$m_{9,10}$	BB_{seq} to LN_{TH}	Low	3.33E-3	d^{-1}	1.03	1.03	1.03	1.03	1.03
$m_{9,10}$	BB_{seq} to LN_{TH}	High	0.03	d^{-1}	0.98	0.98	0.98	0.98	0.98
$m_{11,15}$	$ET2'$ to GI tract	Low	33.3	d^{-1}	0.99	1.00	1.00	0.98	0.98
$m_{11,15}$	$ET2'$ to GI tract	High	300	d^{-1}	1.00	1.00	1.00	1.01	1.01
$m_{12,13}$	ET_{seq} to LN_{ET}	Low	3.33E-4	d^{-1}	1.00	1.00	1.00	1.00	1.00
$m_{12,13}$	ET_{seq} to LN_{ET}	High	0.003	d^{-1}	1.00	1.00	1.00	1.00	1.00
$m_{14,16}$	ET_1 to environment	Low	0.333	d^{-1}	1.00	1.00	1.00	1.00	1.00
$m_{14,16}$	ET_1 to environment	High	3	d^{-1}	1.00	1.00	1.00	1.00	1.00
KI Model (Table 12)					**0.58**	**0.58**	**0.56**	**0.58**	**0.58**

An interesting observation is that for AMAD the effect is the opposite of that observed for doses per unit intake (Table 23). Here higher doses result from a larger AMAD, and lower doses from a smaller AMAD. A larger AMAD results in lower lung deposition and hence lower urinary excretion. Thus a larger intake is assessed from a urine measurement and this more than offsets the lower dose per unit intake. This demonstrates the importance of selecting realistic parameter values. It is possible for a parameter value chosen to be 'conservative' for prospective dose assessments, *i.e.* to overestimate the dose per unit intake, to lead to underestimation of dose in a retrospective assessment.

However, the most striking finding from Table 24 is the importance of the value of the slow dissolution rate, s_s, and how its effect changes with the time between intake and sampling. For a urine sample at 500 days after intake, the dose assessed for a value of s_s at the low end of the range (0.0001 d^{-1}) is about 10 times the dose assessed with the central value (0.002 d^{-1}). The values of s_s do, however, differ by a factor of 20, so the large effect is understandable. At 1000 days greater doses (by a factor of four) are

calculated from values at both ends of the range than from the central value. The effect decreases at later times and reverses: at 5000 and 10,000 days lower doses are calculated from values at both ends of the range than from the central value. Clearly the effect is complex. It suggests that at 500 days after intake the urinary excretion rate is closely coupled to s_s, while at other times there are greater contributions from rapid dissolution and release from secondary deposition sites such as the skeleton. Figure 7 shows rates of uptake to blood from the major sites of deposition of uranium following a single intake. ST0 (ICRP 1995b, Harrison et al, 2007) is a soft tissue compartment that takes a large fraction of the uranium reaching blood, but returns it rapidly, so that it acts as a 'buffer', following total uptake from the other sites. The other two soft tissue compartments are longer term sites of retention. Initially the main inputs are from the lungs and the small intestine (SI), the only compartment in the GI tract model (ICRP 1979) where absorption takes place. As expected, the contribution from the SI falls faster than that from the lungs and the major systemic retention sites (skeleton, ST2, liver). At 10 days its contribution is about 10% of the lungs, and by 500 days, less than 1%. More important, though, is the decrease in the contribution from the lungs, which at 500 days is the largest contribution, but drops below that of the skeleton by 2000 days, and falls rapidly thereafter.

As expected, assessed doses for Type M are very similar to those for the 'high' value of s_s. Doses for Type S are similar to those for the 'low' value of s_s at the later times, but at the earlier times are even higher. This results from the much lower values of f_r and f_1 for Type S than for the central values. Because of these low values, there is far less excreted in urine for a given intake. Hence a much higher intake is assessed from a given amount in urine, and since the dose per unit intake is also higher for Type S, the assessed dose is greater still.

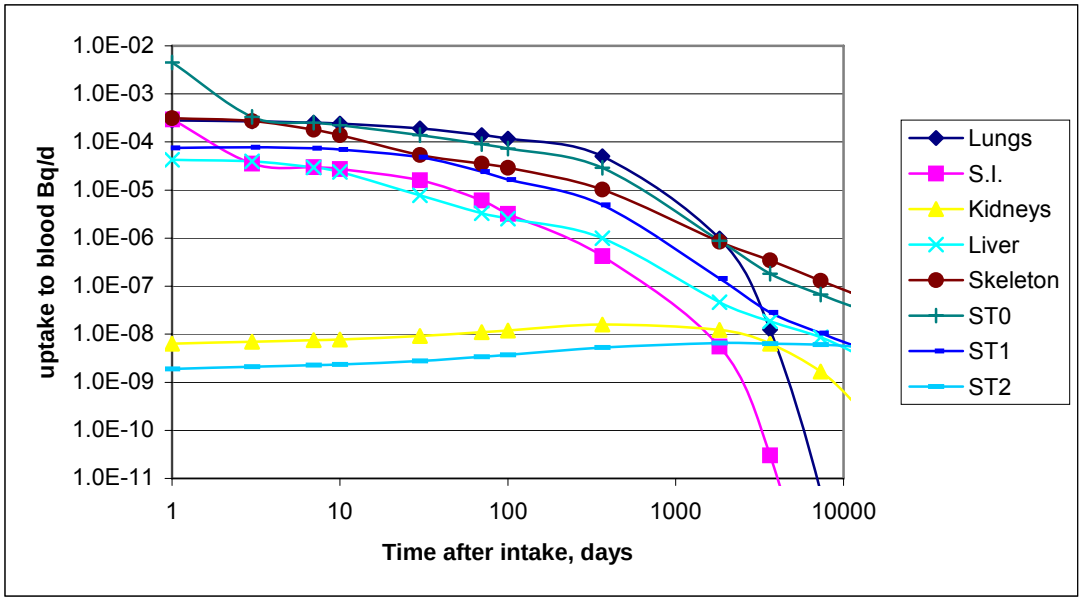

Figure 7 Uptake to blood from lungs, small intestine (SI) and secondary systemic sites of deposition following inhalation of 1 Bq ^{234}U calculated using the central values and the ICRP Publication 69 systemic model for uranium (ICRP, 1995b). STO, ST1 and ST2 are the three soft tissue compartments.

4.2 Uncertainty analysis

Figure 8 shows the median, lower 2.5%-percentile, $L_{2.5\%}$, and upper 97.5-percentile, $U_{97.5\%}$, of the distribution of committed effective dose assessed from 1 ng DU measured in a 24-hour urine sample obtained over the range 10–10,000 days after intake, using the methods described in Section 3.4. It should be noted, however, that this analysis considers only uncertainty and variability in parameters associated with the inhalation model. It does not include uncertainty associated with the measurement itself (which will depend on the technique, and the amount of DU and natural uranium present in the sample), nor of uncertainty and variability in parameters associated with the systemic uranium model.

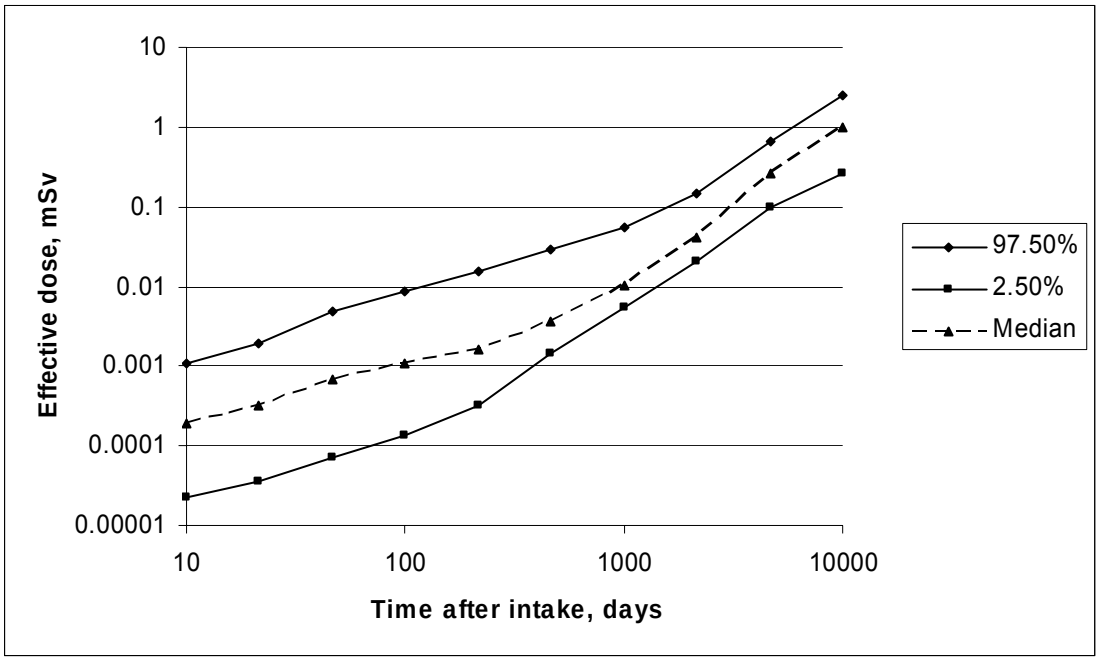

Figure 8 Uncertainty in committed effective dose assessed from 1 ng DU measured in a 24-hour urine sample.

For the median, the committed effective dose assessed from 1 ng DU d^{-1} increases from about 0.1 μSv at 10 days after intake to about 1 mSv at 10,000 days. At 10 days after intake $L_{2.5\%}$ is about a factor of 10 below the median and $U_{97.5\%}$ is about a factor of 6 above it, giving an overall range ($U_{97.5\%}/L_{2.5\%}$) of about 50. As the time between intake and sampling increases, the range decreases, so that between 1000 and 10,000 days, $U_{97.5\%}$ is between 7 and 10 times $L_{2.5\%}$. Despite the large uncertainty, even 'maximum' assessed doses from 1 ng DU d^{-1} are below 1 mSv up to 5000 d.

Figure 9 shows corresponding results for committed equivalent dose to the lungs. As noted above, for inhalation of uranium in moderately soluble or insoluble forms, lung dose makes the dominant contribution to effective dose. Thus the pattern for lung dose is very similar to that for effective doses, with numerical values about 10 times higher, reflecting the value of 0.12 for the lung tissue weighting factor.

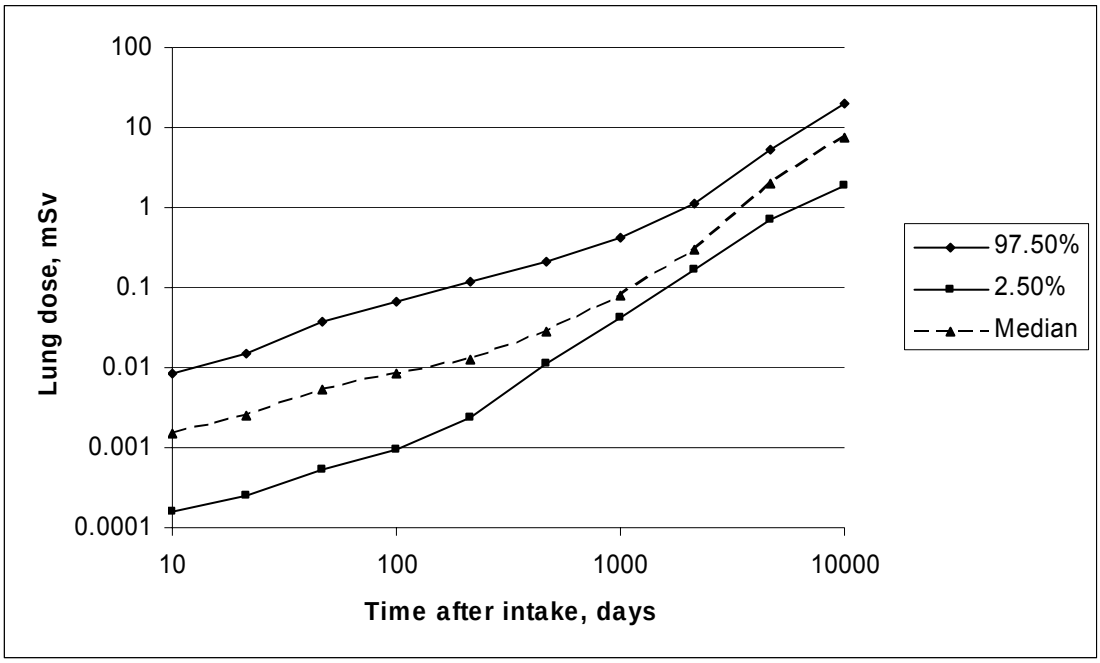

Figure 9 Uncertainty in committed equivalent lung dose assessed from 1 ng DU measured in a 24-hour urine sample

As noted in the Introduction, for the purpose of this study it is assumed that intakes occur entirely by inhalation, although there could be a contribution from ingestion such as that resulting from inadvertent hand-to-mouth transfer. Committed effective doses assessed from 1 ng DU measured in a 24-hour urine sample obtained over the range 10–10,000 days after intake were calculated for f_1 values of 0.02 (the highest value considered), 0.003 and 0.0008 (the central and low values considered in the sensitivity analysis, Table 20). Results are compared with the range obtained in the uncertainty analysis for intake by inhalation in Figure 10. The assessed dose increases as f_1 decreases. At early times (less than about 40 days) and at late times (greater than about 2000 days), doses assessed following intake by ingestion are below the range for inhalation, for all values of f_1 considered. At intermediate times the range of doses assessed following ingestion overlaps with the lower part of the range of doses following inhalation.

An indicative uncertainty analysis was carried out as a preliminary to the full uncertainty analysis, as described in Appendix A. Resulting committed effective doses are compared in Figure 11. The median from the uncertainty analysis lies close to the central value from the indicative analysis, as expected. The range of values obtained in the full uncertainty analysis is narrower than that obtained from the indicative analysis, even though two additional sources of uncertainty were included: intersubject variation in deposition in the extrathoracic airways, and model uncertainties in slow bronchial clearance, demonstrating that the indicative analysis overestimates the range. However, the minimum values from the indicative analysis are close to the $L_{2.5\%}$ values at all times, whereas the maximum values from the indicative analysis are consistently higher than the $U_{97.5}$ values, especially at times up to 1000 days.

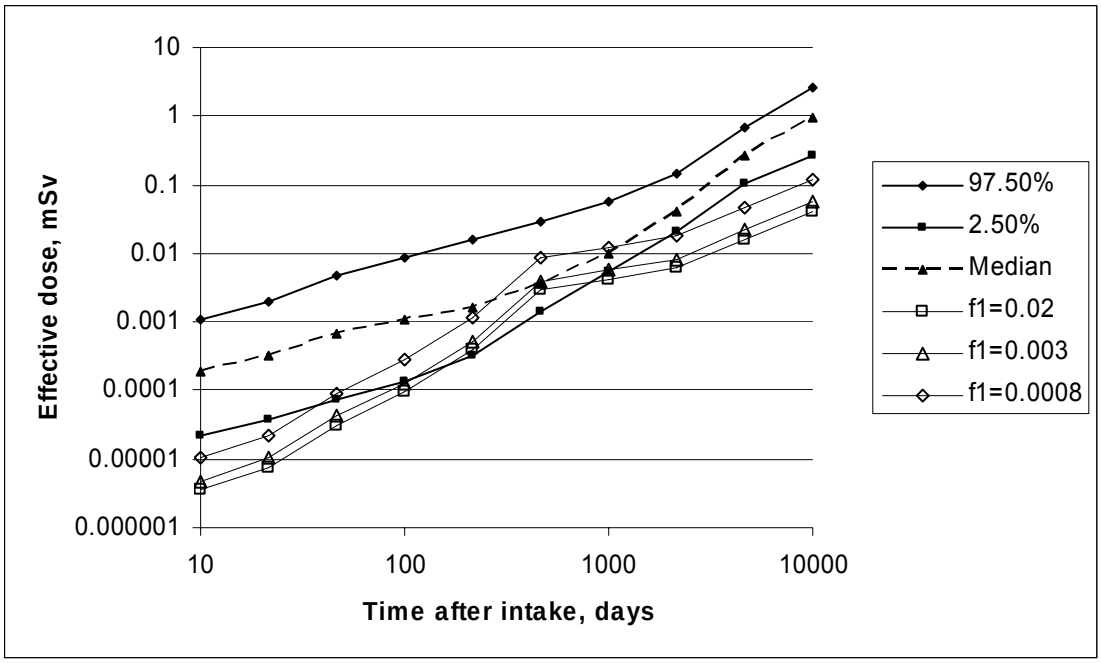

Figure 10 Uncertainty in committed effective dose assessed from 1 ng DU measured in a 24-hour urine sample for intake by inhalation, compared with range assessed for intake by ingestion

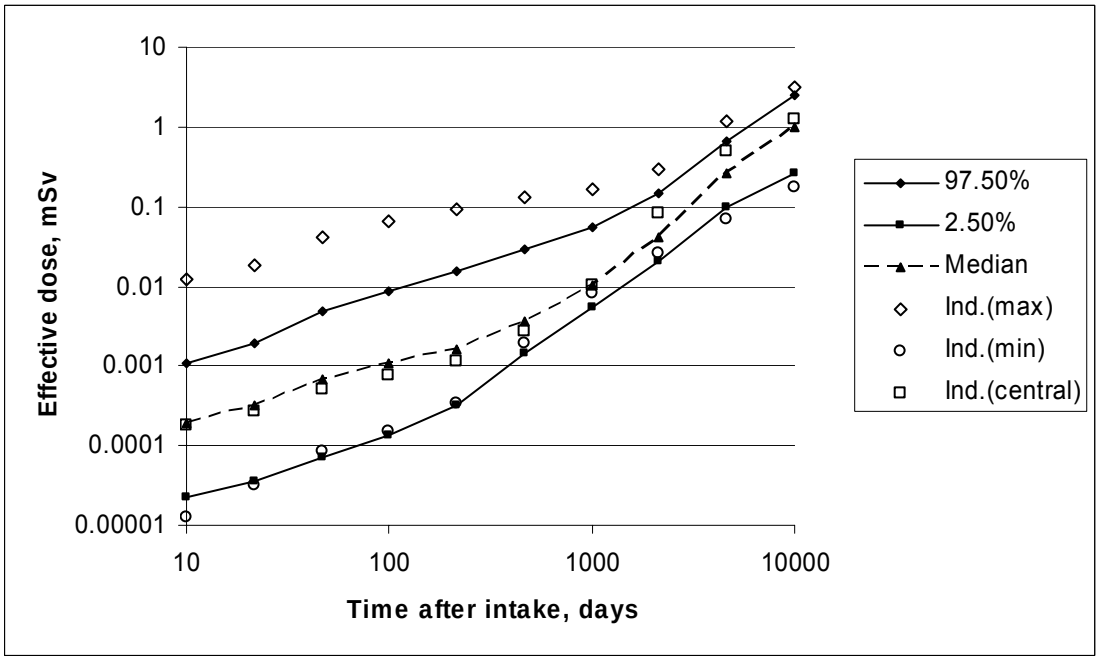

Figure 11 Uncertainty in committed effective dose assessed from 1 ng DU measured in a 24-hour urine sample, compared with 'indicative' uncertainty.

Figure 12 compares the results of the uncertainty analysis with effective doses assessed using Type M and Type S parameter values. Note however, that in these cases all other parameters are at their central values, so that the differences reflect only the differences in absorption parameter values. As expected from consideration of sensitivity (Table 24), results for Type M are similar to the central values, and those for

Type S are much higher, except at late times. Indeed, up to about 500 days after intake results for Type S are above the upper 97.5%-percentile values.

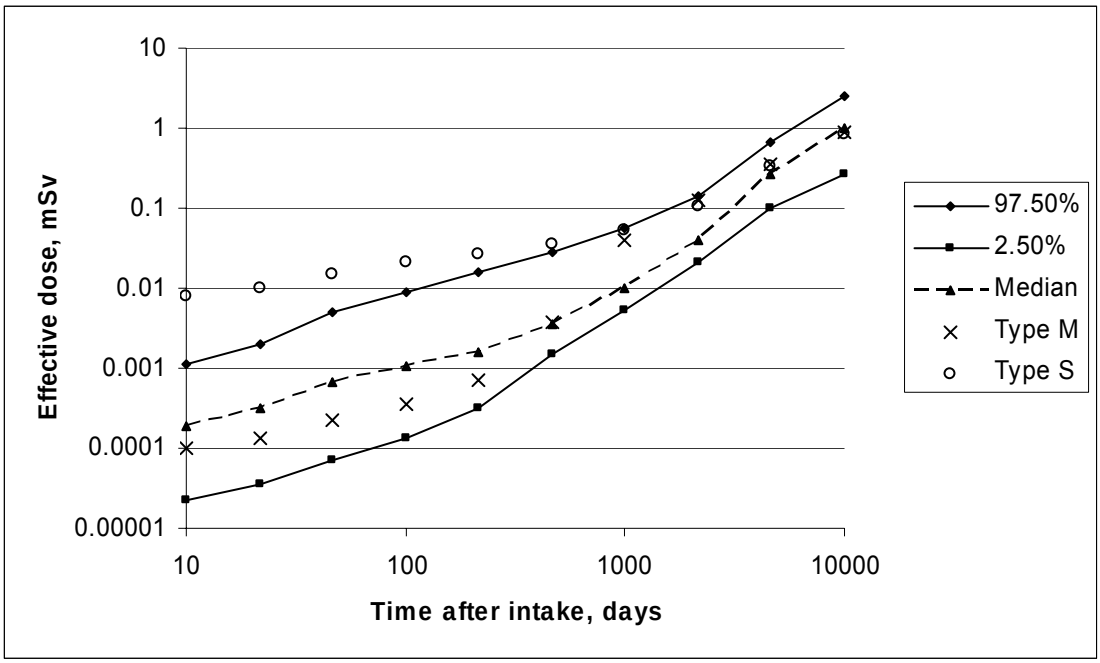

Figure 12 Uncertainty in committed effective dose assessed from 1 ng DU measured in a 24-hour urine sample, compared with default Type M and Type S assumptions.

5 CONCLUSIONS

Information has been reviewed relating to the application of the HRTM to assess intakes, committed doses and maximum concentrations of uranium in the kidneys ($^{max}[U]_k$) from measurements of DU in urine samples taken at long times (100 to 10,000 days) after possible intakes. Consideration was given to Level I and Level II exposure scenarios, because these are considered to have potential to give rise to the highest exposures. There is extensive relevant information that enables reasonable estimates to be made of central values and ranges for relevant parameter values, including those specific to DU exposures following the use of DU munitions in conflicts. A considerable amount of relevant new information has become available since publication of the assessments carried out by the RSWG, in particular the extensive information on the characteristics of aerosols formed by the impact of DU penetrators on armoured vehicles provided by the Capstone Aerosol Study.

For exposures to aerosols formed within a struck vehicle, more than 80 sets of measurements of size distribution made within 5 minutes after impact on non-DU armour are available from the Capstone Study. From these, representative central values and ranges were taken to be: AMAD 2.5 μm (range 0.4 – 13 μm) and GSD 6 (range 2 – 15). The relatively few measurements made outside struck vehicles and through resuspension by disturbance during recovery work activities (about 10 each)

were consistent with these values and so they were chosen to represent all Level I and II exposures.

Based on a review of the literature, HRTM parameter values for heavy exercise and light exercise were taken to be central values for Level I and II respectively. It was considered that ventilation rates (m^3 h^{-1}) might range from 0.5 to 2 times the central value, with similar contributions from variations in breathing frequency and in tidal volume.

For particle transport from the respiratory tract, HRTM default values were taken to be central values. Based on detailed discussion in ICRP Publication 66, which describes the HRTM and its basis, for each particle transport rate, a range of a factor of three either side of the central value was taken here to account for uncertainty in the central value and inter- and intra-subject variability around it. For simplicity, it was assumed that all particle transport rates are correlated, *i.e.* all rates are increased or decreased by a factor of three. For slow clearance in the bronchial tree, an alternative (KI Model) was applied based on the results of recent experimental studies to investigate the phenomenon.

For absorption of uranium from the respiratory tract to blood, consideration was given to both *in vitro* results on materials that are directly relevant, especially those available from the Capstone Study, and *in vivo* results on similar uranium oxides. Central values and ranges were selected for DU dust that might originate from either penetrator impact or combustion. Representative central values and ranges were chosen to be: rapid fraction f_r = 0.15 (range 0.01 – 0.5); rapid dissolution rate s_r = 3 d^{-1} (range 0.3 – 20 d^{-1}) and slow dissolution rate s_s = 0.002 d^{-1} (range 0.0001 – 0.005 d^{-1}).

An analysis was carried out of the sensitivity to uncertainty and variability in each parameter value, of committed lung dose, effective dose, and $^{max}[U]_k$, for unit intake of DU, and for that calculated from a measurement of DU in urine at times in the range 100–10,000 days after intake.

Results for lung and effective dose were very similar. For doses per unit intake (DPUI), some parameters were identified in all four categories (aerosol size; breathing; absorption to blood and particle transport) for which the range in values led to changes in dose greater than 20%. For doses assessed from a measurement of DU in a 24-hour urine sample, generally the same sub-set of parameter values leading to large changes was identified as for DPUI. The most striking finding was the importance of the value of s_s, and how its effect changes with the time between intake and sampling. For example, for a urine sample at 500 days after intake, the dose assessed for a value of s_s at the low end of the range (0.0001 d^{-1}) is about ten times the dose assessed with the central value (0.002 d^{-1}). As expected from inspection of the parameter values, results for Type M are similar to those for the 'high' value of s_s, but some of those for Type S were outside the range, showing the importance of using specific values in such assessments.

Generally a similar sub-set of parameter values leading to changes greater than 20% was identified for assessments of $^{max}[U]_k$ (Appendix A). However, in some cases the effects were in the opposite direction from those for doses. Changes to the absorption parameter values had most effect, especially changes to f_r.

Combinations of high and low parameter values from the ranges were used to give an 'indication' of the overall uncertainty in doses and $^{max}[U]_k$ assessed from measurement of DU in a 24-hour urine sample at times in the range 10–10,000 days after intake (Appendix A). 'Central' values of dose and $^{max}[U]_k$ were calculated using the central values chosen for all parameters. 'Minimum' and 'maximum' values were obtained using all combinations of high and low parameter values as described above.

As well as central values and ranges, probability density functions were estimated for all relevant HRTM parameter values. These were used to carry out a full uncertainty analysis of doses and assessed from measurement of DU in a 24-hour urine sample at times in the range 10–10,000 days after intake.

The median value of committed effective dose assessed from 1 ng DU d^{-1} increased from about 0.1 μSv at 10 days after intake to about 1 mSv at 10,000 days. At 10 days after intake the lower 2.5-percentile, $L_{2.5\%}$, is about a factor of 10 below the median and the upper 97.5-percentile, $U_{97.5\%}$, is about a factor of 6 above it, giving an overall range ($U_{97.5\%}/L_{2.5\%}$) of about 50. As the time between intake and sampling increases, the range decreases, so that between 1000 and 10,000 days, $U_{97.5\%}$ is between 7 and 10 times $L_{2.5\%}$. Despite the large uncertainty, even 'maximum' assessed doses from 1 ng DU d^{-1} are below 1 mSv up to 5000 d. A similar pattern of results was obtained for lung doses.

The range of values obtained in the full uncertainty analysis is narrower than that obtained from the indicative analysis, even though two additional sources of uncertainty were included: intersubject variation in deposition in the extrathoracic airways, and model uncertainties in slow bronchial clearance, demonstrating that the indicative analysis overestimates the range. However, the minimum values from the indicative analysis are close to the $L_{2.5\%}$ values at all times, whereas the maximum values from the indicative analysis are consistently higher than the $U_{97.5\%}$ values, especially at times up to 1000 days.

For the central values, $^{max}[U]_k$ assessed from 1 ng DU d^{-1} increases from about 10^{-5} μg per gram at 10 days after intake, to about 0.1 μg per gram at 10,000 days. At 10 days after intake the minimum is about a factor of four below the central value and the maximum is about a factor of two above it. At later times, the range increases, so that between 200 and 10,000 days, the maximum is between 300 and 900 times the minimum. Nevertheless, despite the large uncertainty, Nevertheless, despite the large uncertainty (which is probably overestimated, as it was for the indicative uncertainty analysis of doses), even maximum assessed values of $^{max}[U]_k$ from 1 ng DU d^{-1} are below 1 μg per gram at all times considered.

For the first part of the sensitivity analyses, consideration is given to doses (and $^{max}[U]_k$) resulting from 1 mg DU. For the second part of the sensitivity analyses, and for the uncertainty analyses, consideration is given to doses (and $^{max}[U]_k$) assessed from a measurement of 1 ng DU in urine. It is considered that the results can be scaled linearly to other intakes and measurements over wide ranges.

6 RECOMMENDATIONS FOR RESEARCH TO REDUCE UNCERTAINTIES

The sensitivity analysis identified some parameters in all four categories (aerosol size; breathing characteristics; absorption to blood and particle transport) for which the range in likely values led to changes in doses (and $^{max}[U]_k$) greater than 20%. However, the largest effects were seen for parameters related to absorption to blood. The Capstone Study included dissolution measurements on nearly 30 samples, and with results from other studies provides a reasonable amount of information, especially about the fraction that dissolves rapidly. However, these studies had two major limitations: (i) they were *in vitro* tests, and leave open the question of extrapolation to dissolution in the human lungs (ii) they were of relatively short duration, 46 days in the case of the Capstone Study, by which time most of the material was still undissolved. While some allowance for the latter was made in the sensitivity and indicative uncertainty analysis carried out here, no additional factor was included for uncertainty related to extrapolation from *in vitro* tests to man. Although one might have been, it would have been a matter of judgement to quantify it.

It is therefore recommended that consideration be given to conducting limited *in vivo* measurements of dissolution of suitable particles. The main objective would be to validate (or provide a correcting factor) for *in vitro* tests, and so would only be applied to a small number of selected samples. Information available to us suggests that no impact tests are planned that might provide samples, but it is likely that material remains from the Capstone Study. To maximise the value of a study:

- Direct comparisons should be made between dissolution *in vivo* and dissolution *in vitro* using exactly the same methodology as used in the Capstone Study, to validate the measurements made there.
- *In vivo* measurements should be made on more than one species (*e.g.* rat and guinea pig) to address the issue of variation between species.
- Measurements should be made over a suitably long period (about a year). To do so *in vivo* might well require mass spectrometric measurements of DU specifically, rather than of total uranium, because of the presence of natural uranium in diet, and hence excreta.
- Comparative measurements should be made under the same conditions on samples of well defined uranium oxides (*e.g.* UO_3 and U_3O_8), to enable the behaviour of DU dusts to be compared to that of materials that have been studied more extensively.

An important feature of the assessments considered here, which limits the potential for research to reduce uncertainties, is the variability associated with the exposure scenario itself. For example, the Capstone Study provides comprehensive information on the size distribution of the DU aerosol as a function of time after impact. However, such a wide range was observed in the central value (AMAD), that however well its frequency distribution is known there will be considerable uncertainty about the value for exposure

of an individual in a particular incident. (In the case of dissolution, there is considerable scope to reduce the uncertainty in the distribution of likely values.)

Thus consideration should also be given to a study to design monitoring programmes that might be carried out on personnel exposed in an incident, to reduce uncertainties in their assessed doses and $^{max}[U]_k$, by providing information on the behaviour of the material to which they were actually exposed. For example, if the exposure were high enough for lung deposition to be measurable directly (by so-called "whole body" or *in vivo* monitoring), comparison of lung content and urinary excretion would provide information on dissolution in the lungs. (However, the minimum detectable activity of DU in the lungs is about 10 mg (WHO 2001), and this requires specialised laboratory facilities). The *in vivo* studies proposed above would provide data sets that could be used as input to such a study. The data sets generated in an *in vivo* experiment would be more extensive than any data set likely to be obtained for an individual exposed in the field, but subsets could be used to give guidance on simulating 'field' data sets. Software such as that being developed for uncertainty analysis could be used to investigate optimisation of monitoring with respect to uncertainty in assessed dose.

7 ACKNOWLEDGEMENTS

T P Fell carried out the calculations of uptake to blood from various deposition sites using PLEIADES, which are shown in Figure 7.

8 REFERENCES

AEPI (Army Environmental Policy Institute) Health and Environmental Consequences of Depleted Uranium Use in the US Army. Technical Report June 1995. on http://www.aepi.army.mil.

Anderson I, Camner P, Jensen PL, et al (1974). A comparison of nasal and tracheobronchial clearance. *Arch Environ Health* **74**, 290–293.

Andersen M, Philipson K, Svartengren M and Camner P (1995). Human deposition and clearance of 6 µm particles inhaled with an extremely low flow rate. *Exp Lung Res* **21**, 187-195.

Anderson E, Braune N, Duletsky S, et al (1985). Development of Statistical Distributions of Ranges of Standard Factors in Exposure Assessments. EPA 600/8.85/010 Environmental Protection Agency, Washington, D.C.

Bailey MR (1994). The new ICRP model for the respiratory tract. *Radiat Prot Dosim* **53**, 107-114.

Bailey MR (2001). Summaries of source documents relating to DU penetrator impacts. Annexe G to the Health Hazards of Depleted Uranium Munitions Part I. Policy Document 6/01, London, United Kingdom. Online report available at www.royalsoc.ac.uk/du.

Bailey MR and Marsh C (2001). Exposures arising from the use of depleted uranium on the Battlefield. Appendix 1 to the Health Hazards of Depleted Uranium Munitions Part I. Policy Document 6/01, London, United Kingdom. Online report available at www.royalsoc.ac.uk/du.

Bailey MR and Phipps AW (2001). Current ICRP models used to assess intakes of uranium. Annexe A to the Health Hazards of Depleted Uranium Munitions Part I. Policy Document 6/01, London, United Kingdom. Online report available at www.royalsoc.ac.uk in the Science Policy Section.

Bailey MR and Roy M (1994). Annexe E. Clearance of particles from the respiratory tract. Human Respiratory Tract Model for Radiological Protection. ICRP Publication 66, *Annals of the ICRP* **24** (1-3), 301–413.

Bailey MR, Guilmette, RA, Jarvis, NS and Roy M (1998). Practical application of the new ICRP Human Respiratory Tract Model. *Radiat Prot Dosim* **79**(1-4), 17-22.

Bailey MR, Ansoborlo E, Guilmette RA and Paquet F (2003). Practical application of the ICRP Human Respiratory Tract Model. *Radiat Prot Dosim* **105**(1-4), 71-96.

Bailey MR, Dorrian M-D and Birchall A (1995). Implications of airway retention for radiation doses from inhaled radionuclides. *J Aerosol Med* **8,** 373–390.

Bailey MR, Harrison JD, Jones KA, et al (1997). Uncertainties in aspects of internal dosimetry relevant to accident consequence assessment codes. Chilton NRPB-M763.

Barber JM and Forrest RD (1995). A study of uranium lung clearance at a uranium processing plant. *Health Phys* **68**, 661-669.

Birchall A, Puncher M, James AC, et al (2003). IMBA Expert^{TM}: Internal dosimetry made simple. *Radiat Prot Dosim* **105**, 421-425.

Birchall A, Puncher M, Marsh JW, et al (2007) IMBA Professional Plus: A Flexible Approach to Internal Dosimetry. *Radiat Prot Dosim.* (in press).

DUOB (Depleted Uranium Oversight Board) Final Report of the Depleted Uranium Oversight Board submitted to the Undersecretary of State for Defence. www.duob.org.uk/final_report_Feb2007.pdf.

Eidson AF (1990). Biological Characterisation of Radiation Exposure and Dose Estimates for Inhaled Uranium Milling Effluents. NUREG/CR–5489 TI90 012914, U.S. Nuclear Regulatory Commission.

Eidson AF and Damon EG (1985a). Biologically significant properties of refined uranium ore, in Int. Conf. on Occupational Radiation Safety in Mining, Stocker, H., Ed., Canadian Nuclear Association, Ontario, Canada, 1, 248.

Eidson AF and Damon EG (1985b). Comparison of uranium retention in dogs exposed by inhalation to two forms of yellowcake, in Int. Conf. on Occupational Radiation Safety in Mining, Stocker, H., Ed., Canadian Nuclear Association, Ontario, Canada, 1, 261.

Ellender M (1987). The clearance of uranium after deposition of the nitrate and bicarbonate in different regions of the rat lung. *Human Toxicol* **6**, 479.

Falk R, Philipson K, Svartengren M, Jarvis NS, Bailey MR and Camner P (1997). Clearance of particles from small ciliated airways. *Exp Lung Res* **23**, 495-515.

Falk R, Philipson K, Svartengren M, Bergmann R, Hofmann W, Jarvis N, Bailey M and Camner P (1999). Assessment of long-term bronchiolar clearance of particles from measurements of lung retention and theoretical estimates of regional deposition. *Exp Lung Res* **25**, 495-516.

Fell TP, Phipps AW and Smith TJ (2007) The internal dosimetry code PLEIADES (submitted to *Radiat. Prot. Dosim.*)

Glissmeyer JA and Mishima J (1979). Characterization of Airborne Uranium from Test Firings of XM774 Ammunition. Pacific Northwest Laboratory. PNL-2944. Richland, WA.

Godfrey S, Davies CTM, Wozniak E and Barnes CA (1971). Cardio-respiratory response to exercise in normal children. *Clin Sci*, **40**, 419–431.

Guilmette RA, Birchall A and Jarvis NS (1998). Effect of uncertainty in nasal airway deposition of radioactive particles on effective dose. *Radiat Prot Dosim* **79**, 245–248.

Harrison JD, Leggett RW, Noßke D, et al (2001). Reliability of the ICRP's dose coefficients for members of the public, II. Uncertainties in the absorption of ingested radionuclides and the effect on dose estimates. *Radiat Prot Dosim* **95**, 295-308.

Harrison JD, Fell TP, Pellow PGD, Phipps AW and Puncher M (2007). Uncertainty analysis of the ICRP systemic model for uranium as applied to interpretation of bioassay data for depleted uranium. Chilton HPA-RPD-024.

Heyder J, Gebhart J, Stahlhofen W and Stuck B (1982). Biological variability of particle deposition in the human respiratory tract during controlled and spontaneous mouth-breathing. Inhaled Particles V, *Ann Occup Hyg,* **26**, 137-148.

Hodgson A, Pellow PGD, and Stradling GN (2007) Influence of nephrotoxicity on urinary excretion of uranium. Chilton HPA-RPD-025.

Hofmann W, Morawska L and Bergmann R (2001). Environmental tobacco smoke deposition in the human respiratory tract: differences between experimental and theoretical approaches. J Aerosol Med 14(3), 317-26.

ICRP (1975). Report of the Task Group on Reference Man, ICRP Publication 23. Pergamon Press, Oxford.

ICRP (1979). Limits for intakes of radionuclides by workers, ICRP Publication 30, Part 1, *Annals of the ICRP* **2**(3/4), Pergamon Press, Oxford.

ICRP (1991). 1990 Recommendations of the International Commission on Radiological Protection, ICRP Publication 60. *Annals of the ICRP* **21**(1–3), Pergamon Press, Oxford.

ICRP (1994a). Human respiratory tract model for radiological protection, ICRP Publication 66, *Annals of the ICRP* **24**(1-3), Elsevier Science Ltd., Oxford.

ICRP (1994b). Dose coefficients for intakes of radionuclides by workers, ICRP Publication 68, *Annals of the ICRP* **24**(4), Elsevier Science Ltd., Oxford.

ICRP (1995a). Age-dependent doses to members of the public from intake of radionuclides: Part 4 Inhalation dose coefficients, ICRP Publication 71, *Annals of the ICRP* **25**(3–4), Elsevier Science Ltd., Oxford.

ICRP (1995b). Age-dependent doses to members of the public from intake of radionuclides: Part 3 Ingestion dose coefficients, ICRP Publication 69. *Annals of the ICRP* **25** (1). Elsevier Science Ltd., Oxford.

ICRP (1996). Age-dependent doses to members of the public from intake of radionuclides: Part 5 Compilation of ingestion and inhalation dose coefficients, ICRP Publication 72. *Annals of the ICRP* **26**(1), Elsevier Science Ltd., Oxford.

ICRP (1997). Individual monitoring for internal exposure of workers, replacement of ICRP Publication 54, ICRP Publication 78, *Annals of the ICRP* **27**(3/4), Elsevier Science Ltd., Oxford.

ICRP (2001). Doses to the embryo and fetus from intake of radionuclides by the mother, ICRP Publication 88, *Annals of the ICRP* **31**(1–3), Elsevier Science Ltd., Oxford.

ICRP (2002). Guide for the practical application of the ICRP human respiratory tract model, Supporting Guidance 3, *Annals of the ICRP* **32**(1–2), Elsevier Science Ltd., Oxford.

ICRP (2004). Doses to infants from ingestion of radionuclides in mother's milk, ICRP Publication 95, *Annals of the ICRP* **34**(3–4), Elsevier Science Ltd., Oxford.

Jarvis NS, Birchall A, James AC, et al (1996). LUDEP 2.0 Personal computer program for calculating internal doses using the ICRP Publication 66 respiratory tract model. Chilton, NRPB-SR287.

Jette SJ, Mishima J and Haddock DE (1990). Aerosolization of M829A1 and XM900E1 Rounds Fired Against Hard Targets, Report PNL-7452, Richland, WA: Battelle Pacific Northwest Laboratory, August 1990. (Reference in AEPI, 1995; OSAGWI, 1998, Tab M). [Restricted circulation, summary #31 in OSAGWI, 2000, Tab L.]

Kreyling WG, Semmler M and Möller W (2004). Dosimetry and toxicology of ultrafine particles. J *Aerosol Med* **17**, 140-152.

Leggett RW and Harrison J.D (1995) Fractional absorption of ingested U in humans. *Health Phys.* **68**, 1-15.

Malarbet JL, Bertholon JF, Becquemin MH, et al (1994). Oral and nasal flowrate partitioning in healthy subjects performing graded exercise. *Rad Prot Dosim* **53**, 179-182.

Mansur ES and Carvalho SM (1988). Solubility classification of yellowcake produced by a Brazilian uranium mill, Report IRPA 1988, vol. III, Pergamon Press, Sydney.

McDiarmid MA, Squibb K, and Engelhardt, SM (2004). Biologic monitoring for urinary uranium in Gulf War I veterans. *Health Phys* **87,** 51-56.

McKay MD, Beckman RJ, Conover WJ (1979). A comparison of three methods for selecting values of input variables in the analysis of output from a computer code. *Technometrics* **21**, 239-245.

Meddings DR and Haldimann M (2002). Depleted uranium in Kosovo: an assessment of potential exposure for aid workers, *Health Phys* **82,** 467-472.

Métivier H, Poncy JL, Rateau G, et al (1992). Uranium behaviour in the baboon after the deposition of a ceramic form of uranium dioxide and uranium octoxide in the lungs: implications for human exposure. *Radioprotection* **27**(3), 263-281.

Miller FW, Martonen TB, Ménache MG, et al (1988). Influence of breathing mode and activity level on regional deposition of inhaled particles and implications for regulatory standards. In: *Inhaled Particles VI. Ann Occup Hyg* **32** (*Suppl* 1), 3–10.

Morrow PE, Gibb FR and Beiter HD (1972). Inhalation studies of uranium trioxide. *Health Phys* **23**, 273-280.

Niinimaa V, Cole P, Mintz S and Shephard RJ (1980). The switching point from nasal to oronasal breathing. *Respir Physiol* **42**, 61–71.

Niinimaa V, Cole P, Mintz S and Shephard RJ (1981). Oronasal distribution of respiratory airflow. *Respir Physiol* **43**, 69–75.

Ough EA, Lewis BJ, Andrews WS, Bennett LG, Hancock RG, and Scott K (2002). An examination of uranium levels in Canadian forces personnel who served in the Gulf War and Kosovo, *Health Phys* **82**, 527-532.

Parkhurst MA, Daxon EG, Lodde GM, et al (2004a). Depleted Uranium Aerosol Doses and Risks: Summary of US Assessments PNWD-3476. Prepared for the US Army by Battelle.

Parkhurst MA, Szrom F, Guilmette RA, et al (2004b). Capstone Depleted Uranium Aerosols: Generation and Characterization, Volumes 1. Main Text. Attachment 1 of Depleted Uranium Aerosol Doses and Risks: Summary of US Assessments. PNNL-14168, Prepared for the US Army by Pacific Northwest National Laboratory, Richland, Washington.

Parkhurst MA, Szrom F, Guilmette RA, et al (2004c). Capstone Depleted Uranium Aerosols: Generation and Characterization, Volume 2. Appendices. Attachment 2 of Depleted Uranium Aerosol Doses and Risks: Summary of US Assessments. PNNL-14168, Prepared for the US Army by Pacific Northwest National Laboratory, Richland, Washington.

Parrish RR, Thirlwall MF, Pickford C, Horstwood M, Gerdes A, Anderson J, and Coggon D (2006). Determination of $^{238}U/^{235}U$, $^{236}U/^{238}U$ and uranium concentration in urine using SF-ICP-MS and MC-ICP-MS: an interlaboratory comparison, *Health Phys* **90,** 127-38.

Philipson K, Falk R, Svartengren M, et al (2000). Does lung retention of inhaled particles depend on their geometric diameter? *Exp Lung Res* **26,** 437–455.

Portuguese Nuclear and Technological Institute, Radiological Protection and Nuclear Safety Department (2001). Report of the Portuguese Scientific Mission to Kosovo and to Bosnia-Herzegovina for assessment of radioactive contamination and of the radiological risk due to the use of depleted uranium ammunitions.

Puncher M, Birchall A. (2007). Estimating uncertainty on dose assessments. (Submitted to *Radiat Prot Dosim*.)

Roth P, Werner E and Paretzke HG (2001). A study of uranium excreted in urine. An assessment of protective measures taken by the German Army KFOR Contingent. GSF - National Research Center for Environment and Health, Institute of Radiation Protection, Neuherberg, Germany. GSF Report 3/01. Available at www.nato.int/du/docu/ge010229a.pdf (2001). Accessed May 2006.

Royal Society (2001) The Health Hazards of Depleted Uranium Munitions Part I. Policy Document 6/01, London, United Kingdom. Online report available at www.royalsoc.ac.uk/du.

Royal Society (2002) The Health Hazards of Depleted Uranium Munitions Part I. Policy Document 5/02, London, United Kingdom. Online report available at www.royalsoc.ac.uk/du.

Scripsick RC, et al (1985a). Preliminary study of uranium oxide dissolution in simulated lung fluid, Report LA-10268-MS, Los Alamos National Laboratory. http://lib-www.lanl.gov/la-pubs/00318819.pdf.

Scripsick RC et al (1985b). Differences in *in vitro* dissolution properties of settled and airborne uranium material, in *Occupational Radiation Safety in Mining,* Stocker, H., Ed., Canadian Nuclear Association 255. http://lib-www.lanl.gov/la-pubs/00374828.pdf.

Smith JRH (2003). Implications of human nasal clearance studies for the interpretation of nose blow and bioassay sample measurements. *Radiat Prot Dosim* **105**, 190–122.

Smith JRH, Bailey MR, Etherington G, Shutt A, Youngman M J. (2007a) Effect of particle size on slow particle clearance from the bronchial tree, (Submitted to *Exp. Lung Res*.)

Smith JRH, Bailey MR, Etherington G, Shutt A, Youngman M J. (2007b) Further study of the effect of particle size on slow particle clearance from the bronchial tree (Submitted to *Radiat Prot Dosim*.)

Svartengren K, Philipson K, Svartengren M, Nerbrink O and Camner P (1995). Clearance in smaller airways of inhaled 6 μm particles in subjects with immotile-cilia syndrome. *Exp Lung Res* **21**, 667-682.

Svartengren M, Sommerer K, Scheuch G, Kohlhaeufl M, Heyder J, Falk R, Bergmann R, Hofmann W, Bailey MR, Philipson K and Camner P (2001). Comparison of clearance of particles inhaled with bolus and extremely slow inhalation techniques. *Exp Lung Res* **27**, 367-386.

Ting BT, Paschal DC, Jarrett JM, Pirkle JL, Jackson RJ, Sampson EJ, Miller DT and Caudill SP (1999). Uranium and thorium in urine of United States residents: Reference range concentrations. Environmental Research Section A 81, 45–51.

West CM, Scott L and Schultz NB (1979). Sixteen years of uranium personnel monitoring experience, in retrospect, *Health Phys* **36**, 665-669.

WHO (2001) World Health Organisation. Depleted Uranium: Sources, Exposure and Health Effects. Report WHO/SDE/PHE/01.1, Geneva, WHO.

APPENDIX A

Indicative uncertainty analysis of the HRTM applied to interpretation of bioassay data for depleted uranium

A1 INTRODUCTION

For a full uncertainty analysis, a frequency distribution is assigned to the value of each parameter, and probability distributions of the outcomes (doses and maximum kidney concentrations, $^{max}[U]_k$) calculated a large number of times using parameter values obtained by sampling each distribution (Section 3.1.4). In order to do this new software had to be designed, written and tested. While this was done, a simpler approach was taken to provide provisional results. This Appendix describes an assessment of 'indicative' uncertainties in doses assessed from a urine sample, based on simple combinations of uncertainties related to individual parameters, which was carried out in advance of the full uncertainty analysis. Again only uncertainty and variability in HRTM parameter values are considered. However, it also includes sensitivity and indicative uncertainty analyses of $^{max}[U]_k$ assessed from a urine sample, although these were beyond the scope of the contract.

The approach follows that adopted (for similar reasons) in the assessments carried out by the Royal Society Working Group on the Health Hazards of Depleted Uranium Munitions (RSWG, Royal Society, 2001, 2002). The RSWG calculated a "central" estimate, which was intended to be a best estimate of the population average, so that multiplying it by the number exposed would give an assessment of the total health impact. This is based on parameter values considered to be "likely", or where information is lacking, unlikely to underestimate exposures greatly. The corresponding parameter values may be considered to be the "most appropriate parameter values for use in biokinetic modelling relating to intakes of DU munitions debris".

The RSWG also made "worst case" estimates, which were intended to be values that it was unlikely that any individual would exceed. These were based on values at the upper end of the likely ranges, but not extreme theoretical possibilities. For some parameters, different values apply to the worst case for radiation dose, from those that apply to the worst case for kidney concentration. Radiation doses tend to be higher when the rate at which the inhaled DU dissolves is low, because of longer retention in the lungs. Conversely, the maximum kidney concentration tends to be higher when the dissolution rate is high, so that uptake to blood and hence kidneys is rapid. Parameter values corresponding to such "worst case" assessments may well correspond to upper or lower ends of ranges.

DU present in a urine sample can be considered as arising mainly from two sources:

- dissolution in the respiratory and gastro-intestinal (GI) tracts followed by "prompt" excretion (within a day or so)
- releases from long-term sites of systemic retention, such as the skeleton.

It is likely that immediately after intake, the former will dominate, but as time goes by its relative contribution will decrease, because both the amount in the respiratory tract, and the dissolution rate, tend to decrease with time.

As described in Sections 2.3 – 2.5 of the main text, there are three main sets of HRTM parameter values relevant to this issue, those that determine:

- the initial pattern of deposition in the respiratory tract;
- particle transport rates from each part of the respiratory tract;
- the rates of absorption to blood.

For both clearance pathways there are two distinct phases, as a result of which, one set of parameter values dominates uptake to blood during the first day or so, and another at later times. In most of the likely scenarios, a large fraction of the inhaled DU is deposited in the upper respiratory tract (URT, the airways of the nose, throat, bronchial tree etc), from which particle transport to the GI tract is rapid (time-scales of minutes to hours). After a few days, most of the inhaled DU remaining in the respiratory tract will be in the alveolar region, from which particle transport to the GI tract is slow (time-scales of months to decades). Similarly, dissolution in the respiratory tract typically shows two phases, represented in the HRTM by rapid and slowly dissolving fractions. Hence, in the first day or so, uptake to blood will be determined by the rapid dissolution acting on the large, but rapidly decreasing, deposit in the URT and by absorption in the GI tract of material cleared from the URT. Subsequent uptake to blood will be determined by slow dissolution acting on the alveolar deposit, since most of the URT deposit will have cleared.

A2 VARIATION IN RESPIRATORY TRACT DEPOSITION

There are four main factors that determine respiratory tract deposition and its variability:

- Aerosol size distribution
- Exercise level and hence ventilation rate
- Breathing mode (nose versus mouth breathing)
- Inter- and intra-subject variability in deposition for a given aerosol size distribution, ventilation rate and breathing mode.

The first three of these are relatively straightforward to consider, and are addressed in the indicative uncertainty analysis below. The fourth is far more complex, because each respiratory tract region acts as a particle filter in series during inhalation and exhalation. Thus deposition in each affects the amount of aerosol reaching the next region (ICRP, 1994a; Bailey et al, 1997; Guilmette et al, 1998). Consideration of the distributions of deposition efficiencies of each region are included in the full uncertainty analysis, but were beyond the scope of this preliminary exercise. It is recognised that neglecting this factor will underestimate ranges in deposition. However, the simple approach used below involves taking maximum and minimum likely values of several parameters simultaneously which will tend to overestimate the likely range.

Appropriate parameter values and ranges are considered in turn below. However, because the analysis here concerns estimates of dose and kidney concentration from a

urine sample, rather than an exposure (time integrated air concentration), the total deposition is not of importance, only the relative distribution between regions. As described above (Section A1), the early phase of uptake to blood is dominated by material deposited in the upper respiratory tract (URT) and the later phase by material deposited in the alveolar region. Therefore to simplify the overall analysis, the effects of these factors were combined to provide sets of parameter values corresponding to a "central" pattern of deposition, and to high and low URT deposition relative to alveolar deposition.

Based on the information reviewed in Section 2.3, central values of regional deposition were based on:

- Aerosol with AMAD 2.5 μm and GSD 6, and particle density of 9 g cm^{-3} (Tables 4 and 5).
- Normal nasal augmenter
  - at light exercise (1.5 m^3 h^{-1}, 20 breaths per minute) for Level II;
  - at heavy exercise (3 m^3 h^{-1}, 26 breaths per minute) for Level I.

To evaluate ranges, other aerosol sizes considered were AMAD 2.5 μm, GSD 2 and 15; AMAD 0.4 μm, GSD 6; AMAD 13 μm, GSD 6 (Section 2.3.1.4). For each aerosol, the minimum and maximum breathing parameters for light and heavy exercise (Table 10) were also applied. For light exercise, habitual mouth breathers were also considered (F_n = 0.4), and for heavy exercise habitual mouth breathers and habitual nose breathers were also considered (F_n = 0.3; F_n = 1.0). For each of the 75 sets of parameter values regional deposition (the fraction of inhaled activity deposited in the respiratory tract was calculated with LUDEP (LUng Dose Evaluation Program, Jarvis et al 1996). LUDEP implements the HRTM, and enables the user to calculate regional deposition fractions by selecting specific values of parameters defining aerosol characteristics, breathing pattern, etc.

As noted above (Section 2.1) the main effect of the deposition pattern on subsequent biokinetics is determined by the distribution between the upper respiratory tract (URT) and deep lungs (alveolar region). Material deposited in the URT (here defined as regions ET_2, BB and bb) is rapidly cleared to the throat and swallowed. Absorption to blood in the first few days is likely to be dominated by the rapid phase of respiratory tract absorption, and uptake in the GI tract. (Material deposited in ET_1 is assumed to be removed by nose blowing and not subject to absorption.) After the first few days, most of the material remaining in the respiratory tract will be in the alveolar (AI) region, and absorption to blood will be dominated by the slow phase of respiratory tract absorption. As a measure of this, the ratio of combined deposition in regions ET_2, BB and bb to deposition in AI was calculated.

Table A1 Estimated ranges of deposition patterns, resulting from variation in each parameter value (a) light exercise

		Ventilation (B and f_R)		Mode (F_n)		AMAD		GSD	
	Central	Low	High	Low	High	Low	High	Low	High
AMAD, μm	**2.5**	2.5	2.5	2.5	2.5	**0.4**	**13**	2.5	2.5
GSD	**6**	6	6	6	6	6	6	**2**	**15**
Mode (F_n)	**1**	1	1	**0.4**	**1**	1	1	1	1
B (m^3 h^{-1})	**1.5**	**0.75**	**3**	1.5	1.5	1.5	1.5	1.5	1.5
f_R (per minute)	**20**	**14**	**28**	20	20	20	20	20	20
Deposition (%)									
ET_1	**24.75**	21.2	28.06	8.08	24.75	15	29.7	30.6	23.27
ET_2	**29.08**	24.76	32.91	22.84	29.08	17.9	32.8	39.4	26.36
BB	**1.42**	1.38	1.45	5.61	1.42	1.85	0.96	2.15	1.48
Bb	**2.21**	3.15	1.56	3.81	2.21	6.69	0.68	1.38	3.6
AI	**9.95**	12.73	7.75	15.41	9.95	21.07	3.37	8.31	11.3
Ratio	**3.3**	2.3	4.6	2.1	3.3	1.3	10.2	5.2	2.8

Note: Central values and varied parameter values in bold. Ratio = (Deposition in ET_2 + BB + bb)/(Deposition in AI)

Table A1 Estimated ranges of deposition patterns, resulting from variation in each parameter value (b) heavy exercise

		Ventilation (B and f_R)		Mode (F_n)		AMAD		GSD	
	Central	Low	High	Low	High	Low	High	Low	High
AMAD, μm	**2.5**	2.5	2.5	2.5	2.5	**0.4**	**13**	2.5	2.5
GSD	**6**	6	6	6	6	6	6	**2**	**15**
Mode (F_n)	**0.5**	0.5	0.5	**0.3**	**1**	0.5	0.5	0.5	0.5
B (m^3 h^{-1})	**3**	**1.5**	**6**	3	3	3	3	3	3
f_R (per minute)	**26**	**19**	**36**	26	26	26	26	26	26
Deposition (%)									
ET_1	**12.4**	10.7	14	6.66	28.04	7.53	14.9	15.3	11.64
ET_2	**27.1**	23.6	30.4	25.39	32.86	14.55	37.7	28.6	27.15
BB	**6.55**	4.95	8.36	8.51	1.45	4.1	5.62	10.9	5.07
Bb	**2.75**	3.56	2.05	3.2	1.57	6.42	1.31	3.07	3.95
AI	**11.9**	15.08	9.12	13.23	8.08	23.74	4.63	12.3	13.32
Ratio	**3.1**	2.1	4.5	2.8	4.4	1.1	9.6	3.5	2.7

Results are shown in Table A1: (a) light exercise; (b) heavy exercise. For both exercise levels, the central parameter values give about three times as much deposition in the URT as in the alveolar region. Also shown in Table A1 is the effect of varying each parameter value separately. Under these conditions, AMAD has the greatest effect, resulting in a ratio of about one for the smallest size and about ten for the largest.

Combinations of parameters were also considered, and Table A2 shows the smallest and highest ratios calculated, with the parameter values giving rise to them. As might be expected the lowest ratio (about 0.9) arises from mouth breathing (F_n = 0.4), low ventilation rate, and a small aerosol size, while the highest ratio (about 25) arises from nose breathing (F_n = 1), high ventilation rate, and a large aerosol size.

Table A2 Estimated ranges of deposition patterns, based on high and low ratio of deposition in the upper respiratory tract to that in the alveolar region

	Light exercise			Heavy exercise		
	Low	Central	High	Low	Central	High
AMAD, μm	0.4	2.5	13	0.4	2.5	13
GSD	6	6	6	6	6	6
Mode (F_n)	0.4	1	1	0.3	0.5	1
B (m^3 h^{-1})	0.75	1.5	3	1.5	3	6
f_R (per minute)	14	20	28	19	26	36
Deposition (%)						
ET_1	4.11	24.8	31.6	3.4	12.4	33.2
ET_2	10.34	29.1	34.6	11.1	27.1	35.8
BB	3.36	1.42	0.9	3.98	6.55	0.81
bb	9.65	2.21	0.41	8.25	2.75	0.24
AI	25.37	9.95	2.09	25.9	11.9	1.38
Ratio	0.92	3.3	17.2	0.90	3.1	26.7

Ratio = (Deposition in ET_2 + BB + bb)/(Deposition in AI)

A3 SENSITIVITY ANALYSIS OF MAXIMUM KIDNEY CONCENTRATIONS TO INHALATION PARAMETER VALUES

The methods used to carry out the sensitivity analysis are described in Section 3. Table 20 lists the parameter values chosen as 'central' (typical) values, and ranges. Results for radiation doses are described in Section 4.1.1.

Doses (and $^{max}[U]_k$) were calculated for an intake of 1 mg DU, using the central parameter values. The value of each parameter in turn was changed to its 'low' and 'high' value, the result recalculated and presented as the ratio to that obtained using all central values, i.e. the 'sensitivity factor'. Thus if a 'low' value gives a ratio greater than 1.0 it means that the dose is higher if calculated with that value than if calculated with the central value. To identify parameters that can have an 'important' impact (worthy of further discussion), ratios ≤ 0.8, and ≥ 1.2 are shown in bold font. (A criterion of 20% difference was chosen because it identified a reasonable number of parameters in each

case.) It should be noted that in many cases the sensitivity of the output (dose or $^{max}[U]_k$) to changes in a particular parameter value will be dependent on the set of central values themselves. For example, the central value of the slow dissolution rate, s_s, is 0.002 d^{-1}, and so changes to the slowest particle transport rate from the AI region 0.0001 d^{-1} will have little effect, because overall retention is dominated by dissolution. Changes to this particle transport rate would have had more effect if a lower central value of s_s had been chosen.

For comparison, results for HRTM default Type M and Type S absorption parameter values are also given. For these, all four absorption parameter values are set to their default values simultaneously, but other parameter values (aerosol, breathing, particle transport) remain at the DU central values given in Table 20:

- For Type M: f_r = 0.1; s_r = 100 d^{-1}; s_s = 0.005 d^{-1}; f_1 = 0.02
- For Type S: f_r = 0.001; s_r = 100 d^{-1}; s_s = 0.0001 d^{-1}; f_1 = 0.002

Note that for Type M the value of f_r is close to the central value (0.15), and that of s_s is the same as the 'high' value. For Type S the value of f_r is only 10% of the 'low' value (0.01), and that of s_s is the same as the 'low' value.

For fractional absorption from the GI tract (f_1), the central value taken for the sensitivity analysis was the default value for Type M (0.02), but central and low values of 0.003 and 0.0008 derived for the uncertainty analysis were included for comparison.

Table A3 Sensitivity to inhalation parameter values of doses (effective and lung) and maximum kidney concentration $^{max}[U]_k$, µg U per gram kidney for unit intake of DU

Parameter	Low/ High	Value	Unit	Ratio to central values		
				E(50)	$H_{Lung}(50)$	$^{max}[U]_k$
Aerosol						
AMAD	Low	0.4	µm	**1.53**	**1.52**	**1.50**
AMAD	High	13	µm	**0.60**	**0.60**	**0.67**
Aerosol GSD	Low	2		**1.39**	**1.40**	1.17
Aerosol GSD	High	15		1.07	1.07	1.07
Breathing						
Nasal fraction (mode), F_n	Low	0.3		**1.21**	**1.21**	1.12
Nasal fraction (mode), F_n	High	1		**0.45**	**0.45**	**0.68**
Ventilation rate, B	Low	0.75	$m^3\ h^{-1}$	0.92	0.92	0.86
Ventilation rate, B	High	6	$m^3\ h^{-1}$	1.05	1.05	1.01
Frequency, f_R	Low	14	$minute^{-1}$	1.09	1.09	**1.20**
Frequency, f_R	High	36	$minute^{-1}$	0.95	0.95	0.91
Absorption to blood						
Rapid fraction, f_r	Low	0.01		1.15	1.16	**0.25**
Rapid fraction, f_r	High	0.5		**0.62**	**0.60**	**2.87**
Rapid dissolution rate, s_r	Low	0.3	d^{-1}	1.01	1.01	**0.64**
Rapid dissolution rate, s_r	High	20	d^{-1}	1.00	1.00	**1.28**
Slow dissolution rate, s_s	Low	1E-4	d^{-1}	**1.59**	**1.62**	0.99
Slow dissolution rate, s_s	High	0.005	d^{-1}	0.84	0.83	1.02

Parameter		Low/ High	Value	Unit	Ratio to central values E(50)	$H_{Lung}(50)$	$^{max}[U]_k$
Type M					0.83	0.82	**1.23**
Type S					**1.80**	**1.83**	**0.03**
GI tract absorption, f_1		Low	0.0008		1.00	1.00	0.83
GI tract absorption, f_1		Central	0.003		1.00	1.00	0.85
Particle transport rates		(Fig. 5; Table 1)					
$m_{1,4}$	AI_1 to bb_1	Low	6.67E-3	d^{-1}	1.01	1.01	1.00
$m_{1,4}$	AI_1 to bb_1	High	0.06	d^{-1}	0.99	0.99	1.00
$m_{2,4}$	AI_2 to bb_1	Low	3.33E-4	d^{-1}	1.04	1.04	1.00
$m_{2,4}$	AI_2 to bb_1	High	0.003	d^{-1}	0.95	0.95	1.00
$m_{3,4}$	AI_3 to bb_1	Low	3.33E-5	d^{-1}	1.00	1.00	1.00
$m_{3,4}$	AI_3 to bb_1	High	3E-4	d^{-1}	1.00	1.00	1.00
$m_{3,10}$	AI_3 to LN_{TH}	Low	6.67E-6	d^{-1}	1.00	1.00	1.00
$m_{3,10}$	AI_3 to LN_{TH}	High	6E-5	d^{-1}	1.00	1.00	1.00
$m_{4,7}$	bb_1 to BB_1	Low	0.67	d^{-1}	1.05	1.05	1.01
$m_{4,7}$	bb_1 to BB_1	High	6	d^{-1}	0.98	0.98	0.99
$m_{5,7}$	bb_2 to BB_1	Low	0.01	d^{-1}	**1.54**	**1.55**	1.00
$m_{5,7}$	bb_2 to BB_1	High	0.09	d^{-1}	**0.79**	**0.78**	1.00
$m_{6,10}$	bb_{seq} to LN_{TH}	Low	3.33E-3	d^{-1}	1.01	1.01	1.00
$m_{6,10}$	bb_{seq} to LN_{TH}	High	0.03	d^{-1}	1.00	1.00	1.00
$m_{7,11}$	BB_1 to ET_2'	Low	3.33	d^{-1}	1.01	1.00	1.04
$m_{7,11}$	BB_1 to ET_2'	High	30	d^{-1}	1.00	1.00	0.98
$m_{8,11}$	BB_2 to ET_2'	Low	0.01	d^{-1}	**1.67**	**1.69**	1.00
$m_{8,11}$	BB_2 to ET_2'	High	0.09	d^{-1}	**0.74**	**0.73**	1.00
$m_{9,10}$	BB_{seq} to LN_{TH}	Low	3.33E-3	d^{-1}	1.03	1.03	1.00
$m_{9,10}$	BB_{seq} to LN_{TH}	High	0.03	d^{-1}	0.98	0.98	1.00
$m_{11,15}$	ET_2' to GI tract	Low	33.3	d^{-1}	1.00	1.00	1.07
$m_{11,15}$	ET_2' to GI tract	High	300	d^{-1}	1.00	1.00	0.98
$m_{12,13}$	ET_{seq} to LN_{ET}	Low	3.33E-4	d^{-1}	1.00	1.00	1.00
$m_{12,13}$	ET_{seq} to LN_{ET}	High	0.003	d^{-1}	1.00	1.00	1.00
$m_{14,16}$	ET_1 to environment	Low	0.333	d^{-1}	1.00	1.00	1.00
$m_{14,16}$	ET_1 to environment	High	3	d^{-1}	1.00	1.00	1.00
KI Model (Table 12)					**0.56**	**0.54**	0.93

A3.1 Results of sensitivity analysis

Table A3 summarises the analysis of the sensitivity to inhalation parameter values of doses (effective and lung) and maximum kidney concentration $^{max}[U]_k$, µg uranium per gram kidney for unit intake of DU. Results for radiation doses are described in Section 4.1.1, but are included in Table A3 for comparison.

Maximum kidney concentration per unit intake

For aerosol size, a smaller AMAD results in an increased value of $^{max}[U]_k$, and a larger AMAD results in a lower value, very similar to the effect on doses, and reflecting differences in lung deposition. Changes to GSD have less effect than for doses.

For breathing parameters, similar to the effect on doses, the fraction breathed through the nose, F_n, is important. As expected, reducing F_n, and correspondingly increasing the fraction breathed through the mouth, increases lung deposition and $^{max}[U]_k$. Reducing the breathing frequency also increases $^{max}[U]_k$, through increased lung deposition. As this occurs mainly in AI, it has less effect on doses than on $^{max}[U]_k$.

Changes to the absorption parameter values have most effect, especially changes to the fraction dissolved rapidly, f_r. The effect is greater than, and opposite to, the effect on doses: an increase in f_r increases $^{max}[U]_k$. This is as expected: increasing f_r increases the amount of uranium reaching blood (and hence kidney) in the first day or so after intake. An increase in s_r also increases $^{max}[U]_k$. A large fraction of the intake deposits in ET_2', which includes the main nasal passage, pharynx and larynx. Dissolution of the rapid fraction competes with particle transport (central rate 100 d^{-1}), so that with a higher value of s_r more of the rapid fraction dissolves before being cleared to the GI tract.

For Type M the value of $^{max}[U]_k$ is higher than for the 'high' value of s_s. This results from the much higher value of s_r (100 d^{-1} for Type M compared to the central value of 3 d^{-1}). For Type S the value of $^{max}[U]_k$ is much lower than for the 'low' value of s_s, because of the much lower values of f_r and f_1. Both these result in much lower absorption to blood and hence deposition in kidney immediately after intake.

Changes to most of the particle transport rates have even less effect on $^{max}[U]_k$ than on doses per unit intake. The exception is the low rate of clearance from ET_2' to the GI tract. As noted above, dissolution of the rapid fraction (central rate 3 d^{-1}) competes with particle transport (central rate 100 d^{-1}), and since particle transport dominates clearance, a decrease in it allows more time for the rapid fraction to dissolve. In other parts of the respiratory tract particle transport rates are lower, and so changes to them have less effect on the proportion of the rapid fraction that dissolves.

Maximum kidney concentration per unit measurement (assessed from a urine sample)

Table A4 summarises the sensitivity to inhalation parameter values of $^{max}[U]_k$ assessed from measurement of DU in a 24-hour urine sample at a series of times in the range 100–10,000 days after intake. Again ratios ≤ 0.8, and ≥ 1.2 are shown in bold font. Generally the same sub-set of parameter values is identified as 'important' as for the value of $^{max}[U]_k$ calculated for a given intake.

As for doses, the effect of AMAD is the opposite of that observed for $^{max}[U]_k$ per unit intake (Table 23). Here higher $^{max}[U]_k$ result from a larger AMAD, and lower doses from a smaller AMAD. Again, as for doses, particle transport from compartment AI_2 is important here, even though no changes to particle transport rates were identified as important for $^{max}[U]_k$ per unit intake.

Changes to breathing parameters tend to have less effect than on $^{max}[U]_k$ per unit intake (Table 23), and none show changes greater than 20%.

The effects of changes to the absorption parameter values have most effect, especially changes to the fraction dissolved rapidly, f_r. and the slow dissolution rate, s_s. At all times a high (or low) value of f_r leads to a $^{max}[U]_k$ 2–5 times higher (or lower) than that calculated with the central values. Changes to the value of s_s, as for doses, have more complex effects: high or low values of s_s lead to increases or decreases in $^{max}[U]_k$ at different times.

For Type M values of $^{max}[U]_k$ are similar to those for the 'high' value of s_s. For Type S values of $^{max}[U]_k$ are much lower than for the 'low' value of s_s, because of the much lower values of f_r and f_1, which lead to much lower absorption to blood, and hence deposition in kidney, immediately after intake.

Table A4 Summary of sensitivity to inhalation parameter values of maximum kidney concentration $^{max}[U]_k$, µg U per gram kidney for 1 ng of DU in a 24-hour urine sample at 100–10,000 days after intake

Parameter	Low/ High	Value	Unit	Ratio to central values				
Days after intake				100	500	1000	5000	10000
Aerosol								
AMAD	Low	0.4	µm	**0.79**	**0.76**	**0.77**	0.84	0.84
AMAD	High	13	µm	**1.55**	**1.68**	**1.64**	**1.34**	**1.33**
Aerosol GSD	Low	2		1.10	1.13	1.12	1.07	1.06
Aerosol GSD	High	15		0.96	0.95	0.96	0.97	0.97
Breathing								
Nasal fraction (mode), F_n	Low	0.3		1.00	1.01	1.00	1.00	1.00
Nasal fraction (mode), F_n	High	1		1.03	1.01	1.01	1.02	1.02
Ventilation rate, B	Low	0.75	$m^3\ h^{-1}$	0.99	0.99	0.99	1.00	1.00
Ventilation rate, B	High	6	$m^3\ h^{-1}$	1.08	1.10	1.10	1.06	1.05
Frequency, f_R	Low	14	$minute^{-1}$	0.89	0.87	0.87	0.92	0.92
Frequency, f_R	High	36	$minute^{-1}$	1.08	1.10	1.10	1.06	1.06
Absorption to blood								
Rapid fraction, f_r	Low	0.01		**0.23**	**0.22**	**0.22**	**0.30**	**0.30**
Rapid fraction, f_r	High	0.5		**3.56**	**4.67**	**4.37**	**2.05**	**2.00**
Rapid dissolution rate, s_r	Low	0.3	d^{-1}	**0.65**	**0.64**	**0.64**	**0.67**	**0.67**
Rapid dissolution rate, s_r	High	20	d^{-1}	**1.25**	**1.27**	**1.27**	1.18	1.17
Slow dissolution rate, s_s	Low	1E-4	d^{-1}	**5.48**	**6.39**	**2.62**	**0.37**	**0.35**
Slow dissolution rate, s_s	High	0.005	d^{-1}	**0.57**	**1.69**	**4.68**	0.90	0.88
Type M				**0.65**	**1.92**	**5.27**	0.99	0.97
Type S				**0.44**	**0.20**	**0.08**	**0.011**	**0.010**
GI tract absorption, f_1	Low	0.0008		0.86	0.83	0.84	0.90	0.90
GI tract absorption, f_1	Central	0.003		0.88	0.85	0.86	0.91	0.85
Particle transport rates	(Fig. 5 ; Table 1)							
$m_{1,4}$ AI_1 to bb_1	Low	6.67E-3	d^{-1}	0.88	0.97	0.99	0.96	0.96

Parameter		Low/ High	Value	Unit	Ratio to central values				
Days after intake					100	500	1000	5000	10000
$m_{1,4}$	AI_1 to bb_1	High	0.06	d^{-1}	1.07	1.00	1.00	1.02	1.02
$m_{2,4}$	AI_2 to bb_1	Low	3.33E-4	d^{-1}	0.96	**0.78**	**0.63**	0.87	0.88
$m_{2,4}$	AI_2 to bb_1	High	0.003	d^{-1}	1.11	**1.89**	**2.29**	**1.23**	**1.22**
$m_{3,4}$	AI_3 to bb_1	Low	3.33E-5	d^{-1}	1.00	0.99	0.98	0.99	1.00
$m_{3,4}$	AI_3 to bb_1	High	3E-4	d^{-1}	1.00	1.02	1.05	1.01	1.01
$m_{3,10}$	AI_3 to LN_{TH}	Low	6.67E-6	d^{-1}	1.00	1.00	1.00	1.00	1.00
$m_{3,10}$	AI_3 to LN_{TH}	High	6E-5	d^{-1}	1.00	1.00	1.00	1.00	1.00
$m_{4,7}$	bb_1 to BB_1	Low	0.67	d^{-1}	1.00	1.01	1.01	1.00	1.00
$m_{4,7}$	bb_1 to BB_1	High	6	d^{-1}	0.99	0.99	0.99	0.99	0.99
$m_{5,7}$	bb_2 to BB_1	Low	0.01	d^{-1}	0.95	1.00	1.00	0.99	0.99
$m_{5,7}$	bb_2 to BB_1	High	0.09	d^{-1}	1.01	1.00	1.00	1.00	1.00
$m_{6,10}$	bb_{seq} to LN_{TH}	Low	3.33E-3	d^{-1}	1.00	1.00	1.00	1.00	1.00
$m_{6,10}$	bb_{seq} to LN_{TH}	High	0.03	d^{-1}	1.00	1.00	1.00	1.00	1.00
$m_{7,11}$	BB_1 to ET_2'	Low	3.33	d^{-1}	1.04	1.04	1.04	1.03	1.02
$m_{7,11}$	BB_1 to ET_2'	High	30	d^{-1}	0.98	0.98	0.98	0.98	0.99
$m_{8,11}$	BB_2 to ET_2'	Low	0.01	d^{-1}	0.91	0.99	1.00	0.97	0.97
$m_{8,11}$	BB_2 to ET_2'	High	0.09	d^{-1}	1.02	1.00	1.00	1.01	1.01
$m_{9,10}$	BB_{seq} to LN_{TH}	Low	3.33E-3	d^{-1}	1.00	1.00	1.00	1.00	1.00
$m_{9,10}$	BB_{seq} to LN_{TH}	High	0.03	d^{-1}	1.00	1.00	1.00	1.00	1.00
$m_{11,15}$	ET_2' to GI tract	Low	33.3	d^{-1}	1.06	1.07	1.07	1.04	1.04
$m_{11,15}$	ET_2' to GI tract	High	300	d^{-1}	0.98	0.98	0.98	0.98	0.98
$m_{12,13}$	ET_{seq} to LN_{ET}	Low	3.33E-4	d^{-1}	1.00	1.00	1.00	1.00	1.00
$m_{12,13}$	ET_{seq} to LN_{ET}	High	0.003	d^{-1}	1.00	1.00	1.00	1.00	1.00
$m_{14,16}$ environment	ET_1 to	Low	0.333	d^{-1}	1.00	1.00	1.00	1.00	1.00
$m_{14,16}$ environment	ET_1 to	High	3	d^{-1}	1.00	1.00	1.00	1.00	1.00
KI Model (Table 12)					0.97	0.93	0.93	0.97	0.98

A4 INDICATIVE UNCERTAINTY ANALYSIS OF HRTM PARAMETER VALUES

A4.1 Methods used in the indicative uncertainty analysis

Combinations of high and low parameter values were used to give an 'indication' of the overall uncertainty in doses and $^{max}[U]_k$ assessed from measurement of DU in a 24-hour urine sample at a series of times in the range 10–10,000 days after intake.

Deposition parameters

As discussed in Sections 2.1 and A2, the aerosol size and breathing parameter values mainly determine the deposition pattern in the respiratory tract, and the distribution between the deposition of uranium in the upper respiratory tract (URT) and the AI region mainly determines the subsequent biokinetics. Hence to reduce the number of parameters varied in the indicative uncertainty analysis, combinations of aerosol size and breathing parameter values were used that gave three sets of values corresponding to high, central and low ratios of deposition in the URT to AI region (Table A2).

Absorption parameters

The absorption parameters f_r, s_r and s_s were taken from the 'low', 'central' and 'high' ranges for *"Impact or combustion aerosols"* given in the final row of Table 19. All three parameters were assumed to vary independently, and thus for this analysis all 27 combinations of f_r, s_r and s_s were considered. The values for default Type M and Type S absorption were also included for comparison purposes.

Particle Transport

It was assumed that all particle transport rates are positively correlated. Dividing the default ICRP particle rate constants (given in Table 1) by a factor of three, or multiplying the constants by a factor of three respectively, produced low and high groups of values (Section 2.6, Table 20). The 'central' (default HRTM) rates were also included in the analysis.

Bioassay and Dose calculations

The steps in a typical set of calculations were as follows:

1. The relevant sets of HRTM parameter values were configured in IMBA by the client program.
2. The predicted 24-hour urine excretion (ng d^{-1}) after an inhalation of 1 mg of DU was calculated at 10, 20, 50, 100, 200, 500, 1000, 5000 and 10,000 days after the intake.
3. $E(50)$ and $H_{Lung}(50)$, were calculated for the 1-mg intake of DU.
4. $^{max}[U]_k$ was calculated for the 1-mg intake of DU.
5. Using the values calculated in steps 3 and 4, and assuming that a quantity of 1 ng of DU had been measured in a 24-hour urine sample, E(50), $H_{Lung}(50)$, and $^{max}[U]_k$ were calculated from the predicted urine bioassay quantities at each time point.

Steps 1 to 5 were repeated using the 'central' sets of values for the deposition and particle transport parameters, but with Type M and Type S absorption parameters.

Data Analysis

The minimum and maximum doses, and the minimum and maximum values of $^{max}[U]_k$, were determined from the results of all 243 calculations in step 5 (above), for each point in the urine bioassay time series.

A4.2 Results of the indicative uncertainty analysis

Figure A1 shows the committed effective dose assessed from 1 ng DU measured in a 24-hour urine sample obtained over the range 10–10,000 days after intake, using central values of all parameters (Table 20). Also shown are the maximum and minimum values obtained using all combinations of high and low parameter values as described above. For the central values, the committed effective dose assessed from 1 ng DU d^{-1} increases from about 0.1 μSv at 10 days after intake to about 1 mSv at 10,000 days. The indicative uncertainty is shown by the curves labelled 'maximum' and 'minimum'. At 10 days after intake the 'minimum' is about a factor of 10 below the central value and the 'maximum' is about a factor of 100 above the central value, giving an overall range of three orders of magnitude. As the time between intake and sampling increases, the range decreases, so that between 1000 and 10,000 days, the maximum is between 10 and 20 times the minimum. Despite the large uncertainty, even 'maximum' assessed doses from 1 ng DU d^{-1} are below 1 mSv up to 5000 d. Also shown in Figure A1 for comparison are effective doses assessed using Type M and Type S parameter values. Note however, that in these cases all other parameters are at their central values, so that the difference from the 'central' curve reflects only the difference in absorption parameter values. As expected from consideration of sensitivity (Table 24), results for Type M are similar to the central values, and those for Type S are much higher, except at late times.

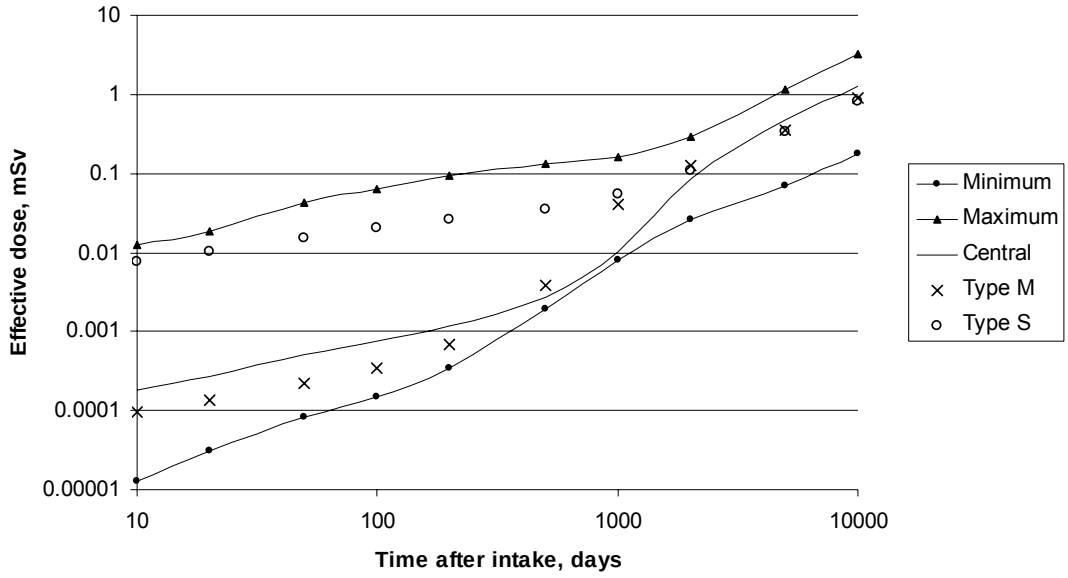

Figure A1 Indicative uncertainty in committed effective dose assessed from 1 ng DU measured in a 24-hour urine sample.

Figure A2 shows corresponding results for committed equivalent dose to the lungs. As noted above, for inhalation of uranium in moderately soluble or insoluble forms, lung dose makes the dominant contribution to effective dose. Thus the pattern for lung dose is very similar to that for effective doses, with values about 10 times higher, reflecting the value of 0.12 for the lung tissue weighting factor.

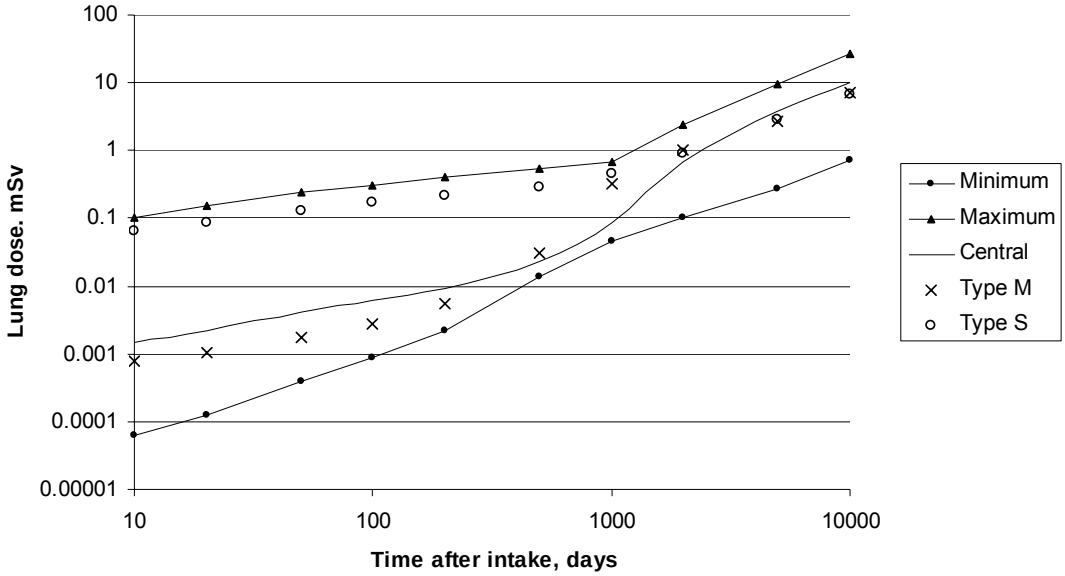

Figure A2 Indicative uncertainty in committed equivalent lung dose assessed from 1 ng DU measured in a 24-hour urine sample

Figure A3 shows corresponding results for maximum kidney concentration $^{max}[U]_k$, µg uranium per gram kidney. For the central values, $^{max}[U]_k$ assessed from 1 ng DU d^{-1} increases from about 10^{-5} µg per gram at 10 days after intake, to about 0.1 µg per gram at 10,000 days. At 10 days after intake the 'minimum' is about a factor of four below the central value and the 'maximum' is about a factor of two above it. The narrow range reflects the close link between urinary excretion and kidney concentration at early times after intake. As the time between intake and sampling increases, the range increases, so that between 200 and 10,000 days, the maximum is between 300 and 900 times the minimum. However, despite the large uncertainty, even 'maximum' assessed values of $^{max}[U]_k$ from 1 ng DU d^{-1} are below 1 µg per gram at all times considered. As expected from consideration of sensitivity (Table A4), results for Type M are similar to the central values, and those for Type S are much lower, especially at later times.

It should be noted, however, that this analysis considers only uncertainty and variability in parameters associated with the inhalation model. It does not include uncertainty associated with the measurement itself (which will depend on the technique, and the amount of DU and natural uranium present in the sample), nor of uncertainty and variability in parameters associated with the systemic uranium model.

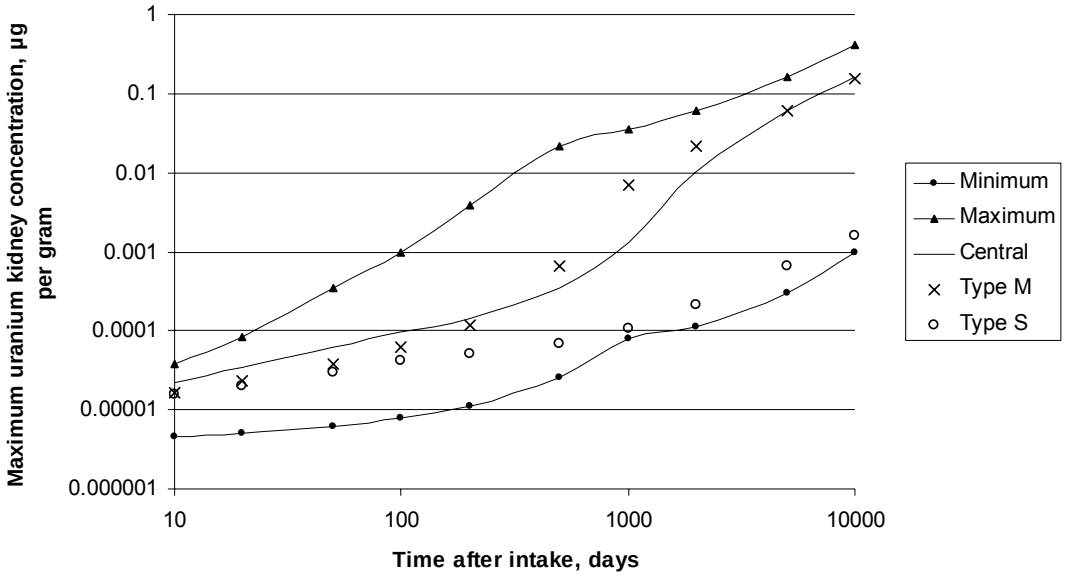

Figure A3 Indicative uncertainty in maximum kidney concentration $^{max}[U]_k$, µg U per gram kidney for 1 ng of DU in a 24-hour urine sample